UNCLASSIFIED

AD 260 731

Reproduced
by the

ARMED SERVICES TECHNICAL INFORMATION AGENCY
ARLINGTON HALL STATION
ARLINGTON 12, VIRGINIA

UNCLASSIFIED

DISCLAIMER NOTICE

THIS DOCUMENT IS BEST QUALITY PRACTICABLE. THE COPY FURNISHED TO DTIC CONTAINED A SIGNIFICANT NUMBER OF PAGES WHICH DO NOT REPRODUCE LEGIBLY.

NOTICE: When government or other drawings, specifications or other data are used for any purpose other than in connection with a definitely related government procurement operation, the U. S. Government thereby incurs no responsibility, nor any obligation whatsoever; and the fact that the Government may have formulated, furnished, or in any way supplied the said drawings, specifications, or other data is not to be regarded by implication or otherwise as in any manner licensing the holder or any other person or corporation, or conveying any rights or permission to manufacture, use or sell any patented invention that may in any way be related thereto.

260731

AFOSR TR 60-139

CORNELL AERONAUTICAL LABORATORY, INC.

CATALOGED BY ASTIA
AS AD No.

REPORT NO. AD-1052-A-12

SUMMARY OF SHOCK TUNNEL DEVELOPMENT AND APPLICATION TO HYPERSONIC RESEARCH

By

A. Hertzberg, Charles E. Wittliff

and

J. Gordon Hall

JULY 1961

Contract No. AF 18(603)-10

ASTIA
AUG 8 1961
TIPDR

BUFFALO, NEW YORK

AFOSR TR 60-139

CORNELL AERONAUTICAL LABORATORY, INC.
BUFFALO 21, NEW YORK

Report No. AD-1052-A-12

SUMMARY OF SHOCK TUNNEL DEVELOPMENT AND APPLICATION TO HYPERSONIC RESEARCH

JULY 1961

Contract No. AF 18(603)-10

MECHANICS DIVISION
AIR FORCE OFFICE OF SCIENTIFIC RESEARCH
AIR RESEARCH AND DEVELOPMENT COMMAND
WASHINGTON 25, D.C.

BY: A. Hertzberg

Charles E. Wittliff

J. Gordon Hall

FOREWORD

This report presents a summary of the development of the hypersonic shock tunnel and related instrumentation at the Cornell Aeronautical Laboratory, Inc. and describes application of the shock tunnel to various research studies. Preparation of this report has been sponsored by the United States Air Force through the Office of Scientific Research (Contract AF 18(603)-10). Mr. Milton Rogers, Chief of the Mechanics Division, AFOSR, provided technical monitoring of this contract. The present report has evolved from the papers "Studying Hypersonic Flight in the Shock Tunnel," presented by A. Hertzberg and C. E. Wittliff at the I. A. S. National Summer Meeting held in Los Angeles, California during June 28-July 1, 1960, and "Hypersonic Research in the Shock Tunnel," presented by C. E. Wittliff at the I. A. S. National Symposium on Hypervelocity Techniques held in Denver, Colorado, on October 20, 21, 1960.

The development of the shock tunnel and the associated instrumentation and the various hypersonic research studies reported herein have been supported by the U. S. Air Force through the Office of Scientific Research (Contracts AF 18(603)-10, AF 18(603)-141, AF 49(638)-782, and AF 49(638)-792), the Wright Air Development Division (Contracts AF 33(616)-2387 and AF 33(616)-6025), the Arnold Engineering Development Center (Contract AF 40(600)-6), the Rome Air Development Center (Contract AF 30(602)-2267), and the Cornell Aeronautical Laboratory, Inc. through its internal research program.

The authors wish to express their thanks to their colleagues in the Aerodynamic Research Department for their assistance in the preparation of this report. They also are pleased to acknowledge the material and cooperation provided by the CAL Applied Hypersonic Research Department.

ABSTRACT

In recent years the shock tunnel has found increasing application in hypersonic research. The early problems associated with this unconventional wind tunnel have been solved, enabling its advantages to be exploited. This report reviews the development of the shock tunnel, discusses its present capabilities, and outlines future prospects.

The ability of the shock tunnel to produce air flows at stagnation temperatures and pressures associated with hypersonic flight has been well established. The chief difficulty associated with this type of tunnel has been the very short (millisecond) testing time. The "tailored-interface" technique has significantly increased the available testing time in a shock tunnel. This testing-time extension, plus the development of effective rapid-response instrumentation, now permits the accurate measurement of pressures, forces, and heat-transfer rates. The hypersonic shock tunnel in its present form is capable of duplicating re-entry flight conditions for various hypersonic vehicles over an important area of the re-entry flight corridor. However, complete duplication over the entire range of interest for re-entry flight cannot be obtained with present shock tunnels. For some regions the techniques of partial simulation must be resorted to. However, the flexibility of the shock tunnel operation permits a wide range of simulation conditions to be studied.

In its present form the shock tunnel has exceeded initial expectations both as to its range of performance and scope of testing. This success has encouraged studies which indicate that significant further developments of a shock tunnel are possible. In particular, exploratory experiments have demonstrated

ABSTRACT

In recent years the shock tunnel has found increasing application in hypersonic research. The early problems associated with this unconventional wind tunnel have been solved, enabling its advantages to be exploited. This report reviews the development of the shock tunnel, discusses its present capabilities, and outlines future prospects.

The ability of the shock tunnel to produce air flows at stagnation temperatures and pressures associated with hypersonic flight has been well established. The chief difficulty associated with this type of tunnel has been the very short (millisecond) testing time. The "tailored-interface" technique has significantly increased the available testing time in a shock tunnel. This testing-time extension, plus the development of effective rapid-response instrumentation, now permits the accurate measurement of pressures, forces, and heat-transfer rates. The hypersonic shock tunnel in its present form is capable of duplicating re-entry flight conditions for various hypersonic vehicles over an important area of the re-entry flight corridor. However, complete duplication over the entire range of interest for re-entry flight cannot be obtained with present shock tunnels. For some regions the techniques of partial simulation must be resorted to. However, the flexibility of the shock tunnel operation permits a wide range of simulation conditions to be studied.

In its present form the shock tunnel has exceeded initial expectations both as to its range of performance and scope of testing. This success has encouraged studies which indicate that significant further developments of a shock tunnel are possible. In particular, exploratory experiments have demonstrated

the usefullness of the shock tunnel for the investigation of hypervelocity rarefied-gas flows associated with the re-entry of manned vehicles. To fully exploit the potential of the shock tunnel for this type research, extremely large size test sections have been shown to be both required and feasible, thus making available the advantages of nearly full-scale testing within the laboratory. In addition, anticipated developments in the technique of operation indicate the possibility of extending the range of complete flight duplication so that nearly the entire range of critical flight re-entry can be conveniently studied.

TABLE OF CONTENTS

TABLE OF CONTENTS (Contd)

LIST OF ILLUSTRATIONS

INTRODUCTION

The ability of the conventional shock tube to generate short-duration flows of known thermodynamic state at high-enthalpy levels was demonstrated approximately 10 years ago by the work of the groups directed by Kantrowitz at Cornell University[1] and LaPorte at the University of Michigan[2]. This capability led to the concept of modifying a shock tube to generate high-enthalpy hypersonic flows[3]. In its earliest form, the modification involved the addition of a diverging nozzle to the end of a conventional shock tube so that the supersonic flow generated behind the shock wave could be expanded to higher Mach numbers. This modified shock tube, termed the shock tunnel, offered a technique for obtaining hypersonic flows within the laboratory with enthalpy levels appropriate to hypersonic flight. While the testing times that could be achieved were brief (on the order of milliseconds), the flexibility and convenience of this device made it an attractive research tool. Hence, the Cornell Aeronautical Laboratory, Inc. embarked on a program to develop the potential of the shock tunnel.

This report reviews the development of the shock tunnel and associated instrumentation. Current research techniques and illustrative results of recent research activities undertaken in CAL shock tunnels will be presented. In addition, consideration will be given to future developments of the shock tunnel which extend its usefulness for the study of the hypersonic aerodynamics associated with manned re-entry vehicles.

The basic theory and techniques of operation of shock tubes and shock tunnels have been extensively reported in the literature (see, for example, Refs. 4, 5, and 6) and therefore will not be discussed here. Furthermore, it

is beyond the scope of this report to review the diversified applications of the shock tube and its modifications in current research activities not related to hypersonic flow. The literature relating to the use of the shock tube and shock tunnel in hypersonic research has proliferated extensively in recent years, attesting to their widespread use (see, for example, Refs. 7-14). While only the application of shock tunnels to hypersonic flow research will be described herein, much of the discussion of tunnel performance, simulation requirements, nonequilibrium effects, and instrumentation techniques is applicable to hypersonic facilities in general.

REVIEW OF SHOCK TUNNEL DEVELOPMENT

Exploratory Experiments

The original shock tunnel studies at CAL were chiefly concerned with the gasdynamic processes involved in terminating the end of a conventional shock tube with a diverging nozzle. Examination of the wave processes following the passage of a shock wave from the shock tube into the expanding nozzle indicated that after a brief period of nonsteady wave motion, steady flow would be established. However, for area ratios required to produce nozzle flow Mach numbers in excess of 4, the steady flow time available from a shock tube of convenient length was less than that required for the establishment of steady flow. Further study showed that by separating the end of a shock tube from the nozzle with a thin diaphragm and by pre-evacuating the nozzle, the time involved in the starting process was small compared to the available testing time[15].

In these early studies it was realized that in order to provide a convenient means of varying the test Mach number and to accommodate the large area

ratios required for hypersonic flows, a multiple-expansion nozzle was desirable. A two-stage nozzle was developed in which the flow first expanded to about Mach 4 and then the central core further expanded to hypersonic Mach numbers. This arrangement allowed the choice of a shock tube of convenient dimensions independent of nozzle size, and also improved the test section flow by partially eliminating the boundary layer generated in the shock tube and in the first expansion nozzle.

These experiments were performed using helium as the driver gas. However, a helium driver could not produce the strong shock waves necessary to obtain the enthalpies typical of hypersonic flight. Even room-temperature hydrogen required pressure levels beyond the techniques then available. Consequently, other available methods for the generation of strong shock waves[1] were examined. Accordingly the use of constant-volume combustion as originally suggested in Ref. 1 was adopted. Studies with a variety of combustible driver mixtures indicated that one of the most effective was a stoichiometric mixture of oxygen and hydrogen diluted with an optimum amount of helium[16]. This particular driver mixture has since been widely adopted for shock tube and gun tunnel use. Operating with this mixture, it was possible to generate at convenient pressure ratios the required shock strengths. In addition, it was found that unusually high shock strengths could be achieved by allowing the diaphragm to rupture before complete combustion (i. e., the so-called constant-pressure technique[17]).

Early Tunnel Development

A shock tunnel was fabricated which embodied the foregoing features (Fig. 1) and a study of the hypersonic flows produced in this tunnel was initiated*. At this time the available instrumentation techniques were limited; in particular, the fast-response techniques of measurement required for the relatively low-density flows in the nozzle were practically nonexistent. Therefore these early experiments were confined to schlieren observation. However, with this prototype shock tunnel, it was observed that Mach numbers of approximately 10 and stagnation temperatures of about 6000°K were obtained. Hence it was felt that the ability of the shock tunnel to develop high-enthalpy hypersonic flows was established, and further research to develop instrumentation to utilize these flows for research was undertaken. This program, which is discussed in detail in a later section, resulted in the development of a reliable technique for heat-transfer measurement with microsecond response based on a thin-film resistance thermometer[18]. This heat-transfer gauge provided the first method of detailed examination of the flow properties in the test section.

Utilizing this new heat-transfer technique, the character of the flow in the test section was carefully studied. The heat-transfer records revealed that even after the tunnel had started, there were continuous systematic changes in heat-transfer rates during the testing period as well as undesirable scatter in the data. This was particularly true when the constant-pressure combustion technique was used. More detailed examination by schlieren and heat-transfer measurements revealed that the flow generated with this type of combustion was

---

* This study and tunnel development were sponsored by the U. S. Air Force Arnold Engineering Development Center, Contract No. AF 40(600)-6.

of relatively poor quality when compared to that obtained using pure gas drivers, such as helium or hydrogen. In particular, shock wave attenuation was extremely severe. Constant-pressure combustion was then abandoned in favor of the more conventional constant-volume method. However, the quality of the flow as indicated by the heat-transfer records was still poor. The attenuation of the shock wave, even with constant-volume combustion, caused a continuous change in the flow properties of the air entering the nozzle. While techniques were developed to correct the data for the nonsteady character of the flow[19], the data reduction was cumbersome.

In addition to the foregoing problem, shock attenuation so reduced the effective performance of the shock tunnel that the advantage of operating with combustion at high pressures was often destroyed. For example, a shock strength of approximately 10 is required for the simulation of flow velocities of 15,000 ft/sec, using a diverging nozzle. Attenuation of 20% in shock strength at this Mach number, which was often exceeded with combustion or even a pure gas driver[16,20], is equivalent to reduction of effective driver pressure by about a factor of 2. Indeed, it was realized that the problems caused by attenuation were perhaps the most severe limitation in the use and development of the shock tunnel as a hypersonic facility.

Another difficulty was encountered when it was observed that small dust particles or diaphragm fragments could lead to flow disturbances in the vicinity of a blunt body increasing the difficulty in the interpretation of the data[21]. Since these fragments were accelerated to high velocity by the test flow, severe damage resulted to the test model. In particular, the abrasive effect of these particles would damage heat-transfer gauges so that it was necessary, in general, to replace the model after each run.

Development of Present Operating Techniques

At the conclusion of these early studies it was realized that the attainment of the promised advantages of the shock tunnel would require significantly more development. The problems which had been revealed were critically re-examined. It was evident that drastic modifications would be required in the technique of operation to achieve reliable and useful data.

The flow produced by combustion drivers was deemed especially unsuitable for high-quality performance. While it was clear that combustion techniques could be improved, it was considered doubtful if the reliability would ever duplicate that obtained with pure gas drivers. Examination of techniques which had become common practice in the chemical industry indicated that hydrogen pressure operation at 30, 000 psi was commonplace and that pressures up to 60, 000 psi were possible[22]. With the availability of pressures of this magnitude, it was decided to abandon the use of combustion in favor of high-pressure pure gas drivers.

In addition to the improvement of flow quality, it was desirable to increase the testing time by gasdynamic means. A study of more sophisticated shock tunnel designs showed that increases in testing time of an order of magnitude could be obtained. Such a large increase in testing time would permit the use of a shorter shock tube giving the same or longer test periods relatively free of attenuation effects. In this modification of the basic shock tube, the incident shock wave was reflected at the downstream end of the shock tube and the conditions of the driver and driven gas at the interface were matched ("tailored") to avoid additional waves from the interaction of the reflected shock and the interface. The wave diagram for this configuration is shown in Fig. 2 and the testing time improvements available with this modification are shown in Fig. 3.

A detailed discussion of the tailored-interface shock tunnel operation is given in Ref. 23. The tailoring condition for the helium and hydrogen driver gases are presented there as well as the corresponding test section flow conditions. Reference 23 also contains a discussion of a number of gasdynamic effects that have important bearing on the design and performance of shock tunnels and warrant special consideration.

In order to exploit the advantages of tailored-interface operation and to take advantage of the availability of high-pressure operating techniques, new driver and driven sections were fabricated capable of safe operation at pressures up to 2000 atm*. The driver tube was 14-feet long with a 3-1/2 inch inner diameter, the driven section, initially 14-feet long and later extended to 28 feet, had a 3-inch inner diameter. Located at the downstream end of the driven tube was a converging-diverging nozzle having a contraction ratio of approximately 19:1 sufficient to insure essentially complete reflection of the incident shock wave. The divergent portion of this nozzle provided a two-stage bilateral expansion. An initial expansion in the horizontal plane ended in a 1-1/2 inch by 12-1/4 inch cross section while a second expansion of 15.4 degrees half-angle in the vertical plane terminated in a test section dimension of 11 x 15 inches. The opening of the second nozzle was made variable in order to conveniently change the test section Mach number and was smaller than the exit of the primary nozzle in order to provide for significant boundary layer bleed.

The first experiments carried out in the tailored-interface shock tunnel were aimed at verifying the predicted tailoring conditions. From these tests,

---

* The tailored-interface shock tunnel development was sponsored by the U. S. Air Force Office of Scientific Research, Contract No. AF 18(603)-10.

pressure histories were recorded at several stations along the driven tube. These measurements showed a relatively constant pressure behind the reflected shock wave for a period of about 4 milliseconds. Indeed, the deviations in stagnation pressure during the useful period of a test was usually less than 2%. Also, it was observed that with shock Mach numbers differing from those theoretically predicted for tailoring, records of the same quality were obtained. Operation at Mach numbers differing from those calculated for tailoring is called "equilibrium-interface" operation as described in Ref. 6. In this latter technique of operation, it has been observed that when the deviation for the theoretically predicted tailoring Mach number is not too large, an equilibrium condition is rapidly established with the nozzle stagnation pressure remaining almost constant. If the shock Mach number is higher than that required for tailoring, somewhat higher temperatures at a somewhat lower pressure are obtained during the useful part of the run for a given driver pressure. If the shock Mach number is less than that predicted for tailoring, the stagnation temperature is reduced, but a certain degree of pressure amplification is obtained. These results indicated that small departures from ideal tailoring conditions do not impair the benefits of tailored-interface operation. In the remainder of this report the term "tailored interface" will be used to describe conditions of operation in which deviations from ideal tailored condition are not deemed significant.

Examination of the heat-transfer records under tailored conditions indicated data of much higher quality than previously obtained. However, the particle damage problem still remained severe, necessitating frequent model replacement. To avoid this particle damage, a simple deflection nozzle was inserted between the two expansion nozzles[24]. The deflector section consisted

of a two-dimensional wedge spanning the entire width of the flow and mounted at a negative angle of attack. The flow passing below the wedge turns upward 10° through a Prandtl-Meyer expansion wave. The terminal nozzle and test section were then mounted behind the wedge, also at 10° inclination. The entrance of this nozzle was thus effectively shielded from diaphragm particles which were completely centrifuged out of the flow. With this modification, no further particle damage to models has been observed. The nozzle, test section, and dump tank arrangement is shown in Fig. 4.

At the time the deflection nozzle was added, techniques for measurement of the low pressures attained in hypersonic nozzle flows had become available. With the realization of both pitot and static pressure measurements, further detailed flow calibration of the shock tunnel was possible. The calibration revealed that additional modifications to the ducting system were required to improve the bypassed air flow. Upon completion of these modifications, calibration of the test section flow with both pressure and heat-transfer instrumentation showed the shock tunnel to produce hypersonic air flows of good quality in the Mach number range 8 to 13 using helium driver gas.

However, during the early experiments with hydrogen as the driver gas and a 14-foot driven tube, it was found that the available testing time was very short. The heat-transfer data exhibited more scatter than observed in the tests using a helium driver gas. For the hydrogen-driver experiments, from 75% to 100% of the available air was theoretically utilized during the useful test flow. Thus mixing or combustion at the hydrogen-air interface reduced the available testing time. To avoid such effects, the driven tube was lengthened to 28 feet, thus doubling the amount of test air available. A considerable improvement was observed in the data obtained from subsequent hydrogen driver-gas experiments

and the data approached the quality of the helium runs. It was also noted that heat-transfer experiments with a helium driver gas gave identical data for the 14- and 28-foot driven tubes even though 60% of the available air was utilized in the first case and only 30% in the second. This result indicates that helium-air interface mixing affects less than 40% of the air under the present operating conditions.

At this stage of its development, the CAL tailored-interface shock tunnel had attained the status of a useful research facility. Operation of the 11 x 15-inch tunnel was now possible with helium or hydrogen driver gases at tunnel stagnation pressures up to 2000 atm. Flow velocities from 6500 ft/sec to 10, 500 ft/sec could be produced with stagnation temperatures ranging from 1800°K to 4200°K. For these conditions, the useful testing times ranged from 4-1/2 milliseconds at 1800°K to 3-1/2 milliseconds at 4200°K using the 28-foot driven tube.

Present CAL Shock Tunnels

In view of the success of the 11 x 15-inch shock tunnel, the Cornell Aeronautical Laboratory constructed a larger shock tunnel incorporating many of the features discussed above. This tunnel, which will be referred to as the 48-inch hypersonic shock tunnel, and is operated by the Applied Hypersonic Research Department of CAL, was built for research and developmental testing[25]. The tunnel has a driver tube 40-feet long 20 feet of which can be heated, and a driven tube 50-feet long. Both tubes have 8-inch inner diameters. The stagnation temperature range is from approximately 1000°K to 4000°K. Helium is used as the driver gas and is either mixed with air, used pure, or heated to obtain tailored-interface conditions over the above range of stagnation temper-

atures. The flow Mach number range available is approximately 6 to 18 at stagnation pressures up to 6000 psi. The test section utilizes a 24-inch diameter 10.5 degree half-angle conical nozzle for studies requiring a wide range of Mach numbers (8 to 18). Contoured nozzles to obtain rectified flow are available for Mach 8 (24-inch diameter) or Mach 16 (48-inch diameter). These nozzles can be operated also at Mach 6 and 14, respectively, by installing a larger throat. It is interesting to note that this 48-inch contoured nozzle was constructed of steel in the throat region and of fiberglas in the rectifying region*.

The 11 x 15-inch shock tunnel has been rebuilt recently to take full advantage of its high-pressure operational capability. The changes have included a new heated driver capable of heating hydrogen to 750°F and a new nozzle having a 6-foot diameter test section. The new nozzle contains two expansion stages and a flow-turning section similar to the 11 x 15-inch tunnel. The primary difference is the second-stage expansion which is a conical nozzle of fiberglas construction. This tunnel, which will be referred to as the 6-foot shock tunnel[26, 27] is described in more detail later in the report.

Having reviewed the development of the hypersonic shock tunnel at CAL, consideration will next be given to its capability in duplicating hypersonic flight conditions and discussion of scale effects. Nonequilibrium effects in hypersonic nozzle flows and in tunnel simulation will also be discussed. Following this the development and use of current instrumentation techniques will be described.

---

* Fiberglas laminate is a convenient method of nozzle fabrication for short-duration wind tunnels which do not experience large wall temperatures during the brief flow times.

SHOCK TUNNEL SIMULATION CAPABILITIES

The purpose of the following discussion is to describe the requirements for duplicating or simulating hypersonic flight phenomena, and to relate the performance capabilities of the shock tunnel to the simulation requirements. It is important that the difference between duplication and simulation be delineated. Duplication of flight conditions requires that the flight velocity and the ambient free-stream conditions of pressure, temperature, density and gas composition be identically matched and that the model and flight vehicle be of identical geometry and size. Simulation refers to testing wherein not all of the flight conditions are duplicated.

Duplication of Ambient Flow Conditions

The capability for simulating flight conditions is a matter of prime importance in any wind tunnel. Mach number, Reynolds number, and specific heat ratio are dimensionless variables of major significance in flight simulation and are commonly used to assess wind tunnel performance. However, many phenomena occurring in hypersonic flight require virtually complete duplication. This is the case, for example, when studying equilibrium and nonequilibrium real-gas effects, radiation phenomena and the interaction of electromagnetic radiation with an ionized gas. These phenomena will be discussed later.

The difficulties in duplicating ambient flow conditions at hypersonic speeds are clearly seen in Fig. 5. This figure is an altitude-velocity map in which are shown the wind tunnel stagnation or reservoir pressures and temperatures*

* In the shock tunnel the conditions behind the reflected shock wave are the stagnation conditions or reservoir conditions for the flow through the nozzle.

necessary for duplicating flight conditions assuming an isentropic expansion of real air in thermo-chemical equilibrium. The "corridor of continuous flight"[28] is also indicated (shaded area) because it represents the flight conditions likely to be encountered by a manned hypersonic vehicle. It is widely appreciated that duplication of hypersonic velocities in a wind tunnel requires stagnation temperatures up to 12,000°K. A less-publicized fact is that very high stagnation pressures are also required. For example, duplication of flight conditions below 200,000 feet altitude requires a stagnation pressure greater than 1000 atm at a velocity of 15,000 ft/sec and greater than 20,000 atm at 20,000 ft/sec.

The performance of a tailored-interface shock tunnel can be related easily to the duplication requirements for hypersonic flight. This has been done in Fig. 5 for the following operating conditions: He/Air tailoring* at an incident shock Mach number $M_s = 3.8$; H_2/Air tailoring* at $M_s = 6.2$; and 750°F H_2 tailoring with room-temperature air at $M_s = 10.5$. These conditions give test-section velocities of about 6500, 10,500 and 17,500 ft/sec, respectively. The last condition is the design point of a new heated-hydrogen driver recently installed at CAL. This driver is similar to the heated-helium driver developed by the CAL Applied Hypersonic Research Department for the 48-inch hypersonic shock tunnel.[25] Operation at shock Mach numbers above 10.5 to obtain flow velocities greater than 17,500 ft/sec can be accomplished by using the equilibrium-interface concept[6,29], by providing more driver-gas heating, or by utilizing the double driver or buffered-shock-tube technique[30,31,32]. The lower limit on altitude duplication is determined by the maximum stagnation pressure

---

*These two cases are for driver (He or H_2) and driven (Air) gases at room temperatures.

capability. This is 2000 atm for the CAL 11 x 15-inch and 6-foot shock tunnels and 400 atm for the CAL 48-inch hypersonic shock tunnel. The 2000 atm and M_s = 10.5 limits are shown in Fig. 5, cross-hatched line. This defines the flight duplication capability of the CAL 6-foot shock tunnel which extends from sea level at 6500 ft/sec to an altitude of 230,000 feet at 17,500 ft/sec. Altitudes below the 2000 atm pressure line are beyond the duplication capabilities of this tunnel, and simulation techniques must be employed.

Simulation Techniques

There are few facilities that can completely duplicate both scale and ambient flow conditions over an extended portion of the flight corridor indicated in Fig. 5. Consequently, simulation is the rule rather than the exception in wind tunnel testing. For example, under certain conditions flight Reynolds numbers can be obtained by testing scale models at high density levels, and hypersonic Mach numbers can be readily obtained using helium rather than air as the test gas because high stagnation temperatures are not required to prevent condensation[33]. Also the shock tube has been used to measure stagnation-point heat transfer at hypervelocities[11, 96] even though the flow Mach number is less than 3. This is permissible because of the Mach number independence of blunt-body flows[34].

Simulation is the technique of duplicating only the dimensionless parameters or flow conditions most intimately associated with the phenomenon being studied. For example, in boundary-layer flows, Reynolds number is generally of prime importance; in force and pressure measurements, generally the hypersonic similarity parameter $M\alpha$ (where α is the thickness ratio or angle of attack) is the governing variable; and in viscous interactions, the important

parameter is a combination of Mach number and Reynolds number, $\chi = M^3/\sqrt{Re}$. Thus each experiment requires an analysis of the flow phenomenon to determine the important parameters or conditions requiring duplication.

Mach number duplication can be obtained in a shock tunnel without having to use extremely high stagnation temperatures. For example, a Mach number of 15 can be obtained with a stagnation temperature of 2000°K by expanding the air to an ambient temperature of 50°K, as illustrated in Fig. 6. Likewise, Mach 23 can be obtained with a stagnation temperature of 4000°K. In contrast to Mach number duplication, however, velocity duplication requires much higher stagnation temperatures. To produce velocities of 15, 000 ft/sec and 23, 000 ft/sec requires stagnation temperatures of about 7000°K and 12, 000°K, respectively, as illustrated in Fig. 5.

Operation at a given stagnation temperature, or more precisely stagnation enthalpy, essentially fixes the test flow velocity in hypersonic tunnels. However, a wide range of flow Mach numbers are available because the nozzle area ratio can be varied by orders of magnitude. In Fig. 6 the nozzle area ratio for equilibrium flow is plotted as a function of Mach number for various stagnation temperatures and a stagnation pressure of 1000 atm. Along each curve the ambient temperature varies from 300°K to 50°K. The shaded area indicates the region of duplication of flight conditions and corresponds to an ambient temperature between 200°K and 300°K, the nominal temperature range of the atmosphere. The condensation limit has been conservatively taken as 50°K, though it is realized that condensation is pressure dependent and may occur at lower temperatures.

It is clear from the high stagnation pressures indicated in Fig. 5 that with small-scale models duplication of flight Reynolds numbers at hypersonic speeds

can rarely be achieved by operating at above-ambient density levels and expanding to the correct ambient temperature. However, a wide variation in Reynolds number can be obtained, even with a limited stagnation pressure capability, by controlling the degree of flow expansion. This is quite analogous to the nozzle area ratio-Mach number relationship shown in Fig. 6. For example, high Reynolds numbers can be obtained by testing at low stagnation temperatures and low Mach numbers. This is illustrated in Fig. 7, which presents Reynolds number per foot for equilibrium flow as a function of Mach number for various stagnation temperatures and a stagnation pressure of 1000 atm. Similar to Fig. 6, the region of duplication of flight conditions is taken as $200°K \leq T_\infty \leq 300°K$. Of course, the usual relation between pressure or density level and Reynolds number is also available for varying the Reynolds number. However, it will be shown in the next section that this is of limited value in hypersonic tunnels because of nonequilibrium phenomena in the nozzle flow. In general, it is necessary to operate at high stagnation pressures to avoid or minimize thermo-chemical nonequilibrium. This pressure dependence of nonequilibrium effects can be a severe limitation to low-density, low Reynolds number research at hypersonic velocities. It appears that the best way to obtain a wide range of Reynolds numbers in hypersonic flows is to operate at high stagnation pressures and to vary the stagnation temperature and flow Mach number. Thus, high Reynolds numbers can be obtained with a low stagnation temperature and low flow Mach number. Conversely, low Reynolds numbers require high stagnation temperatures and high flow Mach numbers.

The foregoing discussion has shown that stagnation pressure capability is a limiting factor in obtaining hypersonic flight duplication. With this limitation in mind, procedures for obtaining a wide range of Mach numbers and Reynolds

numbers have been considered. In all cases, however, duplication of flight velocity essentially requires stagnation enthalpy duplication. This is easily seen from the energy equation, $H_0 = H_\infty + \frac{1}{2} U_\infty^2$, by noting that at hypersonic Mach numbers the ambient enthalpy, H_∞, is small compared to the total enthalpy. Simulation of various other flow conditions, when the required stagnation pressure for duplication cannot be achieved, can be summarized as follows:

1. Velocity and ambient pressure or density can be duplicated jointly by expanding from a slightly higher than flight total enthalpy to a Mach number lower than in flight and an ambient temperature greater than in flight.
2. Velocity and Mach number can be obtained simultaneously by expanding from the exact stagnation enthalpy to the correct ambient temperature. The resulting ambient pressure and density will be lower than in flight.
3. Mach number and ambient density simulation require use of a low total enthalpy and expansion to a very low static temperature, near the condensation limit. The velocity and ambient pressure will be fractions of the flight values.
4. Unit Reynolds number simulation with duplicated ambient temperature requires expansion from a lower total enthalpy to the correct product of the velocity and density. This will mean a moderate Mach number and velocity and a higher ambient pressure and density.

These considerations, which apply to any wind tunnel and are not restricted to shock tunnels, will be illustrated with the following example.

The flight condition to be simulated is taken as a velocity of 21,500 ft/sec at 60,000 feet altitude, an extreme condition. The specific flight conditions are:

U_∞	= 21,500 ft/sec	h	= 60,000 ft.
M_∞	= 22.09	p_∞	= 0.07137 atm
T_∞	= 216.7°K	ρ_∞	= 2.256×10^{-4} slugs/ft^3
H_o	= 2.335×10^{8} ft-lb/slug	S_∞/R	= 25.42

To completely duplicate this flight condition would be impossible since the required stagnation pressure would be greater than 10^6 atm*. It is possible, however, to simulate various parameters of this flight condition. This is illustrated in the following table for a wind tunnel having a stagnation pressure capability of 2000 atm. The air is assumed to be in thermodynamic equilibrium in all cases. Note that in the third case, duplication of Mach number and density, the ambient test section temperature is 6.5°K. It is most likely that air liquefaction would occur in such an expansion. Hence, the specified Mach number and density combination cannot be properly duplicated with a stagnation pressure limit of 2000 atm.

* This is only an estimate based upon extrapolation of existing data for air. The flight conditions require a stagnation pressure beyond the range of existing Mollier diagrams for air.

TABLE I - PARTIAL DUPLICATION CONDITIONS FOR P_o = 2000 atm

Duplicated Quantities	Stagnation Conditions	Other Test Section Conditions
Velocity = 21, 500 ft/sec Pressure = 0. 07137 atm	Enthalpy = 2.73×10^8 ft-lb/slug Temperature = 10, 000°K	Temperature = 2780°K Density = 1.756×10^{-5} slugs/ft^3 Mach number = 6. 72
Velocity = 21, 500 ft/sec Mach number = 22. 09 Temperature = 216. 7°K	Enthalpy = 2.335×10^8 ft-lb/slug Temperature = 10, 050°K	Pressure = 3.668×10^{-6} atm Density = 1.160×10^{-8} slugs/ft^3
Mach number = 22. 09 Density = 2.256×10^{-4} slugs/ft^3	Enthalpy = 7.10×10^6 ft-lb/slug Temperature = 650°K	Temperature = 6. 5°K Pressure = 2.14×10^{-3} atm Velocity = 3700 ft/sec
Unit Reynolds No: $\rho_\infty U_\infty$ = 4. 850 slugs/ft^2-sec T_∞ = 216. 7°K	Enthalpy = 29.03×10^6 ft-lb/slug Temperature = 2300°K	Pressure = 0. 2090 atm Density = 6.611×10^{-4} slugs/ft^3 Velocity = 7330 ft/sec Mach number = 7. 57

It is evident that simulation techniques permit the attainment of a wide range of flow conditions even when operating at a single stagnation pressure. However, application of these techniques to obtain test results that can be related to flight conditions requires a sophisticated knowledge of the flow phenomena being studied so that the proper parameters are duplicated. Also, the state of the gas after expansion through the nozzle must be known, and nonequilibrium effects should be avoided or minimized.

Effects of High-Temperature Phenomena on Simulation

The difficulties of completely duplicating hypersonic flight conditions have been described and are illustrated in Fig. 5. The simulation techniques just discussed provide a means of testing in regions where complete duplication cannot be obtained. However, in the case of real-gas phenomena resulting from the high temperatures encountered in hypersonic flight, complete duplication may be required. The general complexity of the effects of high-temperature phenomena on the simulation of hypersonic flight conditions in a wind tunnel renders any comprehensive treatment beyond the scope of this report. However, some aspects of aerodynamic simulation will be discussed here.

The hypersonic similitude for inviscid flows over slender bodies has been treated by Tsien[35] and Hayes[36] for an ideal gas. Cheng[37] has extended this slender-body similitude to include the effects of nose bluntness and real-gas equilibrium effects. Inclusion of the latter replaces the condition of constant specific heat ratio in the ideal gas similitude by the much more stringent condition that the free-stream flows in the wind tunnel and in flight must have identical thermodynamic and chemical states; i. e., have the same pressures, densities, temperatures and chemical compositions. For the simplest case where the flight and wind tunnel bodies are geometrically similar and the flow is in equilibrium, the similitude allows a free choice of model scale. This is true for the inviscid flow only. The viscous boundary-layer flow would require equal Reynolds numbers and, hence, equal scale in addition to duplication of free-stream conditions.

Cheng[37] has also considered the extension to nonequilibrium inviscid flows about slender bodies. In this case, the free-stream flow conditions must be identical and, in addition, the flow transit time over the body must be the

same for flight and wind tunnel since the relaxation times are unchanged. If geometric similarity is preserved, these conditions require that wind tunnel and flight bodies be of equal scale. Nonequilibrium flows about slender blunt-nosed bodies have been studied by Bloom and Steiger[38] and Whalen[39]. The latter has shown that freezing can considerably alter the pressures, skin friction and heat transfer at the body surface.

For inviscid flow in blunt-nose regions, the equilibrium real-gas effects require duplication of flight stagnation enthalpy, and thus flight velocity, in addition to duplication of flight free-stream thermodynamic state and composition. In this case nonequilibrium aerody namic simulation is not generally possible unless flight and wind tunnel bodies are of equal scale.

For boundary-layer displacement phenomena, full-scale wind tunnel experiments are also likely to be necessary when studying nonequilibrium boundary layers which are particularly complex from the simulation viewpoint because of the interrelated dependence of chemical relaxation times, flow transit times, and Reynolds number on density, flow velocity, and scale.

As indicated in Fig. 5, extremely high stagnation pressures are required to duplicate free-stream conditions of flight at hypersonic speeds. If the flight density level is not achieved, the local gas composition and normalized thermodynamic variables do not duplicate the flight condition even for equilibrium flow. A sufficient mismatch in free-stream thermodynamic state can cause the simulation to fail badly. An interesting illustration of this point is shown in Fig. 8, reproduced from Ref. 37. The figure shows Cheng's similitude correlations of Feldman's calculated results[40] for the temperature of equilibrium air flow about wedges at hypersonic speeds. Correlations are shown for two altitudes (100, 000 ft. and 250, 000 ft.) for which the ambient densities differ by

a factor of the order of 200 and the ambient temperature by only about 14%. The difference in normalized temperatures behind the oblique shock wave at the two altitudes is seen to be substantial (about 34%) at values of the similarity parameter $M\alpha$ around 10. An appreciable difference (about 20%) also exists between the normalized densities[37].

In the above example the free-stream density levels differ by several orders of magnitude, and generally a much closer matching than this of tunnel and flight densities would be possible. In view of the fact that the local normalized thermodynamic variables undergo only percentage changes when the density level undergoes order of magnitude changes, it may be anticipated that moderate mismatch in density levels can be tolerated for certain problems. For example, this would appear to be the case for surface pressures when governed by Newtonian flow. This is evidenced by experimental studies of blunt-nose pressure distributions[34]. This particular behavior is not unexpected since pressure is governed by momentum changes. In the example of Fig. 8, the effect of density mismatch on the wedge pressure is almost an order of magnitude less than the corresponding effect on temperature[37].

Where the phenomena of interest are very sensitive to local chemical and thermodynamic state, as in the case of gas radiation, the density is very important. In particular, the occurrence of nonequilibrium in the flow about a body can strongly affect the local thermo-chemical state. The complex dependence of nonequilibrium processes in air on density and temperature renders any simulation at reduced scale very difficult. Even granting the characterization of complex air kinetics by individual and uncoupled species relaxation times, which is dubious as shown in the next section, the different density dependence of the various rate processes involved still remains a major diffi-

culty. Considering, for example, flow behind a normal shock wave, the density dependence of relaxation times for NO formation, molecular vibration, and dissociation are approximately as given by Logan[41]

$$\tau_{NO} \sim \rho^{-1/2} \qquad \tau_{VIB} \sim \rho^{-1} \qquad \tau_{DISSOC} \sim \rho^{-3/2}$$

Thus the flight ratio of relaxation time to a characteristic flow transit time can be maintained for only one relaxation process at other than flight density or scale. In actual fact, the kinetic situation is even much more complex than this since the relaxation times are strongly coupled. For example, those processes involving chain reactions (such as NO formation) do not scale in the same manner with pressure or density as the processes involving three-body collisions (such as recombination) except in fortuitous circumstances. In addition, electron-ion rate processes may also be an important consideration.

The scaling problem is similarly complex when studying combined radiative and convective heat transfer in regions where nonequilibrium may occur[42]. Here, not only the gas radiation, but also the reaction kinetics within the boundary layer are strongly density dependent. Several investigators have shown[43, 44] that high-altitude hypersonic flight may lead to conditions in which the boundary layer is not in thermo-chemical equilibrium. This may lead to significant reductions in convective heat transfer if the boundary layer is essentially frozen in the presence of a noncatalytic wall.

Another aspect of the complexity of real-gas scaling is involved when one considers the interaction of electromagnetic waves, such as used for communications, with the plasma sheath surrounding the body. Here, the kinetics of the ionization process and the wavelength of the electromagnetic radiation must be considered simultaneously in the scaling problem. Again experiment and flight will not scale except in certain restricted cases.

The foregoing discussion, while giving a simplified picture, serves to illustrate the need for as near a duplication of flight conditions as is possible for the study of equilibrium and nonequilibrium real-gas flows, radiation of the hot gas in the shock layer about a body, combined radiative and convective heat transfer and interaction of electromagnetic radiation with an ionized shock layer. As these problems increase in importance with the development of sophisticated hypersonic vehicles, it becomes increasingly difficult to interpret small-scale experiments. It is also clear that additional similitude studies of basic aerophysical-chemical phenomena could prove of considerable value in delineating and extending the range of useful simulation in hypersonic tunnels, particularly when use is made of recently acquired knowledge of the phenomena concerned.

Apart from the difficulty of employing full-scale models, the problem of attaining the flight density or pressure level severely limits the application of most hypersonic wind tunnels in studying the phenomena discussed above. It is worth noting that the extremely high stagnation pressures required to duplicate flight conditions, Fig. 5, can certainly be obtained more readily in a short-duration facility such as a shock tunnel or an electric-arc discharge tunnel[45] than in any other type of wind tunnel.

An additional complexity is brought into the simulation problem if the nozzle flow is not in thermodynamic and chemical equilibrium. If significant chemical freezing occurs, the duplication of flight conditions cannot be attained. The occurrence of freezing or chemical nonequilibrium in nozzle flows and the resulting effects on the test section conditions will be discussed in some detail in the next section.

NONEQUILIBRIUM PHENOMENA IN HYPERSONIC NOZZLE FLOWS

At tunnel stagnation enthalpies required to duplicate hypersonic flight conditions, significant excitation of molecular vibration, dissociation, electronic excitation, and ionization exists. Unlike translation and rotation, these modes of energy storage generally require large numbers of collisions to equilibrate to sudden changes of thermodynamic state. In the expansion of high-enthalpy air in a supersonic nozzle, where state changes are generally very rapid, it is possible that collision frequencies can be insufficient to maintain such modes in local thermo-chemical equilibrium. In this event, the state of the air after nozzle expansion to hypersonic speeds from a high-enthalpy level can be very different from the equilibrium state desired for duplication of flight conditions, both with respect to thermodynamic and gasdynamic variables as well as detailed chemical composition. In particular, if energy modes containing a significant fraction of the total enthalpy are frozen out during expansion, the test flow temperature and pressure can be drastically reduced below the corresponding equilibrium values desired.

The possible effects of such nonequilibrium phenomena on high-enthalpy tunnel performance represent a serious problem as regards duplication of equilibrium, free-stream flight conditions. While the potential importance of this problem has long been appreciated, its serious consideration has come about only recently with the actual development of high-enthalpy tunnels. Our present understanding of the problem rests almost entirely upon theoretical or numerical studies done over the past two or three years. These numerical studies have largely employed chemical-kinetic rate data obtained from shock-

tube experiments at high temperatures. As yet, comprehensive experimental studies of nonequilibrium expanding air flows have not been reported, although such studies are badly needed.

The results obtained from theoretical and numerical studies will be reviewed here with emphasis on recent work undertaken at CAL. While these results provide valuable insight into the nonequilibrium problem, they are theoretical only. The specific physical-chemical models assumed are idealized and simplified with respect to real air flow situations of interest. For example, the possible important effects of impurities which may be present are not considered. It is apparent that with our existing state of knowledge, nonequilibrium effects in any specific wind tunnel must ultimately be determined by experimental measurement.

Nonequilibrium Regimes

A useful indication of the nonequilibrium rate processes important for the gross thermodynamic and gasdynamic behavior is obtained by considering the important internal energy modes of the equilibrium reservoir air prior to expansion. The range of tunnel stagnation conditions of present interest is roughly from 2000 to 10,000°K in temperature and from 10 to 1000 atm in pressure. The higher part of this pressure range, say above 50 to 100 atm, is of somewhat greater interest because of the suppression of nonequilibrium effects at high pressures. For the above range of conditions, the detailed chemical composition and other properties of equilibrium air are available from several reports (see, for example, Refs. 46 and 47). Figure 9 illustrates the important compositional changes in equilibrium air as a function of pressure at temperatures of 4000, 6000, and 8000°K.

For sufficiently low temperatures, molecular dissociation is unimportant and molecular vibration of oxygen and nitrogen constitutes the only internal energy sink to be considered. At a temperature of 2000°K, the total vibrational energy of equilibrium air is about 0.11 H at 100 atm pressure, where H is the enthalpy. Above 2000°K, the vibrational energy increases only slightly and does not exceed about 0.13 H (at 100 atm) before dropping at high temperatures when significant dissociation of nitrogen sets in (see Figs. 9 and 10). By comparison, the total chemical energy involved in the dissociation of oxygen and nitrogen and in nitric oxide formation, is only about .01 H at 2000°K and 100 atm pressure. Above 2000°K, the total chemical energy increases rapidly with temperature due to the dissociation of oxygen, initially, and then nitrogen. At 4000°K and 100 atm, the total chemical and vibrational energies are about equal at 0.13 H. Above 4000°K the chemical energy becomes dominant, exceeding 0.50 H beyond about 9000°K at 100 atm. The foregoing trends are illustrated in Fig. 10 which shows the detailed internal energy distribution in equilibrium air at 100 and 1000 atm for temperatures from 4500 to 8000°K.

The temperature below which the chemical energy of air is small compared to the vibrational energy increases with increasing pressure. At 100 atm this temperature lies in the range from 2000 to 2500°K. To date, little attention has been given to vibrational nonequilibrium in this relatively low-temperature region where chemical effects are unimportant. This is due, in part, to the inherent greater interest in substantially higher temperatures as well as to the supposition that the maximum thermodynamic effects of vibrational nonequilibrium are quite limited because the maximum energy involved is only about 11% or less of the total enthalpy. However, it may be noted that if vibrational

energy equal to 11% of the total enthalpy is assumed to be frozen out, the effects are not exactly negligible for expansion to hypersonic Mach numbers. For example, at 2000°K the complete freezing of all vibration for expansion to a Mach number of about 12 reduces the stream pressure and temperature below equilibrium values by about 15 and 20 per cent, respectively, and increases the effective Mach number by about 6 per cent. These effects suggest that some consideration need be given to possible vibrational nonequilibrium in this regime, particularly at lower pressures since the collision frequency is proportional to density.

The extensive work of Montroll and Shuler on the relaxation of various diatomic oscillator models (see, for example, Ref. 48) provides a suitable basis for the calculation of finite-rate vibrational effects without dissociation. An important result of their work is the finding that during any relaxation process the distribution of oscillator vibrational energy remains Boltzmann-like if it is initially so, provided the collisional transition probabilities are those of Landau and Teller[49]. To date, no comprehensive experimental studies bearing on vibrational nonequilibrium in nozzle air flows have been reported; the only experimental work appears to be that of Ref. 50. This work involved measurement by sodium line reversal of the air stagnation temperature on a blunt body located in the test section of a hypersonic gun tunnel. For the relatively low stagnation temperature of about 1500°K and a stagnation pressure of 2500 psia, the results obtained suggest the possibility of substantial vibrational freezing in the nozzle expansion.

Above stagnation temperatures of about 4000°K the total chemical energy becomes so large, as previously indicated, that chemical nonequilibrium becomes the primary consideration as far as the nozzle-flow thermodynamics

is concerned. Vibrational nonequilibrium is likely to be of secondary importance in this higher temperature range, although the coupled effects of vibrational lag on the chemical rate processes involved could be of significance. Such coupling has not been included in nozzle-flow studies to date.

Ionization rate processes are likewise unimportant insofar as the nozzle air flow thermo-chemistry is concerned, at least for the present range of nozzle stagnation conditions. For these conditions, the electron and ion concentrations are very small compared to concentrations of the important neutral species (see Fig. 9). Relative to the total chemical energy, the total energy involved in equilibrium ionization of air remains very small to temperatures well beyond 10,000°K for pressures above 10 atm. Calculations of the nonequilibrium flow behind strong shock waves in air, carried out by Duff and Davidson[51] and more recently at CAL, show the ionization kinetics to have negligible influence on the kinetics of the important neutral species in the present temperature range. It is reasonable, therefore, to neglect ionization phenomena completely in considering chemical nonequilibrium in nozzle air flows.

Chemical Nonequilibrium

The critical aspect of the chemical nonequilibrium problem is the degree to which oxygen and nitrogen atoms recombine and maintain equilibrium dissociation as the dissociated air expands in the nozzle. The energy involved in dissociation is so large that a lag in atom recombination can produce substantial effects on the flow thermodynamics. As illustrated in Fig. 10, oxygen dissociation is the principal energy sink at lower temperatures, but nitrogen dissociation eventually dominates at high temperatures. The degree of atom recombination attained in the nozzle expansion depends on the chemical kinetic rate processes involved, as well as on the nozzle geometry.

The chemical kinetics of high-temperature air containing dissociated oxygen and nitrogen is complicated by the formation of small but kinetically significant amounts of nitric oxide. A number of authors (e. g. Ref. 52) have considered this problem with the object of reducing to a minimum the number of reactions needed to provide realistic kinetics of the important neutral species. There seems to be some measure of general agreement that the coupled reactions

$$(1)\quad O_2 + M \underset{k_F}{\overset{k_R}{\rightleftharpoons}} 2O + M$$

$$(2)\quad N_2 + M \rightleftharpoons 2N + M$$

$$(3)\quad NO + M \rightleftharpoons N + O + M$$

$$(4)\quad O_2 + N \rightleftharpoons NO + O$$

$$(5)\quad N_2 + O \rightleftharpoons NO + N$$

are of basic importance in the present temperature range. This picture is supported by theoretical and experimental studies (e. g. Refs. 51, 53) of the kinetics of high-temperature air flows produced behind strong shock waves.

Reactions (1) to (3), where M is any colliding body, provide atom recombination by three-body collisions. The kinetics of pure dissociated oxygen or nitrogen flows, for example, are governed by reactions (1) or (2) alone. The bimolecular reactions (4) and (5), the so-called nitric-oxide shuffle reactions, involve two-body collision processes only. Their significance lies in the fact that commonly such two-body reactions are very fast compared to the three-body recombination reactions of (1) to (3) (see, for example, Ref. 54).

The system of reactions (1) to (5) leads to a set of coupled differential equations expressing the rates of change of species concentrations as sums of

products of concentrations and temperature-dependent reaction rate coefficients (see, for example, Ref. 55). The latter are usually not well known; the determination of such coefficients is a major concern of chemical kinetics. For reactions (1) to (5), however, sufficient basic experimental data is available to provide values, or at least estimates, for the rate coefficients involved.

Calculation of the nozzle expansion of dissociated air thus entails solving a coupled system of differential rate equations simultaneously with the appropriate gas dynamics equations for specified reservoir conditions and nozzle geometry. In general, the chemical rate equations are very nonlinear and the analytic problem is intractable even for the simplest gas dynamics of pseudo-one-dimensional and inviscid flow. Resort must, therefore, be made to numerical methods. However, numerical solution for multiple reactions proves to be far from simple even with high-speed computing machines. Difficulties arise because of singularities in the rate equations at the equilibrium reservoir conditions from which forward integration must be started, and because the nozzle mass flow is unknown, a priori. Partly as a consequence of the inherent computational difficulties, most numerical studies to date of nonequilibrium nozzle flows have been confined to the simplest chemistry of a pure dissociating diatomic gas, with or without inert diluents (Refs. 56-62). In this case, only a single chemical rate equation is involved. Recently an IBM-704 computer program has been developed at CAL for handling the multiple-reaction problem in expanding flows. Before discussing recent applications of this program to nozzle airflows[63], it is instructive to review earlier studies involving a single finite-rate reaction.

A considerable body of numerical results exists for pseudo-one-dimensional nozzle flows with a single reaction[56-62]. Bray[60], as well as Hall and Russo[61], give exact numerical solutions for pure dissociated oxygen

flows where reaction (1) alone determines the kinetics. These solutions show a characteristic and important feature: the atom mass concentration is rapidly frozen, i. e. becomes constant, downstream of the nozzle throat. This results from the eventual vanishing at low densities of the three-body collisions required for recombination. In addition to exact numerical solutions, these authors also develop convenient approximate methods for determining the frozen level of dissociation in such flows on the basis of the corresponding solutions for equilibrium flow. In Ref. 61, these approximate methods are applied to a simplified kinetic model of air in which only the oxygen dissociation-recomination kinetics of reaction (1) are considered. Here, species other than oxygen atoms or molecules are considered only as inert colliders M. This approach to air is further extended in Ref. 62 to obtain results for nozzle stagnation temperatures up to 6000°K, stagnation pressures from 100 to 1000 atm, and for a wide range of nozzle shape and scale.

The approximate solutions for the simplified air model[61, 62] exhibit the same general characteristics as the pure diatomic gas case. Figure 11 shows typical results for the frozen degree of oxygen dissociation α_f, versus a nozzle geometry parameter $L/\tan\theta$. Here L is the throat radius and θ the asymptotic semi-angle of the hyperbolic, axisymmetric nozzle illustrated. Hypersonic nozzles typically have values of $L/\tan\theta$ of the order of 1 cm. The recombination rate coefficient and throat radius L occur as a product in the problem, so that the plot also illustrates the dependence on rate coefficient at fixed L.

Figure 11 shows that substantial freezing of atomic oxygen occurs at high stagnation temperatures and low stagnation pressures. The frozen level of dissociation decreases markedly with decrease in temperature and increase

in pressure. Increased pressure not only reduces the initial dissociation prior to expansion, but also delays the onset of freezing. This influence of pressure indicates the need for high nozzle stagnation pressures in order to minimize nonequilibrium effects. Fortunately, this need is compatible with that for duplication of hypersonic flight pressure levels. Another aspect of Fig. 11 is the influence of nozzle geometry. An increase in $L/\tan\theta$, produced either by an increase in throat radius or a decrease in expansion angle, reduces the frozen degree of dissociation. However, the influence of nozzle geometry is substantially less than that of pressure. As regards the location of freezing, for $L/\tan\theta$ values of the order of 1 or less freezing is complete at area ratios less than 10 for the conditions of Fig. 11. Freezing occurs earlier for decreased values of $L/\tan\theta$, stagnation pressure, and stagnation temperature.

The validity of these results, obtained for a simplified model of air which considers oxygen kinetics alone, can be assessed only by comparison with results for more complete models which include coupled reactions. In recent work at CAL, the IBM program referred to above for coupled reactions has been applied to calculate nonequilibrium nozzle airflows controlled by the complete system of reactions (1) to (5) over a wide range of stagnation temperature and pressure[63]. The results of these calculations, which are given in detail in Ref. 63, show that the nitric-oxide shuffle reactions (4) and (5) can play an important role as regards the nitrogen atom concentration under conditions where the energy of dissociation of nitrogen is significant.

In these solutions for the coupled system, the bimolecular reactions (4) and (5) depart slowly from equilibrium. The activation energies of these reactions are such that the net direction of reaction is that of removing nitrogen atoms and producing oxygen atoms. The bimolecular reaction rates are so

fast that reactions (4) and (5), rather than the three-body recombination reactions, control the freezing of atomic nitrogen. As a consequence, there is a very strong tendency for nitrogen atoms to remain equilibrated. Significant nitrogen freezing is thereby postponed to very much lower stagnation pressure levels than would otherwise be the case. In contrast, the freezing of oxygen atoms is still effectively controlled by three-body recombination.

The significance of the bimolecular shuffle reactions for the nozzle-flow thermodynamics depends on the amount of nitrogen dissociation and on the pressure or density level. Appreciable energetic effects due to these reactions require significant nitrogen dissociation energy (compared to oxygen say), and not too low pressures in order that the difference between two- and three-body collision processes be pronounced. At low stagnation temperatures and high stagnation pressures, for example in the range 4000 - 6000°K and 100 - 1000 atm, the energy of nitrogen dissociation is unimportant. Here the simplified model of air previously discussed[61, 62] gives reasonably good estimates for the frozen level of oxygen dissociation. On the other hand, at high temperatures and very low pressures, for example at 8000°K and below 10 atm, the energy of nitrogen dissociation is very large. However, here the density level is so low that even the bimolecular reactions are not sufficiently fast to prevent almost immediate freezing of atomic nitrogen.

Between the above two extremes lies a range of intermediate stagnation conditions, important for hypersonic shock tunnel operation, where the energy of nitrogen dissociation equals or exceeds that for oxygen, and where the pressure is sufficiently high that the shuffle reactions play a very significant role. At these conditions, the present solutions for the coupled system[63] show that the shuffle reactions prevent freezing of the large amount of energy due to

dissociation of nitrogen which would otherwise be frozen out on the basis of three-body recombination. This is illustrated in Fig. 12, reproduced from Ref. 63, which gives species mass concentrations versus nozzle area ratio for the exact coupled-reaction solution at a stagnation temperatue of 8000°K and a stagnation pressure of 100 atm. Here, the energy due to dissociation of nitrogen before expansion exceeds that of oxygen, being about 25% of the stagnation enthalpy. It is seen from Fig. 12 that, whereas oxygen atoms freeze almost immediately at their reservoir concentration, the fast shuffle reactions delay the freezing of nitrogen atoms until their concentration is less than one percent of the reservoir value. Thus, the bimolecular reactions permit the energy due to nitrogen dissociation to be fully recovered in the nozzle expansion, whereas with three-body recombination, it would be almost completely frozen out. In this intermediate regime, the shuffle reactions are thus important as regards the nozzle-flow thermo-and-gas-dynamics. Simple models of air which neglect these reactions in this regime can lead to large errors.

The detailed results of Ref. 63 for coupled reactions verify the validity of previous simplified kinetic models[61, 62] for airflows where the dissociation of nitrogen is energetically unimportant. In addition, these results indicate how such models may be extended with respect to detailed chemical composition (e. g. N, NO, and O_2, say) and to high temperatures where nitrogen dissociation is energetically important.

Ionization Nonequilibrium

In hypersonic flow studies concerned with electromagnetic phenomena, the free-electron concentration in the nozzle airflow can be important. As previously mentioned, the energy stored in ionization is very small over a wide range of nozzle stagnation conditions for air, so that the electron-ion

kinetics exert negligible influence on the flow thermodynamics. This fact facilitates solution of the electron-ion rate problem. The rate equations governing electron-ion kinetics can be solved for a thermodynamic and gasdynamic history predetermined from consideration of chemical nonequilibrium alone.

The CAL computer program, previously discussed for the numerical solution of expanding flows with arbitrary coupled rate processes, has not yet been applied to the ionization problem. In lieu of exact numerical solutions, the approximate calculation methods developed for chemical nonequilibrium in nozzle airflows[61] have been carried over to ionization nonequilibrium by Eschenroeder and Daiber[64, 65] to estimate the freezing of electron mass concentration. The main source of electrons in high-temperature air, at least up to 8000°K, is nitric oxide because of its low ionization potential. The calculations of Ref. 64 consider only nitric oxide to be ionized, and assume the electron concentration to be determined by the kinetics of the two reactions:

$$M + e^- + NO^+ \rightleftharpoons NO + M$$

$$e^- + NO^+ \rightleftharpoons N + O$$

which are believed to dominate. The first reaction is the classical Thomson recombination by three-body collision, analogous to the three-body recombination of atoms. The second reaction, termed dissociative recombination, provides a two-body collision path for recombination. Here the recombination energy is taken up in dissociation of the nitric oxide molecule and in translation of the atoms.

For the above reactions, a rate equation governing the electron concentration can be written. In the work of Refs. 64 and 65, this rate equation was solved by approximate methods for nozzle airflows at stagnation temperatures of 4000 and 8000°K and stagnation pressures of 100 and 1000 atm. The local

thermo- and gas-dynamic state of the flow was taken to be that for chemical equilibrium, and the electron and gas translational temperatures were assumed equal. Calculations were made of the initial departure from electron equilibrium and of the electron mass concentration frozen out for a wide range of axisymmetric, hyperbolic nozzle geometries[65].

The results of these calculations for airflow ionization nonequilibrium show electron freezing to occur in a manner qualitatively similar to atom freezing in the case of chemical nonequilibrium. The electron mass concentration freezes out relatively quickly in the nozzle expansion. In general, electron freezing precedes any significant departure from chemical equilibrium. As with chemical nonequilibrium, increased pressure and nozzle scale and decreased temperature reduce nonequilibrium effects. With ionization, the difference between two-body (dissociative) and three-body recombination is not nearly as marked as in the chemical case. This is because inelastic energy transfer between the electron and the NO ion substantially increases the effectiveness of three-body recombination. Also, the effect of nozzle scale is much more pronounced in the case of electron freezing.

On the basis of the results for electron freezing, Ref. 65 gives calculated electron densities for the test airflow of a hypersonic shock tunnel. Over a wide range of tunnel scale and stagnation conditions, the test-section electron density has rather limited variation. Attenuation of electromagnetic radiation by the test flow was also considered. Calculated results here show that waves of frequencies greater than about 1 KMC are essentially unattenuated for unseeded airflow over a wide range of tunnel conditions.

Effects of Free-Stream Nonequilibrium on Hypersonic Testing

The foregoing sections have considered various regimes and aspects of the general problem of nonequilibrium airflow in hypersonic nozzles. Recent calculation studies, as those discussed for coupled chemical reactions (Ref. 63), provide a sounder basis than hitherto attained for considering the important question which remains. This question, of course, is that of the importance of nonequilibrium in the ambient hypersonic airflow to the duplication or simulation of local flow fields generated about hypersonic bodies in flight through an equilibrium atmosphere.

Nonequilibrium in the free stream will affect both the detailed chemical composition and the gross aero-thermodynamic characteristics of the body flow-field. Considering aerodynamic effects first, it is useful to look at the quantitative departures from equilibrium in the thermodynamic variables of the hypersonic test airflow on the basis of the solutions for coupled reactions of Ref. 63. Table II, reproduced from Ref. 63, lists the ratios of actual to equilibrium values of the thermodynamic and gasdynamic test-section variables for air expansions from 6000 and 8000°K at nozzle stagnation pressures of 100 and 1000 atm. The nozzle geometry is hyperbolic axisymmetric with $L/\tan\theta = 1$ cm. At each set of stagnation conditions, the area ratio of the expansion is that giving an equilibrium Mach number of 20. It may be noted that the tabulated ratios are only weakly dependent on the expansion ratio so that the results are representative of an appreciable range of equilibrium test Mach number.

While the nitric-oxide shuffle reactions essentially eliminate the problem of nitrogen freezing except at very low stagnation pressures, they have essentially no effect on oxygen freezing and this problem still remains. The chemical energy frozen out, H_F, is seen from Table II to be a substantial part of the

TABLE II - RATIOS OF ACTUAL TO EQUILIBRIUM AIRFLOW VARIABLES FOR COUPLED-REACTION EXPANSIONS GIVING EQUILIBRIUM MACH NUMBER 20

L/tan θ = 1 cm.

T_o	6000°K		8000°K	
P_o	100 atm.	1000 atm.	100 atm.	1000 atm.
H_F/H_o	.155	.048	.194	.0813
p/p_{EQ}	0.425	0.875	0.159	0.544
T/T_{EQ}	0.359	0.855	0.121	0.497
ρ/ρ_{EQ}	1.095	1.014	1.110	1.045
U/U_{EQ}	0.913	0.987	0.901	0.957
M/M_{EQ}	1.455	1.06	2.30	1.305
$Re_x/Re_{x_{EQ}}$	2.79	1.17	8.25	2.01

total enthalpy H_o at high temperatures and low pressures. Essentially all of H_F is frozen dissociation energy of oxygen; that of nitrogen is negligible. As a consequence of freezing, the flow temperature and pressure are drastically reduced below equilibrium values. Effects on flow density and velocity, which are increased and decreased respectively by nonequilibrium, are substantially smaller than on temperature and pressure. As a result of the large reduction of temperature, the test-flow Mach number defined by

$$M = U \Big/ \sqrt{\frac{d\rho}{dx} \Big/ \frac{dp}{dx}}$$

and in particular the test-flow Reynolds number, are greatly increased over the equilibrium values.

The previous remarks on the significant advantage of operation at high-pressure levels in order to suppress nonequilibrium effects are further emphasized by Table II. At 1000 atm stagnation pressure, nonequilibrium effects are greatly reduced compared with those at 100 atm.

The effects of free-stream nonequilibrium on the aerodynamics of the body flow field have received some consideration in Ref. 60 for the stagnation region of blunt bodies in pure oxygen flows. Here, numerical calculations were carried out for the equilibrium stagnation point flow on a blunt body over a wide range of oxygen freezing in the free stream. The results indicate relatively limited effects on the equilibrium stagnation point quantities. Even for complete freezing giving H_F/H_o of the order of 0.60, stagnation point heat transfer, pressure and density are reduced by only about 20 to 25% from values for an equilibrium free stream. Shockwave standoff distance and shape, however, are more strongly affected. Because of the density increase in the free stream and the consequent density decrease behind the bow shock compared to equilibrium-flow values, the density ratio across the shock can be affected appreciably. For complete equilibrium behind the shock, the standoff distance is thereby increased as compared to that for an equilibrium free stream. Far from the body where the shock wave is weak, the shock angle is reduced from equilibrium free-stream values because of the increase in effective stream Mach number.

In hypersonic airflows, the aerodynamic effects of free-stream nonequilibrium on equilibrium stagnation-point flows may likewise be expected to be relatively small. For hypersonic conditions the stagnation pressure p_o' behind a normal shock wave is approximately $\rho_\infty U_\infty^2$, regardless of real-gas phenomena. The product $\rho_\infty U_\infty$ is very little affected by nozzle-flow nonequilibrium.

Thus the free-stream nonequilibrium effect on pitot pressure is essentially that on stream velocity U_∞ . Reference to Table II shows that nonequilibrium effects on U_∞ are quite small, less than about 10% for all conditions tabulated. For large expansions where the stream temperature is very low, the departures from equilibrium are given approximately by:

$$\frac{p_0' - p_{0_{E2}}'}{p_{0_{E2}}'} \simeq \frac{U - U_{E2}}{U_{E2}} \simeq \frac{1}{2} \frac{H_F}{H_0}$$

assuming H_F/H_0 is small. The equilibrium stagnation state is determined by any two thermodynamic quantities, in particular by H_0 and p_0' . Since H_0 is fixed for an adiabatic flow, and since free-stream nonequilibrium effects on p_0' are small, the equilibrium stagnation state, in general, cannot be greatly affected by departures from free-stream equilibrium. Assuming local equilibrium flow to prevail, the above conclusion can be extended to include the surface flow a short distance away from the stagnation point on the basis of Newtonian flow concepts.

Whereas the surface aerodynamic characteristics of the immediate stagnation zone on a blunt body are only weakly dependent on free-stream nonequilibrium, the same is not generally true for the downstream flow fields of slender bodies. This is demonstrated by the calculations of Ref. 39 for the inviscid and viscous aerodynamic characteristics of various slender bodies in frozen hypersonic flows. The results of these calculations show the similitude for surface heat transfer, pressure, and lift to fail badly when appreciable enthalpy is frozen in the nozzle expansion process. Further studies of problems in this class, which are generally much more complex than the stagnation-point case, are needed to fully elucidate the effects involved.

The foregoing discussion has been concerned only with the aerodynamic consequences in the body flow field of free-stream nonequilibrium. Of course, the detailed chemical composition about the body will also be affected. At and near equilibrium stagnation points, the foregoing arguments indicate that chemical composition will generally be little changed. However, nonequilibrium rate processes in the shock layer flow may be very strongly affected, since the chemical boundary conditions immediately behind the shock envelope may be very different from those for an equilibrium free stream. Thus free-stream nonequilibrium could have substantial effects on the chemical composition of much of the shock layer flow. Studies of such effects are needed as they would likely be important for consideration of radiation and ionization phenomena.

INSTRUMENTATION TECHNIQUES

The collection of accurate data under high-temperature, high-velocity and millisecond-long test conditions imposes special requirements on the measuring and recording instruments. Cathode-ray-tube oscilloscopes have been available since the conception of the shock tunnel, so that adequate recording instrumentation has never been a real problem. On the other hand, during the early years of the shock tunnel, adequate measuring instrumentation did not exist. It was necessary to devote a considerable effort to instrumentation development concurrent with the shock tunnel program in order to exploit the potentiality of this tunnel as a research tool. In 1953, a CAL-sponsored internal research program was undertaken to investigate the feasibility of instrumenting models for testing in a hypersonic shock tunnel. It was concluded from

this study that suitable techniques could be developed for measuring forces, pressures, and heat-transfer rates. In particular, it was decided that force and heat-transfer instrumentation were in the greatest need of development. Some commercial pressure transducers already appeared promising, and further development of pressure instrumentation was being carried on by several companies. As a result of the conclusions reached in this study, the U. S. Air Force, through the Wright Air Development Center*, sponsored a program to develop force and heat-transfer instrumentation. This program produced a successful accelerometer force balance and the widely used thin-film resistance thermometer for heat-transfer measurements[18]. In recent years, further instrumentation development has been performed by CAL's Applied Hypersonic Research Department as an internal research program. This development has produced small sensitive piezoelectric-crystal pressure transducers, strain-gauge and piezoelectric-crystal force balances, and a dynamic stability testing technique.

In the following sections the techniques used for heat-transfer, pressure and force measurements, optical studies, and a newly developed method for dynamic stability measurement will be described. Instrumentation development has advanced to the status where the shock tunnel is capable of many types of aerodynamic studies requiring force, pressure, heat-transfer or static and dynamic stability measurements. Future developments should serve to extend the range of application and convenience of use of the present instrumentation.

Heat Transfer Instrumentation

The measurement of heat-transfer rates in the shock tunnel relies on sensing the transient surface temperature of the model[18]. The early CAL in-

* Contract No. AF 33(616)-2387.

ternal research program found only one commercial temperature transducer[66] suitable for sensing rapid surface temperature changes. However, this instrument, which was developed for gun barrel temperature measurements, was not entirely suitable for shock tunnel application because of its low sensitivity. The lack of suitable temperature transducers led to the development* of the thin-film resistance thermometer which has been described quite thoroughly in Refs. 18, 67 and 68. This instrument consists of a thin-metallic-film resistance thermometer mounted on an insulator. The thermometer measures the surface temperature of the insulator, and the one-dimensional theory of heat conduction in a solid is used to relate the surface-temperature history to the heat-transfer rate[18]. The short test time in the shock tunnel eliminates the need for corrections for axial and circumferential heat conduction effects.

At CAL the thin-film thermometers are sprayed on fused quartz or Pyrex glass using Hanovia 05-X platinum paint**. After spraying, the model is placed in an oven and baked. Details of the technique have been described in Refs. 18 and 67. This procedure produces a durable platinum alloy film that is about 0.1 micron thick. The films can be placed on models that are made entirely of fused quartz or Pyrex glass or on small inserts that are mounted in metal or plastic models. Other research groups have used evaporated or sputtered techniques for producing similar resistance thermometers[69, 70]. The thin-film thermometers have proven capable of measuring heat-transfer rates from less than 1 BTU/ft^2-sec to more than 1000 BTU/ft^2-sec. Recently, Vidal and Golian

---

* Air Force Contract No. AF 33(616)-2387 with the Wright Air Development Center

** This paint is available from the Hanovia Chemical and Manufacturing Company of East Newark, New Jersey.

have succeeded in measuring a heat-transfer rate of 0.02 BTU/ft^2-sec with a 5% noise level through the use of a very low-noise amplifier ahead of the analog network described later in this section.

A recent improvement* in gauge construction has been the addition of a thin dielectric coating over the metallic film to insulate it from an ionized gas stream[71]. The coating consists of an evaporated silicon-monoxide film about 800 to 1000 Å thick which is heated in an oven to convert it to silicon-dioxide, a better insulator. This insulates the gauge from an ionized gas without impairing its thermal response. This coating permits accurate heat-transfer measurements to be made in regions where the gas is highly ionized and its conductivity is high enough to affect the signal of an uncoated gauge by producing a short circuit.

A further development in thin-film thermometry has resulted from a study of the effect of surface catalysis on heat transfer at hypersonic speeds**. This study required a technique of applying a thin metal foil over the silicon-dioxide coating with no electrical contact to the thin-film thermometer. Foils of gold (0.1 μ thick), silver (0.15 μ), palladium (≃ 0.15 μ), and nickel (≃ 1.0 μ) have been applied directly over the silicon dioxide using a gelatin-water solution[71]. The rise time of these doubly-coated thin-film gauges has been measured as 4 μ-sec compared to 2 μ-sec for a silicon-dioxide coated gauge and about 1 μ-sec for an uncoated gauge.

The surface-temperature history measured by the resistance thermometer is related to the heat-transfer rate according to the equation

---

* Development supported by AFOSR, Contract No. AF 18(603)-141.

** Supported by AFOSR, Contract No. AF 18(603)-141.

$$q(t) = \frac{1}{2}\sqrt{\pi k \rho c}\left\{\frac{T(t)}{\sqrt{t}} + \frac{1}{\pi\sqrt{t}}\int_0^t \frac{\sqrt{\tau}\,T(t) - \sqrt{t}\,T(\tau)}{(t-\tau)^{3/2}}\,d\tau\right\}$$

where $q(t)$ = heat-transfer rate

k = thermal conductivity

ρ = density

c = specific heat

} of the dielectric backing material

$T(t)$ = surface-temperature history

t = time

τ = time variable of integration

This equation is derived from the theory of one-dimensional heat conduction and contains the assumptions that the resistance thermometer has negligible heat capacity and that the model is a semi-infinite slab[18]. Analysis has shown these assumptions to be valid for the 0.1-micron-thick gauges mounted on quartz or Pyrex glass during the short test periods occurring in the shock tunnel[18].

Data reduction, utilizing the above equation, has been performed on a high-speed computer (IBM 704) for several years. Recently, an analog network has been devised, under CAL internal research sponsorship, to perform this data-reduction calculation[72]. During a test the thin-film thermometers are operated at a constant electrical current (about 5-20 ma) so that as the resistance changes with surface-temperature variations, a transient voltage appears across the gauge proportional to the change in temperature. Previously, this voltage was amplified, recorded and interpreted as the surface-temperature history. Now, the voltage is applied to the input of the analog network, and the voltage output, which is proportional to the heat-transfer rate, is recorded.

Several research investigations in which the thin-film resistance thermometers have been used to measure local heat-transfer rates on models in the hypersonic shock tunnel will be described in the next section, Research Applications.

Pressure Transducers

During a typical shock tunnel test, it is customary to measure pressures in the driver and driven tubes and in the test section. These pressures may range from 2000 atm in the driver to 10^{-3} atm in the test section -- a factor of 10^{6} difference. The problem is further complicated by the need for some of the transducers to have microsecond response during millisecond test durations. In addition, the pressure transducers must be insensitive to temperature changes and accelerations. As indicated previously, in the early phases of instrumentation development it was hoped that commercial pressure gauges which met the shock tunnel requirements would become available. To a large extent, this hope has been fulfilled, and a variety of pressure transducers are presently available which fulfill the shock tunnel needs. The transducers in current use at CAL to measure pressures in the various sections of the shock tunnel are listed in the following tables.

TABLE III - DRIVER TUBE AND STORAGE RESERVOIR PRESSURE

Make:	Baldwin-Lima-Hamilton	Foxboro
Model:	"STD" Pressure Cell	(Part of Control System)
Type:	Strain Gauge	Helical Bourdon Tube
Range:	0-20,000 psi 0-50,000 psi	0-40,000 psi
Sensitivity:	7 mv Full Scale	15 psi Full Scale
Recorder:	Brown Recording Potentiometer	Foxboro Pen Chart

The Baldwin-Lima-Hamilton pressure cells are used to measure pressure in the storage reservoirs and are read and recorded on a Minneapolis-Honeywell Brown self-balancing potentiometer. The Foxboro pressure cell is part of a system that automatically controls the loading of the driver and the chamber between the two diaphragms. This system contains a pressure transmitter unit which sends a low-pressure signal (3-15 psi) to a Foxboro pen-and-ink recorder.

TABLE IV - DRIVEN TUBE PRESSURE*

Make:	Norwood	Kistler	Kistler
Model:	Model 104	PZ-6S	PZ-14 (SLM)
Type:	Strain Gauge	Piezoelectric Crystal	Piezoelectric Crystal
Range:	0-30, 000 psi	0-5000 psi	0-3000 psi
Sensitivity:	0. 75 μv/psi	0. 5 μμ coul. /psi	0. 4 μμ coul. /psi
Natural Frequency:	45, 000 cps	200, 000 cps	50, 000 cps
Size:	1 inch O. D. 2-1/2 inches long	1/4 inch O. D. 1/2 inch long	5/8 inch O. D. 2 inches long

These transducers are used to measure the pressure behind the incident and reflected shock waves in the driven tube with the Kistler gauges being used at pressures below 5000 psi and the Norwood at higher pressures. All three transducers have proven to be quite reliable. The PZ-6 is considerably smaller than the other two and has the fastest rise time; however, it has been found that the calibration tends to change with time, more so than the PZ-14. Also, the

* Initial pressure of the test gas in the driven tube is measured with various bourdon-tube gauges and manometers. The transducers listed here are used to measure pressure behind the incident and reflected shock waves.

PZ-6 is somewhat more temperature sensitive than the PZ-14. Both the PZ-14 (SLM) and the Norwood are easier to mount than the PZ-6, and only the Norwood is suitable for measuring pressures above 5000 psi. These transducers are shock-mounted in the driven tube to isolate them from accelerations arising from recoil of the shock tube and the elastic wave traveling down the tube.

TABLE V - TEST SECTION PRESSURE*

Make:	Altec-Lansing	CAL	CAL
Model:	21 BR-200-2 21 BR-180-2	BT	PZT
Type:	Capacitive Microphone	Barium-Titanate Crystal	Lead Zirconate-Lead Titanate Crystal
Range:	0-3 psi 0-0.3 psi	0-10 psi	0-1.0 psi
Sensitivity:	1.4 v/psi 6.9 v/psi	0.15 v/psi	2 v/psi
Natural Frequency:	12,800 cps 10,000 cps	9000 cps	10,000 cps
Size:	11/16 inch O.D. 3 inches long	1/2 inch O.D. 1/8 inch thick	1/2 inch O.D. 1/8 inch thick

Test section static pressure is measured on the tunnel sidewall with the Altec-Lansing microphone. The microphone is modified for use as a pressure transducer by the addition of a perforated plate over the diaphragm and by sealing the bleed hole in the case. It is necessary to shock-mount this transducer because of its acceleration sensitivity. Although the Altec-Lansing microphone possesses a high-pressure sensitivity (6.9 v/psi), it is relatively large (11/16 inch OD by 3 inches long with the cathode-follower base) and not readily usable

* The initial pressure in the test section prior to a run is in the range of 1 to 100 microns Hg abs. and is measured with Pirani or McLeod gauges. The transducers listed here measure static, pitot, and model surface pressures during a test run.

in small models. Consequently, CAL's Applied Hypersonic Research Department undertook the development of small piezoelectric crystal transducers. The characteristics of two transducers now in use have been quoted in Table V. These pressure gauges are 1/2 inch in diameter and 1/8 inch thick. Their small size makes them well suited for model instrumentation, and even smaller transducers (3/8 inch diameter) are under development. An interesting feature of the CAL pressure transducers is the incorporation of a duplicate crystal and diaphragm within the gauge to provide acceleration compensation. A general description of these gauges is given in Ref. 73. Measurements made in the CAL shock tunnels with these transducers have proven their capability. The barium-titanate transducer has been used extensively to measure pitot pressures during tunnel calibration tests. Also, a flat-plate model, instrumented with both types of transducers, has been tested as part of a study of hypersonic flow over a flat plate. Typical results are presented in the section on Research Applications.

Force Measurements

Force balance systems for shock tunnel application share with pressure transducers the requirement of high sensitivity and fast response time. The need for a relatively high natural frequency can best be met by using a stiff, lightweight model and a stiff balance. Stiff balances, however, often produce large interactions from the various forces. Consequently, more flexible balance designs are generally used to reduce interaction effects.

The first successful force measurements made at CAL[67] were on a cone model using an accelerometer balance system[18], developed under the WADC program* mentioned previously. This system consisted of a lightweight model

* Air Force Contract No. AF 33(616)-2387.

instrumented with accelerometers mounted parallel and perpendicular to the cone axis to measure axial force, normal force and pitching moment. The model was very lightly supported from the sting to provide a small amount of unrestrained motion during which the accelerations are measured.

Recently, under an internal research program, the CAL Applied Hypersonic Research Department has been developing force balances using strain gauges and piezoelectric crystals as the sensing elements[73]. A "compensated" balance utilizing a combination of strain gauges and accelerometers has been built. The accelerometer signals are used to "correct" the strain gauge outputs for inertial loads and produce a resulting signal proportional to the aerodynamic forces. An analog computer network has been developed to do this. Crystal balances have been developed for various configurations and geometries. One of these is a six-component crystal balance. This balance has a 0.75 inch diameter, is 2.5 inches long and has a typical sensitivity to drag force of about 0.8 v/lb. The crystal balances have wider dynamic range than strain gauge balances and better meet the wide variation of loads inherent in hypersonic tests.

Typical force-measurement results from tests of a hypersonic aircraft configuration, utilizing an early three-component, barium-titanate crystal balance, are shown in Fig. 13. These tests were run in the CAL 24-inch shock tunnel at Mach 8.

Static and Dynamic Stability Testing

The development of fast response instrumentation techniques suitable for shock tunnel application has now been extended to the field of static and dynamic stability testing. Early work in this field was done by the group under Slawsky

at NOL[74] using a free-flying model technique, to obtain both force and stability data. This method has also been used by the GE-MSVD group[75] and by the CAL 48-inch shock tunnel group. The procedure consists of supporting a model of small moment of inertia in the test section by fine threads. Free flight occurs as the initial air flow breaks the supporting threads. The motion of the model during the test is then recorded by high-speed schlieren photography. The static derivative C_{M_α} may be obtained from the observed frequency of oscillation in pitch and the dynamic derivatives $\left(C_{M_q} + C_{M_{\dot\alpha}}\right)$ from the logarithmic decrement of the oscillation. In addition, lift and drag coefficients may be obtained by doubly differentiating the vertical and axial displacements of the model to determine accelerations.

The free-flight method is straightforward in principle and has been used successfully at NOL, GE-MSVD and CAL. However, the development of force balances at CAL has provided an alternate means of obtaining force and static stability data. In applying the free-flight technique to the determination of dynamic stability measurements, some practical limitations are encountered. To obtain a sufficiently accurate decrement for a damping measurement, several cycles of oscillation are desirable. The number of cycles in a given time interval is proportional to $\left[\left(\frac{C_{M_\alpha} q_\infty}{d^2}\right) t^2\right]^{1/2}$, assuming the model mass is proportional to d^3. Hence, it is desirable to have a high dynamic pressure, long testing time, and a small model. On the other hand, the streamwise displacement due to drag is proportional to $\left(\frac{C_D q_\infty}{d}\right) t^2$, again assuming $m \sim d^3$. Since, in any given shock tunnel, there is limit to the amount of streamwise displacement allowable, there are practical upper limits on $q_\infty t^2$ (the product of the dynamic pressure and the square of the flight time) and, therefore, on the number of cycles possible. Decreasing the model size per-

mits increasing $q_\infty t^2$, provided streamwise displacement does not become greater than the test section length or field of view of the camera. However, decreasing the model size decreases the Reynolds number, which may be undesirable.

As a result of internal research studies at CAL utilizing the 48-inch hypersonic shock tunnel, it was concluded that the free-flying model technique may be well suited for determining the static derivative C_{M_α} , but that it has severe limitations in determining the dynamic derivatives, $(C_{M_{\dot{q}}} + C_{M_{\dot{\alpha}}})$. To overcome these difficulties a flexure-pivot technique has been developed by the CAL Applied Hypersonic Research Department under an internal research program[73]. The restrictions imposed by the streamwise displacement may be removed by restraining the model in this degree of freedom. The model is mounted on a stiff flexure pivot having a natural frequency considerably greater than that of the free model. The static derivative is then determined from the difference in natural frequency for wind-off and the actual test, and the dynamic derivative from the difference in decrements. The flexure pivot is instrumented with strain gauges to measure the frequency of the oscillatory model. During a test, the model, mounted on the flexure pivot and sting support, is cocked to an initial angular displacement and released just before the air flow hits the model. In this manner, wind-off and test data are determined during the same run.

The advantages of this method are: more cycles of oscillation occur during the test time permitting determination of both static and dynamic pitching derivatives; data may be obtained more simply and more accurately from the strain gauge output than from interpretation of photographs; there is a lesser degree of restriction on model size; there is more versatility in tunnel oper-

ation (i.e., variation of Reynolds number, etc.); the model is not destroyed each run. The disadvantages are that: accurate results depend on accurate calibration; the method gives $(C_{M_{q'}} + C_{M_{\dot{\alpha}}})$ but does not separate them since the model is rotating about a fixed point. On the whole, it appears a more attractive technique for obtaining static and dynamic stability derivatives.

The technique has been used in a series of tests on a family of cones at Mach 12, a Reynolds number per foot of 1.2×10^6 and a stagnation temperature of 1800°K in the CAL 48-inch hypersonic shock tunnel. Conical models were used so that the results could be compared with theoretical predictions. Cones of 15°, 22.5° and 30° half-angle were tested with the center of rotation of 50% of the cone length, and the 22.5° cone was tested with the center of rotation at 40% and 60% also. The results for C_{M_α} and $C_{M_{q'}} + C_{M_{\dot{\alpha}}}$ are presented in the following table along with coefficients obtained by Newtonian theory.

TABLE VI - RESULTS OF CONE STABILITY TESTS

		C_{M_α}			$C_{M_{q'}} + C_{M_{\dot{\alpha}}}$		
θ_c	$X_{c.g.}/L$	Newtonian	Modified Newtonian	Experiment	Newtonian	Modified Newtonian	Experiment
15°	0.5	-0.400	-0.438	-0.44	-0.205	-0.224	-0.30
22.5°	0.4	-0.650	-0.692	-0.74	-0.378	-0.402	-0.40
22.5°	0.5	-0.479	-0.511	-0.54	-0.265	-0.282	-0.31
22.5°	0.6	-0.309	-0.329	-0.25	-0.186	-0.198	-0.16
30°	0.5	-0.583	-0.612	-0.53	-0.375	-0.393	-0.35

The theoretical results have been calculated from Newtonian theory using the general equations of C_{M_α} and $C_{M_{q'}} + C_{M_{\dot{\alpha}}}$ given by Tobak and Wehrend[76]. The modified Newtonian theory was based on the work of Linnell and Bailey[77]. Although the agreement is not uniform for all cases, the results are very en-

couraging and indicate the method is a significant contribution to shock tunnel technology.

Schlieren Methods.

Standard schlieren techniques are used in the CAL shock tunnels. Single-shot pictures are taken using a spark light source having an extremely short duration, about 0.1 microsecond. High-speed schlieren movies are taken using a continuous light source and Fastax or Fairchild cameras. Such movies are valuable for studying flow establishment as well as in the stability experiments previously described.

An innovation at CAL is a high-speed, multiple-spark light source[78]. This light source, developed under CAL internal research sponsorship, consists of five individual spark sources mounted in a series, each separated by a lens assembly. In this system each spark is focused on the spark gap ahead of it and, hence, finally on an external prism which transmits the light to the schlieren system. When used in conjunction with a drum camera, this light source permits the taking of five schlieren photographs during a test at preselected time intervals. An added advantage of this system and the drum camera is that the luminosity frequently present during the flow process does not fog the schlieren picture. Initially, a rotating-drum camera was used[78] with this light source. The drum speed of this camera limited the usefulness of the light source by requiring small images when using short time delays between sparks. Recently, a CAL-built rotating-prism camera was adapted to the schlieren system. This camera, having an air-turbine driven prism, does not have the speed limitation of the rotating-drum camera.

Flow Calibration

Calibration of the test flow in the CAL shock tunnels is based on sidewall static-pressure measurement and pitot-pressure surveys. In addition, flow angularity has been determined from heat-transfer measurements on slender wedges[79] and a slender cone[80].

The calibration of the 11 by 15-inch shock tunnel is an example of this technique and is reported in Refs. 79, 80, 81 and 82. Typical calibration results are shown in Fig. 14, where the Mach numbers obtained from the sidewall static pressure and a pitot pressure rake are shown as a function of time for stagnation pressures of 1030 psi and 4350 psi. At the lower pressure the flow Mach number has a value of 11.25 ± 0.2 and shows little variation across the flow. At the higher stagnation pressure, a centerline Mach number of about 12.3 ± 0.1 is obtained from the pitot pressure measurement while the static pressure indicates a Mach number of 12.0 ± 0.1. Away from the centerline, the Mach number drops to 11.75 ± 0.1. Thus the thicker nozzle wall boundary layer at the lower stagnation pressure compensates quite well for the diverging nozzle walls producing fairly uniform flow. On the other hand, at the higher stagnation pressure, the boundary layer is thinner; the flow Mach number is higher; and there is gradient across the flow as would be expected in a wedge nozzle.

Measurements of local pitot pressure and flat-plate heat transfer (at a fixed point on the plate) at different longitudinal stations on the nozzle centerline have indicated very small longitudinal gradients over a distance of three to four inches in the test region used. The maximum Mach number gradient is estimated to be less than 0.1 per inch.

Flow angularity has been determined in the pitch and yaw planes of the 11 by 15-inch shock tunnel with a multiple-wedge rake instrumented for heat-transfer measurements on the upper and lower surfaces of the wedges[79]. These measurements indicated a varying angularity in the pitch plane as would be expected in a wedge-shaped nozzle. Also, a small relatively constant angularity was found in the yaw plane (the plane of symmetry of the nozzle). Additional information on the flow angularity in this nozzle has been obtained from the results of heat-transfer studies of a yawed slender cone[80]. The cone results indicated a net angularity of 1 degree on the nozzle centerline with components of -0.8 degrees in the pitch plane and 0.6 degrees in the yaw plane. These values are in good agreement with the data obtained from the multiple-wedge rake. The centerline angularity in the pitch plane can be attributed to boundary-layer growth on the flow-turning wedge. The yaw-plane angularity results either from the primary nozzle or a slight misalignment of the various nozzle sections.

RESEARCH APPLICATIONS

To illustrate the application of the shock tunnel to hypersonic research, several investigations conducted in the CAL 11 by 15-inch shock tunnel will be described. These include a study of hypersonic flow over sharp and blunt flat plates, an investigation of laminar heat transfer to a slender cone including yaw and nose-bluntness effects, and stagnation-point heat transfer at low Reynolds numbers. The programs will be briefly outlined, and the important results will be presented and discussed.

In addition to the research performed in the 11 by 15-inch shock tunnel, a variety of research and development programs have been conducted in the 48-inch shock tunnel. These include pressure, force, dynamic stability and heat-transfer experiments on various hypersonic aircraft and missiles.

Flow Over Sharp and Blunt Flat Plates

A comprehensive study* has been completed in the shock tunnel of hypersonic air flow over sharp and blunt flat plates[82-84]. The basic purpose of the work was to investigate the effects of leading-edge bluntness and boundary-layer displacement on the viscous and inviscid characteristics of the flow. The study entailed measurement of surface heat transfer and pressure distributions, as well as schlieren measurement of shock-wave shapes, under essentially ideal gas conditions but with low wall-to-stagnation temperature ratios. Advantage was taken of the available wide range in tunnel stagnation pressures to encompass the limiting cases of dominant bluntness and dominant viscous interaction.

The studies of surface heat transfer and shock shape were carried out in the CAL 11 by 15-inch hypersonic shock tunnel at air flow Mach numbers around 12. A stagnation temperature of 2000°K with a wall-to-stagnation temperature ratio of 0.15 was employed in most of the tests. At zero angle of attack and zero yaw, leading-edge Reynolds numbers ranged from 3 to 15,000 and stream Reynolds number per inch from 1.4×10^4 to 1.8×10^5. These extremes of Reynolds number covered the complete range of interaction of bluntness and displacement effects. Studies of angle-of-attack effects without yaw and yaw

* The experimental program, including a portion of the accompanying similitude study, was performed under the sponsorship of the Air Force Office of Scientific Research, Contract No. AF 18(603)-10.

effects without angle of attack were made at small and large leading-edge Reynolds numbers. Heat-transfer measurements were also made on a sharp plate at stagnation temperatures up to 4000°K giving wall-to-stagnation temperature ratios down to .075.

Surface pressure measurements were carried out with a sharp plate at zero angle of attack at Mach numbers 9, 14.6, and 16.1 in the CAL 48-inch hypersonic shock tunnel, and at Mach number 12 in the 11 by 15-inch tunnel. Pressure measurements on a blunt plate were also made at Mach number 12. The wall-to-stagnation temperature ratio for the pressure studies was also about 0.15.

Detailed results of these experimental studies have been reported in Refs. 82 to 84. The experimental data were reduced to nondimensional forms indicated by an extension of hypersonic viscous similitude for an ideal gas to include the effects of leading-edge bluntness[82, 85]. Comparisons of the data were also made with the leading or zero-order approximation ($\gamma \to 1$) of a general theory by Cheng[82, 85] for the combined effects of bluntness, viscous displacement, and angle of attack*.

Typical schlieren photographs of shock-wave shapes are shown in Fig. 15. The shock shapes permitted an assessment of the degree to which the experimental flows met the assumptions of the theory of strong shocks and small flow deflection angles. These assumptions effectively place upper and lower bounds on the local shock-wave angle. With due allowance for this, the schlieren and heat-transfer data are correlated by the viscous similitude extended for bluntness over the entire range of varying bluntness and viscous-interaction effects.

* The theoretical study was done under the sponsorship of the Office of Naval Research, Contract No. Nonr 2653(00).

Typical correlations of shock shape and heat-transfer data for zero angle of attack are shown in Figs. 16 and 17. Here, the abscissa $\beta = \chi_\epsilon K_\epsilon^{-2/3}$ involves the variable χ_ϵ characterizing viscous-interaction effect, and the variable K_ϵ characterizing leading-edge bluntness effect. Large values of β (~ 1 to 10) give dominant viscous interaction, while small values ($\sim 10^{-1}$ to 10^{-2}) give dominant bluntness effect. Also shown in these figures is the zero-order prediction of the bluntness-displacement theory. The agreement between experiment and theory is fairly good considering the restrictive assumptions of the latter.

Typical surface pressure results are shown in Fig. 18 in nondimensional form for a sharp plate at zero angle of attack. With the low wall-to-stagnation temperature ratios of the tests, the laminar boundary layers were highly cooled. The induced pressures were thus substantially less than for adiabatic wall conditions. The data show a transition from weak to strong interaction behavior over a range of the viscous interaction variable $\bar{\chi}$ from 1 to about 38. The Mach number 9 and 12 data appear to follow the second-order weak interaction theory of Lees and Probstein[86] to $\bar{\chi}$ values of about 9. At the highest values of $\bar{\chi}$ the data appear to cross the strong interaction theory[82, 85]. This trend appears similar to that observed by Nagamatsu and Sheer[87].

Heat Transfer to Slender Cones

The second research investigation to be discussed is a recent study* of laminar heat transfer to a slender cone including the effects of yaw and nose bluntness[80]. The experiments were conducted in the 11 by 15-inch shock tunnel

* This program has been sponsored by the Aeronautical Research Laboratory of the Air Force Research Division, Contract No. AF 33(616)-6025.

over a Mach number range from 11.3 to 13.0, a free-stream Reynolds number range from 2×10^5 to 2×10^6 per foot, and at a nominal stagnation temperature of 2000°K. A 5° semi-apex angle cone was instrumented with thin-film resistance thermometers at three axial stations and various circumferential positions.

The results for the zero-yaw, pointed-cone experiments were reduced to a Stanton number and were compared with theoretical predictions. The theory for laminar boundary layer on a cone[80] gives

$$St = \frac{q}{\rho U (H_{aw} - H_w)} = 0.3321 \, Pr^{-2/3} \sqrt{\frac{3C}{Re_x}}$$

For the conditions of these experiments, this reduces to

$$St = 0.675 \, Re_x^{-1/2}$$

where the Stanton and Reynolds numbers are evaluated at local condition at the outer edge of the boundary layer and the Prandtl number is taken as 0.71. On the average, the data lie about 20% above this theoretical curve. Most of this 20% discrepancy can be attributed to boundary-layer displacement and transverse-curvature effects. Utilizing available theory, these effects may be accounted for and the Stanton number expressed as

$$St = 0.3321\sqrt{3} \, Pr_w^{-2/3} \sqrt{\left(\frac{C}{Re_x}\right)_c} \left\{ 1 + \left[-0.350 + 0.111 \frac{T_w}{T_c} + (0.429\gamma - 0.028) M_c^2 \right] \frac{\alpha_c F_1 \bar{x}_c}{\gamma M_c^2} \right.$$

$$\left. + \left[0.517 + 0.913 \frac{T_w}{T_c} + 0.121(\gamma - 1) M_c^2 \right] \frac{\sqrt{(C/Re_x)_c}}{\sqrt{3} \tan \theta_c} \right\}$$

where the second and third terms within the braces are the corrections for boundary-layer displacement and transverse-curvature effects, respectively. At the lowest free-stream Reynolds number (2.4×10^5/ft), the data and the theory are in good agreement. At $Re_\infty = 9.0 \times 10^5$/ft, the data lie about 10%

above the theory at the most forward instrumented station ($x = 3.0$ in.), are within 10% at the second station ($x = 5.1$ in.) and scatter about the theory at the aft station ($x = 6.6$ in.). At the highest free-stream Reynolds number ($Re_\infty = 17.4 \times 10^5$/ft), the data lie from 10% to 40% above the theory at the first station ($x = 3.0$ in.) and within 10% of the theory at the aft station.

The effect of yaw on the heat transfer along the most-windward or stagnation streamline of the pointed cone is shown in Fig. 19. Here the ratio of the local heat-transfer rate at yaw to the zero-yaw rate is plotted as a function of yaw angle for yaw angles up to almost three times the cone half-angle. A theoretical curve, based on an extrapolation of Reshotko's results[88], has been calculated for yaw angles up to 8 degrees. The agreement is seen to be good at yaw angles up to 3 degrees. Above 3 degrees yaw, the data lie increasingly above the theory. Also shown in Fig. 19 are theoretical curves for large yaw angles obtained from Reshotko and Beckwith's theory for a yawed cylinder[89]. The theory has been calculated using both Newtonian theory and the second-order Stone theory to obtain the pressures. The data do not agree with either of these theoretical curves.

The circumferential heat-transfer distributions at the two largest yaw angles (9.5 and 13.7 degrees) showed a locally high heat-transfer rate along the most leeward streamline[80]. This strongly suggests the formation of a pair of separated vortices resulting from the large cross flow. Schlieren pictures could not be taken to verify this fact because the model was yawed rather than pitched.

For the blunt-nose experiments the cone was tested with flat noses having diameters of 0.059, 0.1925, 0.2995 and 0.4000 inches. These produced a variation in length-to-diameter ratios from 1.75 to 112 at the instrumented sta-

tions. The experimental heat-transfer rates are shown in Fig. 20 and are compared with the zero-order ($\gamma \to 1$) blunt-cone theory of H. K. Cheng[85]. The correlation is made in terms of the parameters

$$\frac{(\epsilon k)^{1/4} C_H \sqrt{Re_D}}{M_\infty \theta_c^2 \sqrt{C}} \quad \text{and} \quad \frac{\theta_c^2 \chi}{\sqrt{\epsilon k}\, D}$$

which appear in Cheng's theory. Note that the heat-transfer parameter, C_H, is defined in terms of free-stream rather than local flow conditions. Considering the zero-order nature of the theory[85] the agreement shown in Fig. 20 is thought to be reasonably good. As indicated in Ref. 85, the oscillations shown in the theoretical curve are not really anticipated in actuality, but result from the zero-order nature of the theory, i. e. $\gamma \to 1$.

The analyses of both Cheng[85] and Chernyi[90] predict that the pressure on the cone will overexpand from the high stagnation-point value to a pressure less than that on an equivalent sharp-cone value, and then decay to a pressure equal to that on a pointed cone of the same cone angle. The experimental pressure distributions reported by Bertram[91] do not show an overshoot above the sharp-cone pressure. However, a recent correlation[92] of blunt-cone pressures obtained in both a shock tunnel and a wind tunnel clearly indicate an overshoot in the recompression followed by a decay to the sharp-cone pressure. The heat-transfer data presented in Fig. 20 also show such a variation.

Stagnation-Point Heat Transfer in Low-Density Flows

Heat transfer to the stagnation point of blunt bodies at high Reynolds number has been the subject of various theoretical[43, 44, 93] and experimental[94-96] investigations within the past five years. Recently, low Reynolds number analyses of this flow have appeared in the literature[97-102]. There exists little ex-

perimental data at hypersonic speeds with which to judge the accuracy of these theories. Most of the available experimental data on low-density flows have been restricted to Mach numbers of 6 or less[103-106]; therefore, it is desirable to extend experimental hypersonic research into the rarefied gas region. Just recently, several such investigations have been reported, Refs. 81, 101, 107 and 108.

To investigate the capability of the shock tunnel as a low-density hypersonic research tool and to obtain experimental data in this flow regime, a study* was undertaken in the CAL 11 by 15-inch shock tunnel of stagnation-point heat transfer to two and three-dimensional bodies. The initial results for flow about a transverse cylinder at Mach numbers from 8.4 to 11.5 and Reynolds numbers from 11 to 1000, based on flow conditions behind the bow shock wave and the body radius, were reported at the Second International Symposium on Rarefied Gas Dynamics[109]. A more complete description of these experiments as well as the results of a brief series of tests with an axisymmetric model is given in Ref. 81.

As in other investigations described, the free-stream Mach number was found somewhat dependent on the Reynolds number because of changes in the nozzle boundary-layer thickness. In the transverse-cylinder experiments, three models were used having nominal diameters of 1/8, 1/4, and 1 inch. For each model, the free-stream Reynolds number was varied from about 1460 per inch to 21,300 per inch. The corresponding Mach number range was from 9.7 to 11.6. The 1/4 and 1-inch models had three thin-film resistance thermometers

---

* Sponsored by the Aeronautical Research Laboratory of the Air Force Research Division, Contract No. AF 33(616)-6025.

located along the stagnation line. They were located at the tunnel centerline and about one inch on either side. The 1/8-inch model had a single stagnation-line thermometer located at the tunnel centerline.

All three models were tested at a nominal stagnation temperature of 1800°K. In addition, the 1/4-inch model was tested at 3600°K. In the latter tests, the Mach number varied from 8.4 to 10.3 for free-stream Reynolds numbers from 560 to 3400 per inch. The effect of the higher stagnation temperature is to produce a lower Mach number and free-stream Reynolds number for a given stagnation pressure.

The experimental heat-transfer rates for the transverse cylinders are presented in Fig. 21 and are compared with two theoretical predictions. The data have been reduced to the heat-transfer coefficient, $C_H = q/\rho_\infty U_\infty (H_0 - H_w)$, and are plotted as a function of the parameter, $K^2 = \rho_\infty R/\mu_\infty U_\infty C$, which is proportional to the Reynolds number based on flow conditions behind the bow shock and the model radius. At large values of K^2, the compressible laminar boundary-layer theory of Cohen and Reshotko[110] has been calculated for $\epsilon = 0.10$ and 0.15, where $\epsilon = \frac{\rho_s}{2\rho_s H_s} \cong \frac{\gamma - 1}{2\gamma}$. For lower values of K^2, the theoretical curves are previously unpublished solutions obtained by H. K. Cheng for a viscous shock-layer flow. These solutions, which are also calculated for $\epsilon = 0.10$ and 0.15, are similar to those reported by Cheng in Ref. 111 for the axisymmetric case.

At the higher Reynolds numbers (large values of K^2), the data show fairly good agreement with the compressible boundary-layer theory. In the viscous layer region, the 1800°K stagnation temperature data ($\epsilon \simeq 0.13$) on the average fall somewhat below the theoretical curve. The 3600°K stagnation temperature data ($\epsilon \simeq 0.10$) are in better agreement with the corresponding theoretical curve;

however, they also are slightly below the theory. For values of $K^2 \rightarrow 1$, the data show no significant deviation from the theoretical curve. It is planned to extend the range of experiments to values of K^2 of about 0.1 utilizing the CAL six-foot shock tunnel. In addition, the effects of yaw on the stagnation-point heat transfer to a cylinder will be investigated.

Subsequent to the transverse-cylinder tests, a brief series of experiments with a hemisphere-cylinder model* was undertaken in the 11 by 15-inch shock tunnel. The model was 1/2 inch in diameter and was instrumented to measure stagnation-point heat transfer. The tests covered a range of K^2 from 3 to 80. The results of the experiments are presented and discussed in Ref. 81. Within the scatter of the data, good agreement was obtained with Cheng's viscous shock-layer theory[111]. An additional comparison is made in Refs. 81 and 111 of the shock tunnel data with wind tunnel data reported by Ferri[101]. Both sets of data are in good agreement when compared in terms of the parameters C_H and K^2. As with the transverse-cylinder investigation, it is planned to utilize the CAL six-foot shock tunnel to extend the range of the experiments to lower Reynolds number (lower values of K^2).

The results already obtained have shown that successful low-density experiments could be made in a shock tunnel that was not designed for operation in this flow regime. This has led to a fuller investigation of the application of the shock tunnel to research studies of rarefied gasdynamic phenomena at hypersonic speeds[81, 109].

---

* Supported by U. S. Navy Office of Naval Research, Contract No. Nonr 2653(00).

FUTURE DEVELOPMENTS OF THE SHOCK TUNNEL

In the previous sections the state of the art with respect to shock tunnel operation has been reviewed. The shock tunnel in its present form is being extensively utilized to study problems of hypersonic flight. The technical problems associated with its use have largely been solved, and constant improvements in operating techniques are being made. However, further development of the shock tunnel should be considered, particularly in relationship to future prospects for hypersonic flight.

The present reality of hypersonic flight is exemplified by the re-entry of ballistic missile nose cones. However, the problems of the future are related to manned, recoverable hypersonic vehicles. While the plunging re-entry of the ballistic vehicle carries it to hypersonic Mach numbers at low altitudes, the permissible maximum decelerations require that the re-entry path of a manned vehicle be at a glancing angle with respect to the atmosphere. Hence these manned vehicles will experience high Mach number hypersonic flight at extremely high altitudes for relatively extended periods. The variety of modes of re-entry (see, for example, Refs. 112-114) which have been suggested make it difficult to define the corridor of flight rigorously. These vehicles combine various forms of heat sinks or shields with the use of lift in varying degrees to control the re-entry trajectory. However, the glancing re-entry trajectory, which is always employed, indicates a flight Mach number region of interest between 15 and 25 and an altitude zone starting at approximatel 150,000 feet and extending to 300,000 feet. It is within this zone that vehicles will experience their critical heating and aerodynamic effects.

Re-entry vehicles of the future will also have requirements which are not dictated by the problem of survival. Indeed, the re-entry path may often times be compromised by the requirements of mission rather than by the requirements of structures. For example, a vehicle designed for reconnaissance over the electromagnetic spectrum must select a trajectory such that the interaction of electromagnetic waves with the plasma sheath will not adversely affect observation. Also, a vehicle designed to utilize advanced command and guidance techniques cannot operate in a zone which will lead to communications blackout.

In previous sections, the limitations of scaling with respect to many important hypersonic phenomena have been indicated. It appears that in many cases duplication of ambient flow conditions with full scale is necessary. With duplication, the problems dealing with Mach number, Reynolds number, real-gas effects, as well as the interaction of electromagnetic radiation with the plasma sheath can be studied simultaneously or separately as desired.

This discussion of future re-entry flight provides a background for consideration of further development of the shock tunnel. In the following paragraphs, the requirements for duplication of flight conditions will be discussed and compared with the potentialities of the shock tunnel. In particular, the form of future shock tunnels will be discussed. Requirements as to stagnation pressure and temperature, scale of facility and testing time will be outlined.

Stagnation Pressure Requirements

Examination of Fig. 5 shows the stagnation pressures and temperatures required to duplicate velocity, Mach number, and altitude by equilibrium expansion

in a hypersonic nozzle. This graph applies to any facility achieving duplication by direct expansion. As pointed out in the earlier section discussing nonequilibrium nozzle flows, operation at pressures in the order of 1000 atm is mandatory if the effects of nonequilibrium are to be minimized. However, it can be seen that duplication in the high altitude, high Mach number region of flight requires tunnel stagnation pressures on the order of tens of thousands of atmospheres. Thus duplication creates pressure requirements beyond those of nonequilibrium.

At the present time the design capability of the CAL six-foot shock tunnel is 2000 atm. Doubling this pressure level by existing techniques is certainly feasible. However, to operate at still higher pressures will require the development of new techniques. For example, techniques similar to those presently being used in light gas guns might be employed [115]. In such cases amplification of driver gas pressure would be obtained by the inertia of a rapidly moving piston. In addition, more sophisticated techniques such as employed in the buffer type of shock tube[30, 32] can be further exploited. While such techniques appear promising, nonetheless they have not yet been developed, and the shock tunnels of the near future will probably be limited to pressures below 10,000 atm.

The high-pressure levels required for duplication of flight conditions and suppression of nonequilibrium effects also prove advantageous in minimizing nozzle boundary-layer development. Hypersonic nozzles operating in the low-density region tend to have extremely thick boundary layers[116]. This thickening of the boundary layer limited the maximum Mach number which could be obtained in the 11 x 15 inch nozzle of the CAL shock tunnel. The effective expansion ratio of this nozzle was found to be approximately one-half the geometric ratio at

a Mach number of 12 and at stagnation pressures of about 700 atm; it decreased rapidly at lower pressures. On the other hand, with the 24-inch conical nozzle the effective area ratio at Mach 16 is about two-thirds the geometrical area ratio at a stagnation pressure of about 150 atm. These results are in fair agreement with predictions of the empirical relationship presented by Lee in Ref. 117. The difference in boundary-layer effects between the two nozzles is attributed to the axisymmetrical conical shape of the 24-inch nozzle as contrasted to the two-dimensional expansion nozzle used in the 11 x 15-inch tunnel. Two-dimensional nozzles are known to have more rapid boundary layer buildup than axisymmetric nozzles.

In order to estimate the effect of this boundary-layer problem on future facilities, calculations of the boundary-layer displacement thickness have been made using the results of Lee. The results of these calculations, presented in Fig. 22, show the relative effect of stagnation pressure, Mach number, and nozzle size. It can be seen that at high Mach numbers, high stagnation pressures reduce the nozzle boundary layer to manageable proportions. Nozzle boundary-layer data is difficult to apply in general since the particular configuration (i. e., technique of contouring, nozzle back pressures, etc.) of each facility has a significant effect. It is felt that the results of Fig. 22 do indicate that the high stagnation pressures required for duplication are also necessary to obtain large cores of uniform hypersonic flow in the nozzle.

In addition to the beneficial effects on nonequilibrium and nozzle boundary-layer phenomena, high pressure operation can be expected to alleviate certain shock tube problems such as interface mixing, reflected-shock boundary-layer interaction and shock -wave attenuation. Several investigators have shown[118-120]

that there is a severe decrease of flow duration in shock tubes operating at very low pressures. This has been attributed to low-speed gas in the boundary layer "leaking" past the interface. Roshko[120] has shown that this effect decreases with increasing initial pressure ahead of the shock. The interaction of the reflected shock wave and the shock-tube wall boundary layer has been studied by Mark[121] and Byron and Rott[122] who have shown that large effects can result. Again, however, increasing the pressure level markedly decreases these effects. Lastly, attenuation of the shock wave as it travels down the tube has been the subject of theoretical[123-126] and experimental[16, 20, 127-129] studies. Being a viscous phenomenon, this has also been found to be pressure dependent and to decrease as the overall pressure level is raised. Thus operating shock tubes at the high pressures necessary to obtain flight duplication nearly eliminates the viscous problems associated with shock tube flow.

Stagnation Temperature Requirements

In the section relating to simulation capabilities, it was shown that stagnation enthalpy duplication was required for velocity duplication. In a tailored-interface shock tunnel, room-temperature helium as a driver gas provides a stagnation enthalpy corresponding to an air stagnation temperature of 2000°K and a velocity of 6900 ft/sec. Using helium heated to about 1000°K or room-temperature hydrogen provides a stagnation temperature of approximately 4000°K in air, yielding a velocity of 10, 500 ft/sec. With the development of the high-pressure heated-hydrogen driver* recently installed at CAL, hydrogen

* The present heated-hydrogen driver consists of a high-strength alloy steel tube with a stainless steel inner liner to protect the tube from attack by the hydrogen. The driver and liner is surrounded by heating units so that the entire driver may be heated without the introduction of thermal stress.

temperatures of up to 750°F are presently available, yielding a stagnation temperature in the range from 6000 to 8000°K and a velocity of 17,000 ft/sec. The efficiency of this heated hydrogen driver compares very favorably with the best performance obtainable from combustion drivers. Of course, considerably higher temperatures can be obtained by operating the shock tube nontailored, either as a conventional reflected or nonreflected type of shock tunnel. However, the loss in performance due to attenuation and the loss of pressure when operating nontailored severely limits the performance possibilities.

With the stipulated requirement that the conditions of hypersonic flight are to be duplicated, higher velocities are desired. It is anticipated that the performance of the heated-hydrogen driver can be extended to obtain maximum temperatures of around 1000°F corresponding to a stagnation temperature range from about 8000 to 10,000°K with a velocity of approximately 20,000 ft/sec. Further increases in stagnation temperature would then require further shock-tube development. For example, the possibility of utilizing the equilibrium-interface technique[6] has been discussed in the section on Shock Tunnel Simulation Capabilities. The practical operating limitations involved have not yet been seriously explored; however, it is anticipated that some increase in stagnation temperature may possibly be obtained by utilizing this technique. In addition, the technique of the buffer shock tube has been suggested as a method for preheating a driver for tailored-interface operation[30]. As yet the development of this type of shock tube is still in a preliminary stage[32]. The utilization of electrical-heating techniques to suddenly heat the driver gas in a manner similar to that of the hot-shot type tunnel has been considered. However, estimates indicate that a very large amount of electrical energy storage capacity is necessary. An additional example is the pressure amplification scheme util-

izing piston compression suggested in the discussion of pressure requirements. This would also serve as a technique of heating hydrogen beyond the 1000°F temperature limit. Nonetheless, at the present time it appears that the shock tunnels of the immediate future will be limited to stagnation temperatures in the range 8000 to 10,000°K with a corresponding velocity of approximately 20,000 ft/sec.

Tunnel Scale

The limitations of scaling with respect to many important hypersonic phenomena have been indicated in previous sections. In view of the objective of the duplication of flight conditions within the laboratory, it appears that only full-scale testing can completely satisfy our requirements. Hence, studies have been carried out at CAL to explore the size limitations of hypersonic shock tunnels. These design studies indicate that nozzle diameters up to 50 feet are well within the capabilities of existing technology. Thus, it is now appropriate to consider full-scale testing within the laboratory under conditions closely duplicating re-entry flight. Indeed, when the cost of a flight test program is considered, the cost of such a shock tunnel is relatively small. Such a facility serves as a useful and complementary adjunct to flight test. Indeed, the relative flexibility possible with instrumentation allows studies involving subtle delineations of flight phenomena which can be carried out with greater precision and certainty in the laboratory. However, such a facility does not completely replace flight test since in the final analysis the composite integrity of any system must be proved in the field. The use of a large-scale shock tunnel would serve to aid in the planning of flight programs, to limit the number of firings required to those involving critical design features, and to materially aid in interpreting the results of such tests.

Design studies carried out at CAL have shown that small-diameter shock tubes can provide sufficient mass flow to supply large-scale nozzles. For example, the 3-inch I. D. shock tube now in use can supply a 6-foot diameter hypersonic nozzle for Mach numbers greater than 15, and the 8-inch diameter shock tube used with the 48-inch shock tunnel could supply at least a 20-foot diameter nozzle.

While at first glance full-scale shock tunnels would seem to require a monumental facilities effort, it must be remembered that the inherent simplicity of a shock tunnel is not appreciably affected by scale. The ability of the shock tube to supply the power required for the brief period of testing is beyond the capability of any continuous tunnel. Indeed, since continuous pumping is not required, relatively small-scale vacuum and high-pressure pumping equipment are quite satisfactory.

Much of the technology of such large-scale shock tunnels has already been developed. For example, at the present time diaphragms for the 8-inch diameter shock tube have been developed to withstand pressures of about 500 atm, and the development of single diaphragms to withstand even higher pressures does not seem difficult. However, the technique of multiple-diaphragm operation has been generally adopted at CAL. In this technique the pressure load on the diaphragms can be divided equally between diaphragms by adjustment of the intermediate pressure and the diaphragms are burst by relieving the intermediate pressure. Hence, multiple diaphragms make it possible to obtain controlled diaphragm rupture at any pressure desired for a full-scale tunnel. The fabrication of relatively large (up to 15 or 16 inches) diameter tubes to withstand high pressure is an engineering art which men have assiduously developed over the previous few centuries.

While the limitations of scaling have been introduced as the chief argument for full-scale shock tunnels, additional advantages also can be anticipated. It has been pointed out that high-pressure operation is an important factor in suppressing nozzle nonequilibrium phenomena. However, increased scale is also helpful in this respect, particularly at high temperatures. While pressure also plays a dominant role in minimizing nozzle boundary-layer buildup, Fig. 22 indicates that increasing nozzle scale is also favorable in reducing boundary-layer effects. In addition to these advantages, relatively large-scale models generally simplify the problems of model instrumentation.

Testing Time Requirements

The testing time of a shock tunnel need be no longer than that required for flow establishment and instrumentation response. As discussed in Ref. 15, starting and stopping times in a hypersonic nozzle are very brief, and the theory of Ref. 15 has proven adequate for engineering estimates. For example, the testing time loss associated with nozzle starting and stopping is less than a millisecond for all CAL shock tunnels. In practice, the techniques of instrumentation determine the minimum duration of the steady flow. These testing time requirements have been discussed in the section relating to instrumentation. They vary, for example, from a few microseconds in the case of the thin-film heat-transfer gauge to the relatively long time, on the order of several milliseconds, required to measure dynamic forces or motion of a model.

However, with the increasing performance levels of shock tunnels, structural heating problems are expected to limit the permissible testing time. For example, present CAL shock tunnels have been operated at pressures up to 1000 atm, and stagnation temperatures of approximately 4000°K for testing times of 3 milliseconds, with no damage observed at the nozzle throat. How-

ever, with increase of stagnation temperature and pressure, it is possible that damage to the nozzle throat could be a serious problem (see, for example, Ref. 130). With the shorter testing times permitted by anticipated improvements in instrumentation response, it is felt that this problem will not seriously limit the capability of the shock tunnel. In addition, while it has not yet been necessary to resort to special throat protection, suitable modification of the nozzle geometry can appreciably increase the heat-sink capability of the throat. Thus, it is expected that the trend in shock tunnel design will be towards ever decreasing test durations as both instrumentation is improved and performance levels are increased.

It must be kept in mind that as the testing time is reduced, the time for the establishment of steady flow around the model may become a consideration. While both theory and experiments show that the boundary-layer flows within the nozzle and about models are established in times comparable to the starting time of the nozzle, recent tests indicate that flows involving upstream separation may require significantly longer test times for the establishment of steady flow. For example, experiments reported in Ref. 29 show that a flat plate with an upstream facing step takes significantly longer to establish steady flow than the equivalent simple flat plate. While this establishment time was still comparable to the starting time of the nozzle, other configurations may exhibit longer establishment times. Shock tunnels must always be used with due discretion for flow establishment time.

The CAL Six-Foot Shock Tunnel

The foregoing sections have outlined the requirements of future shock tunnels for the investigation of manned re-entry flight. In order to study at first hand the problems associated with future facilities of this type and to pro-

vide a research facility of increased capability, CAL undertook extensive modifications to the 11 by 15-inch shock tunnel. The driver section has been replaced with a heated driver of 4.75 inches inner diameter utilizing hydrogen up to 750°F at 30,000 psi. This driver is connected to the existing 28-foot driven section. The shock tube is terminated in a convergent-divergent nozzle having a contoured two-dimensional expansion to produce a uniform flow at a Mach number of about 4.5 (Fig. 23). A Prandtl-Meyer deflection section is installed to centrifuge particles out of the flow; the air is finally expanded in a conical nozzle of 15° half-angle into a test section having a diameter of 6 feet. A photograph of this nozzle system is shown in Fig. 24.

The performance curve for this tunnel, indicated by the shaded line in Fig. 5, covers a significant area of the critical re-entry region. It is anticipated that flow Mach numbers up to 25 with large inviscid flow regions will be obtainable. Thus, relatively large-scale test models (up to one foot in diameter) may be utilized to explore scaling effects. Part of the conical section of this nozzle is fabricated with fiberglas to permit the study of the interaction of electromagnetic radiation with the plasma sheath surrounding the model.

At the present time the shock tunnel is undergoing shakedown tests and flow Mach numbers in excess of 20 have been obtained. It is anticipated that this tunnel will make it possible to study within the laboratory many of the problems associated with hypersonic flight. In particular, the problems associated with very high-altitude, low-density flight can be examined at relatively large scale under flow conditions which duplicate an important area of re-entry flight. In addition, the test program contemplated should serve to supply data for the planning of future full-scale shock tunnels which will provide complete duplication.

CONCLUDING REMARKS

The development of the shock tunnel has proceeded rapidly following the success of the tailored-interface technique and the development of adequate instrumentation. In its present form the shock tunnel has far exceeded the initial estimates of performance. It is a useful and versatile tool for hypersonic research. The continued refinement of techniques of operation and instrumentation are expected to further improve its capabilities and convenience of operation.

This success has encouraged studies which indicate that significant further developments of the shock tunnel are possible. The CAL 11 by 15-inch shock tunnel has been modified for higher performance by the addition of a heated hydrogen driver and six-foot diameter nozzle. This tunnel should prove a useful tool for the study of problems of high-altitude, hypersonic flight, and provide valuable data for subsequent development of full-scale tunnels providing complete duplication of flight conditions.

REFERENCES

1. Resler, E. L., Lin, S. C. and Kantrowitz, A., The Production of High Temperature Gases in Shock Tubes, Journal Applied Physics, Vol. 23, No. 12, December 1952, pp. 1390-1399.
2. Hollyer, R. N., Hunting, A. C., Laporte, O., Schwarcz, E. N., and Turner, E. B., Luminous Effects in the Shock Tube, Phys. Rev., Vol. 87, 1952, pp. 911-912a.
3. Hertzberg, A., A Shock Tube Method of Generating Hypersonic Flows, Journ. Aero. Sci., Vol. 18, No. 12, December 1951, pp. 803-805.
4. Lukasiewicz, J., Shock Tube Theory and Applications, Nat'l Aero. Est., Canada, Report 15, 1952.
5. Glass, I. I. and Patterson, G. N., A Theoretical and Experimental Study of Shock-Tube Flow, J. Aero. Sci., Vol. 22, No. 2, February 1955, pp. 73-100.
6. Hertzberg, A., Smith, W. E., Glick, H. S., and Squire, W., Modifications of the Shock Tube for the Generation of Hypersonic Flow. CAL Report No. AD-789-A-2, AEDC-TN-55-15, AD-63559, March 1955.
7. Bleakney, W., Weimer, D. K., and Fletcher, C. H., The Shock Tube: A Facility for Investigations in Fluid Dynamics, Rev. Sci. Inst., Vol. 20, 1949, p. 807.
8. Yoler, Y. A., Hypersonic Shock Tube, GALCIT Memo No. 18, July 1954.
9. Seigel, A. E. and Slawsky, Z. I., A Hypervelocity Gun Using a Shock-Compressed Steam-Heated Propellant, NavOrd Report 4345, 1956.
10. Hertzberg, A., The Application of the Shock Tube to the Study of the Problems of Hypersonic Flight, Jet Propulsion, Vol. 26, No. 7, July 1956, pp. 549-554.

11. Rose, P. M., Physical Gas Dynamics Research at the AVCO Research Laboratory, AVCO Res. Lab. Rept. No. 9, May 1957 (Also AGARD Rept. 145, July 1957).

12. Rabinowicz, J., Aerodynamic Studies in the Shock Tube, GALCIT Hypersonic Research Proj. Memo. No. 38, June 1957.

13. Vitale, A. J., Kaegi, E. M., Diaconis, N. S., and Warren, W. R., Results from Aerodynamic Studies of Blunt Bodies in Hypersonic Flows of Partially Dissociated Air, G. E. Document No. 58SD214, February 1958 (also Proceedings of the 1958 Heat Transfer and Fluid Mechanics Institute).

14. Nagamatsu, H. T., Geiger, R. E., and Sheer, R. E. Jr., Hypersonic Shock Tunnel, ARS Journal, Vol. 29, No. 5, May 1959.

15. Glick, H. S., Hertzberg, A., and Smith, W. E., Flow Phenomena in Starting a Hypersonic Shock Tunnel, CAL Report No. AD-789-A-3, AEDC-TN-55-16, AD-63558, March 1955.

16. Wittliff, C. E. and Wilson, M. R., Shock Tube Driver Techniques and Attenuation Measurements, CAL Report No. AD-1052-A-4, AFOSR TN 57-546, AD 136531, August 1957.

17. Hertzberg, A. and Smith, W. E., A Method for Generating Strong Shock Waves, J. Appl. Phys., Vol. 25, No. 1, January 1954, pp. 130-131.

18. Vidal, R. J., Model Instrumentation Techniques for Heat Transfer and Force Measurements in a Hypersonic Shock Tunnel, CAL Report No. AD-917-A-1, WADC TN 56-315, AD-97238, February 1956.

19. Vidal, R. J., Wittliff, C. E., Bartlett, G. E., and Logan, J. G., Investigation of Stagnation Point Heat Transfer in the CAL Hypersonic Shock Tunnel, CAL Rept. No. AA-966-A-1, November 1955.

20. Jones, J. J., Experimental Investigation of Attenuation of Strong Shock Waves in a Shock Tube with Hydrogen and Helium as Driver Gases, NACA TN 4072, July 1957.

21. Hertzberg, A., The Shock Tunnel and Its Application to Hypersonic Flight, CAL Report No. AD-1052-A-5, AFOSR TN 57-268, AD-126567, June 1957. Presented at the Seventh Meeting of the AGARD Wind Tunnel and Model Testing Panel at Scheveningen, Netherlands, July 1957.

22. Series of papers presented at High Pressure Symposium, Indust. and Engin. Chemistry, Vol. 49, No. 12, December 1957, pp. 1945-2050.

23. Wittliff, C. E., Wilson, M. R., and Hertzberg, A., The Tailored-Interface Hypersonic Shock Tunnel, ASME-ARS Aviation Conference, Dallas, Texas, March 1958. CAL Report No. AD-1052-A-8, AFOSR TN 59-31, AD 209203, Jan. 1959. J. Aero/Space Sci., Vol. 26, No. 4, April 1959.

24. Wittliff, C. E., Hypersonic Nozzle Design to Avoid Particle Damage, Paper presented at the 11th Meeting, Supersonic Tunnel Assn., April 21-23, 1959.

25. Cornell Aeronautical Laboratory, Inc. 24" Hypersonic Shock Tunnel. October 1959.

26. Hertzberg, A. and Wittliff, C. E., Studying Flight in the Hypersonic Shock Tunnel, IAS Paper No. 60-67, June 1960.

27. Wittliff, C. E., Hypersonic Research in the Shock Tunnel, Proceedings of the IAS National Symposium on Hypervelocity Techniques, October 1960.

28. Masson, D. J. and Gazley, C. Jr., Surface Protection and Cooling Systems for High-Speed Flight, Aero. Eng. Rev., Vol. 15, No. 11, November 1956, pp. 46-55.

29. Holder, D. W. and Schultz, D. L., On the Use of Shock Tunnels for Research on Hypersonic Flow, Paper presented at the International Congress Aero. Sci. 1960.

30. Russo, A. L., and Hertzberg, A., Modifications of the Basic Shock Tube to Improve Its Performance, CAL Rept. No. AD-1052-A-7, AFOSR TN 58-716, AD 162251, August 1958.

31. Slawsky, Z. I., and Seigel, A. E., A Two-Stage Driver for Shocktubes and Shock Tunnels (U), NAVORD Rept. 5669, January 5, 1960.

32. Chapin, S. G. and Heyman, R. J., Performance Characteristics of a Chambered Buffered Shock Tube, Proceedings of the Hypervelocity Techniques Symposium, IAS, Denver, Colorado, October 20-21, 1960.

33. Bogdonoff, S. M. and Hammitt, A. G., Fluid Dynamic Effects at Speeds From M=11 to 15, J. A. S. Vol. 23, No. 2, February 1956, pp. 108-116.

34. Lees, L., Hypersonic Flow, Proceedings of the Fifth International Aeronautical Conference, June 20-24, 1955, pp. 241-276. (Also IAS Preprint No. 554).

35. Tsien, H. S., Similarity Law of Hypersonic Flow, J. Math. and Phys., Vol. 25, 1946, pp. 247-251.

36. Hayes, W. D., On Hypersonic Similitude, Quart. Appl. Math., Vol. 5, 1947, pp. 105-106.

37. Cheng, H. K., Similitude of Hypersonic Real-Gas Flows Over Slender Bodies with Blunted Noses, J. Aero/Space Sci., Vol. 26, No. 9, September 1959, p. 575.

38. Bloom, M. H. and Steiger, M. H., Inviscid Flow with Nonequilibrium Molecular Dissociation for Pressure Distributions Encountered in Hypersonic Flight, J. A. S. Vol. 27, No. 11, pp. 821-835, November 1960.

39. Whalen, R. J., Viscous and Inviscid Nonequilibrium Gas Flows, IAS Paper No. 61-23, Presented at IAS 29th Annual Meeting, New York, N. Y., January 23-25, 1961.

40. Feldman, S., Hypersonic Gas Dynamic Charts for Equilibrium Air, AVCO Research Report 40, January 1957.

41. Logan, J. G., Jr., Relaxation Phenomena in Hypersonic Aerodynamics, IAS Preprint 728, Presented at IAS 25th Annual Meeting, New York, January 28-31, 1957.

42. Kivel, B., Radiation from Hot Air and Stagnation Heating, AVCO-Everett Res. Report 79, October 1959.

43. Fay, J. A. and Riddell, F. R., Theory of Stagnation Point Heat Transfer in Dissociated Air, AVCO Research Rept. 1, April 1957. (Also J. Aero. Sci., Vol. 25, No. 2, February 1958, pp. 73-85.

44. Reshotko, E. and Cohen, C. B., Heat Transfer at the Forward Stagnation Point of Blunt Bodies, NACA TN 3513, July 1955.

45. Perry, R. W. and MacDermott, W. N., Development of the Spark-Heated Hypervelocity Tunnel -- Hotshot, AEDC-TN-58-6, June 1958.

46. Logan, J. G. and Treanor, C. E., Tables of Thermodynamic Properties of Air From 3000°K to 10,000°K at Intervals of 100°K, CAL Report No. BE-1007-A-3, January 1957.

47. Hilsenrath, J., Klein, M., and Woolley, H. W., Tables of Thermodynamic Properties of Air Including Dissociation and Ionization From 1500°K to 15,000°K, AEDC-TR-59-20, December 1959.

48. Montroll, E. W., and Shuler, K. E., Studies in Nonequilibrium Rate Processes: I. The Relaxation of a System of Harmonic Oscillators, Jour. Chem. Phys., Vol. 26, No. 3, March 1957, pp. 454-464.

49. Landau, L. and Teller, E., Physik. Z. Sowjetunion 10, 34 (1936).

50. Stollery, J. L., Stagnation Temperature Measurements in a Hypersonic Gun Tunnel Using the Sodium Line Reversal Method, Imperial College of Science and Technology, Report No. 16, September 1960.

51. Duff, R. E. and Davidson, N., Calculations of Reaction Profiles Behind Steady State Shock Waves: II. The Dissociation of Air, Jour. Chem. Phys., Vol. 31, No. 4, October 1959, pp. 1018-1027.

52. Davidson, N., Rates of Selected Reactions Involving Nitrogen and Oxygen, AVCO Res. Report 32, June 1958.

53. Wray, K., Teare, J. D., Kivel, B., and Hammerling, P., Relaxation Processes and Reaction Rates Behind Shock Fronts in Air and Component Gases, AVCO Res. Report 83, December 1959.

54. Zinman, W. G., Recent Advances in Chemical Kinetics of Homogeneous Reactions in Dissociated Air, ARS Jour., March 1960, pp. 233-238.

55. Penner, S. S., Chemical Reactions in Flow Systems, Butterworths Scientific Pub., London, 1955.

56. Krieger, F. J., Chemical Kinetics and Rocket Nozzle Design, Jour. Amer. Rocket Soc., Vol. 21, No. 6, November 1951, pp. 179-185.

57. Wilde, K. A., Effect of Radical Recombination Kinetics on Specific Impulse of High Temperature Systems, Jet Propulsion, Vol. 28, No. 2, February 1958, pp. 119-120.

58. Heims, S. P., Effect of Oxygen Recombination on One-Dimensional Flow at High Mach Numbers, NACA TN 4144, January 1958.

59. Reynolds, T. W. and Baldwin, L. V., One-Dimensional Flow with Chemical Reaction in Nozzle Expansions, Symposium on "Thermodynamics of Jet and Rocket Propulsion," Preprint No. 6, A. I. Ch. E. 40th National Meeting, Kansas City, Mo., May 17-20, 1959.

60. Bray, K. N. C., Atomic Recombination in a Hypersonic Wind-Tunnel Nozzle, Jou. Fluid Mech., Vol. 6, Pt. 1, 1959, pp. 1-32.

61. Hall, J. G. and Russo, A. L., Studies of Chemical Nonequilibrium in Hypersonic Nozzle Flows, Proc. of 1st Conference on Kinetics, Equilibria and Performance of High Temperature Systems, Butterworth and Co. Ltd. London, 1959.

62. Boyer, D. W., Eschenroeder, A. Q., and Russo, A. L., Approximate Solutions for Nonequilibrium Airflow in Hypersonic Nozzles, CAL Report No. AD-1345-W-3, August 1960.

63. Eschenroeder, A. Q., Boyer, D. W., and Hall, J. G., Exact Solutions for Nonequilibrium Expansions of Air with Coupled Chemical Reactions, CAL Report No. AF-1413-A-1, AFOSR TN 622, May 1961.

64. Eschenroeder, A. Q. and Daiber, J. W., Nonequilibrium Ionization in a Shock Tunnel Flow, ARS Jour., January 1961, p. 94.

65. Eschenroeder, A. Q. and Daiber, J. W., Ionization Nonequilibrium in Expanding Airflows, CAL Report No. AF-1441-A-2, RADC TN 60-231, September 1960.

66. Bendersky, D., A Special Thermocouple for Measuring Transient Temperatures, Mech. Eng., Vol. 75, No. 2, February 1953, pp. 117-121.

67. Wittliff, C. E. and Rudinger, G., Summary of Instrumentation Development and Aerodynamic Research in a Hypersonic Shock Tunnel, CAL Rept. No. AD-917-A-2, Part I, WADC TR 58-401, AD-155758, August 1958.

68. Hall, J. G. and Hertzberg, A., Recent Advances in Transient Surface Temperature Thermometry, Jet Propulsion, Vol. 28, No. 11, Nov. 1958.

69. Chabai, A. J. and Emrich, R. J., Measurement of Wall Temperature and Heat Flow in Shock Tube, J. Appl. Phys., Vol. 26, June 1955, pp. 779-780.

70. Rabinowicz, J., Jessey, M. E. and Bartsch, C. A., Resistance Thermometer for Heat Transfer Measurement in a Shock Tube, GALCIT Hypersonic Research Project Memo. No. 33, July 1956.

71. Marrone, P. V. and Hartunian, R. A., The Performance of Thin-Film Thermometers in Partially Ionized Shock-Tube Flows, CAL Report No. AD-1118-A-5, AFOSR TN 59-1046, November 1959.

72. Skinner, G. T., Analog Network to Convert Surface Temperature to Heat Flux, CAL Report No. CAL-100, February 1960.

73. MacArthur, R. C., The Eyes and Ears of a Shock Tunnel, CAL Research Trends, Vol. VIII, No. 3, Fall 1960.

74. Seigel, A. E., Millisecond Measurement of Forces and Moments in Hypersonic Flow, Paper presented at NOL Aeroballistic Research Facilities Dedication and Decennial, NAVORD Rept. NOLR 1238, May 1959.

75. Geiger, R., Experimental Lift and Drag of a Series of Glide Configurations at Mach Numbers 12.4 and 17.5, IAS Paper No. 60-92, Presented at the National Summer Meeting, Los Angeles, California, June 1960.

76. Tobak, M. and Wehrend, W. R., Stability Derivatives of Cones at Supersonic Speeds, NACA TN 3788, September 1956.

77. Linnell, R. C. and Bailey, J. Z., Similarity Rule Estimation Methods for Cones and Parabolic Noses, J. Aero. Sci. Readers' Forum, Vol. 23, No. 8, August 1956, pp. 796-797.

78. Wilson, M. R. and Hiemenz, R. J., High-Speed Multiple-Spark Light Source, Rev. Sci. Instr., Vol. 29, No. 11, November 1958, pp. 949-951.

79. Wittliff, C. E. and Wilson, M. R., Nozzle Flow Study and Flow Angularity Measurements in the Hypersonic Shock Tunnel, CAL Report No. AD-917-A-3 (WADC TR 58-401, Part II, AD 207615) December 1958.

80. Wittliff, C. E. and Wilson, M. R., An Investigation of Laminar Heat Transfer to Slender Cones in the Hypersonic Shock Tunnel, CAL Report No. AF-1270-A-2 (WADD TN 59-6) May 1961.

81. Wittliff, C. E. and Wilson, M. R., Low-Density Stagnation-Point Heat Transfer in Hypersonic Air Flow, CAL Report No. AF-1270-A-3, (ARL Tech. Rept. 60-333) December 1960.

82. Cheng, H. K., Hall, J. G., Golain, T. C., and Hertzberg, A., Boundary-Layer Displacement and Leading-Edge Bluntness Effects in High-Temperature Hypersonic Flow, Jour. Aero/Space Sci., Vol. 28, No. 5, May 1961, pp. 353-410.

83. Hall, J. G., and Golian, T. C., Heat Transfer to Sharp and Blunt Yawed Plates in Hypersonic Airflow, Jour. Aero/Space Sci. Vol. 28, No. 4, April 1961, pp. 345-346.

84. Hall, J. G. and Golian, T. C., Shock-Tunnel Studies of Hypersonic Flat-Plate Airflows, CAL Report No. AD-1052-A-10, AFOSR TN 60-142, December 1960.

85. Cheng, H. K., Hypersonic Flow with Combined Leading-Edge Bluntness and Boundary-Layer Displacement Effect, CAL Report No. AF-1285-A-4, August 1960.

86. Lees, L. and Probstein, R., Hypersonic Viscous Flows Over A Flat Plate, Rept. No. 195, Dept. Aero. Eng., Princeton Univ., 1952.

87. Nagamatsu, H. T. and Sheer, R. E., Hypersonic Shock Wave-Boundary Layer Interaction and Leading Edge Slip, ARS Jour., Vol. 30, No. 5, May 1960, p. 454.

88. Reshotko, E., Laminar Boundary Layer with Heat Transfer on a Cone at Angle of Attack in a Supersonic Stream, NACA TN 4152, December 1957.

89. Reshotko, E. and Beckwith, I. E., Compressible Laminar Boundary Layer Over a Yawed Infinite Cylinder with Heat Transfer and Arbitrary Prandtl Number, NACA TN 3986, June 1957.

90. Chernyi, G. G., Flow Past a Thin Blunt-Nosed Cone at High Supersonic Speed. RAE Library Translation No. 737, May 1958 (from Dokl. Akad. Nauk SSSR, 115 (1957) 4, pp. 681-3).

91. Bertram, M., Tip-Bluntness Effects on Cone Pressures at Mach 6.85, J. Aero. Sci. Readers' Forum, Vol. 23, No. 9, September 1956, pp. 898-900.

92. Curtis, J. T., Aerodynamic Analysis of the Flow Over a Double Compression Cone at Hypersonic Speeds, CAL Report No. AM-1509-Y-1, May 1961.

93. Sibulkin, M., Heat Transfer Near the Forward Stagnation Point of a Body of Revolution, J. Aero. Sci. Readers' Forum, Vol. 19, No. 8, pp. 570-571, August 1952.

94. Winkler, E. M. and Danberg, J. E., Heat Transfer Characteristics of a Hemisphere Cylinder at Hypersonic Mach Numbers, IAS Preprint No. 622, January 1956.

95. Hartwig, F. W., Development and Application of a Technique for Steady State Aerodynamic Heat Transfer Measurements, GALCIT Hypersonic Research Project Memo. No. 37, June 1957.

96. Rose, P. H. and Riddell, F. R., An Investigation of Stagnation Point Heat Transfer in Dissociated Air, AVCO Research Rept. 7, April 1957 (Also, 1957 Heat Transfer and Fluid Mechanics Institute, Preprint of papers, Stanford Univ. Press, 1957).

97. Probstein, R. F. and Kemp, N. H., Viscous Aerodynamic Characteristics in Hypersonic Rarefied Gas Flow, J. A./S. S., Vol. 27, No. 3, pp. 174-192, March 1960.

98. Herring, T. K., The Boundary Layer Near the Stagnation Point in Hypersonic Flow Past a Sphere, J. Fluid Mech., Vol. 7, Part 2, February 1960, pp. 257-272.

99. Hoshizaki, H., Shock-Generated Vorticity Effects at Low Reynolds Numbers, Lockheed M. S. D. Rept. LMSD-48381, Vol. 1, January 1959, pp. 9-43.

100. Ho, H. T. and Probstein, R. F., The Compressible Viscous Layer in Rarefied Hypersonic Flow, Brown University, ARL TN 60-132, August 1960.

101. Ferri, A., Zakkay, V. and Ting, L., Blunt Body Heat Transfer at Hypersonic Speed and Low Reynolds Numbers, PIBAL Rept. No. 611 (ARL TN 60-140), June 1960.

102. Oguchi, H., Hypersonic Flow Near the Forward Stagnation Point of a Blunt Body of Revolution, J. A./S. S., Vol. 25, No. 12, December 1958, pp. 789-790.

103. Stalder, J. R., The Use of Low-Density Wind Tunnels in Aerodynamic Research, Paper presented at the 1st International Symposium on Rarefied Gas Dynamics, Nice, France, July 1958 (Published in the proceedings of the Symposium "Rarefied Gas Dynamics," Edit. by F. M. Devienne, Pergammon Press, New York, 1959).

104. Drake, R. M. and Backer, G. H., Heat Transfer from Spheres in Supersonic Flow to a Rarefied Gas, Trans. ASME, Vol. 74, October 1952.

105. Tewfik, O. K. and Giedt, W. H., Heat Transfer, Recovery Factor, and Pressure Distributions Around a Circular Cylinder Normal to a Supersonic Rarefied-Air Stream, J. A./S. S., Vol. 27, No. 10, October 1960, pp. 721-729.

106. Weltmann, R. N. and Kuhns, P. W., Heat Transfer to Cylinders in Crossflow in Hypersonic Rarefied Gas Streams, NASA TN D-267, March 1960.

107. Hoshizaki, H., Neice, S. and Chan, K. K., Stagnation Point Heat Transfer Rates at Low Reynolds Numbers, IAS Paper No. 60-68, presented at the Nat'l Summer Meeting, Los Angeles, Calif., June 1960.

108. Varwig, R. L., Measurements of Free Molecule Heat Transfer in Air at Mach Numbers from 10-18, Space Tech. Lab. Rept. No. STL/TR-60-0000-94324, October 1960.

109. Wittliff, C. E. and Wilson, M. R., Low-Density Research in the Hypersonic Shock Tunnel, Proceedings of the 2nd Internat'l Symp. on Rarefied Gas Dynamics, Univ. of California, Berkely, Calif. Academic Press, 1961.

110. Cohen, C. B. and Reshotko, E., Similar Solutions for the Compressible Laminar Boundary Layer with Heat Transfer and Pressure Gradient, NACA TN 3305, February 1955.

111. Cheng, H. K., Hypersonic Shock-Layer Theory of the Stagnation Region at Low Reynolds Number, CAL Report No. AF-1285-A-7, April 1961 (Also Proceedings of 1961 Heat Transfer Fluid Mechanics Institute).

112. Allen, H. J., Hypersonic Flight and the Re-Entry Problem (21st Wright Brothers Lecture), J. Aero. Sci., Vol. 25, No. 4, April 1958, pp. 217-229.

113. Ferri, A., Feldman, L., and Daskin, W., The Use of Lift for Re-Entry from Satellite Trajectories, Jet Propulsion, Vol. 27, No. 11, November 1957, pp. 1184-1191.

114. Lees, L., Hartwig, F. W., and Cohen, C. B., Use of Aerodynamic Lift During Entry Into the Earth's Atmosphere, ARS Journal, Vol. 29, No. 9, September 1959, pp. 633-641.

115. Brown, W. S., Boyd, W. A., Cannon, E. T. and Partridge, W. S., Construction of a High Pressure, High Temperature, Light-Gas Gun, Proceedings of the Hypervelocity Techniques Symposium, IAS, Denver, Colorado, October 1960.

116. Baradell, D. L., Experimental Verification of Boundary-Layer Corrections in Hypersonic Nozzles, J. Aero/Space Sci. Vol. 26, No. 7, July 1959, pp. 454-455.

117. Lee, J. D., Axisymmetric Nozzles for Hypersonic Flows, OSU Rept. No. TN (ALOSU) 459-1, WADC TN 59-228, June 1959.

118. Duff, R. E., Shock-Tube Performance at Low Initial Pressure, Phys. Fluids, Vol. 2, No. 2, March-April 1959, pp. 207.

119. Anderson, G. F., Shock-Tube Testing Time, J. A./S. S., Vol. 26, No. 3, March 1959, p. 184.

120. Roshko, A., On Flow Duration in Low-Pressure Shock Tubes, Phys. Fluids, Vol. 3, No. 6, p. 835, November-December 1960.

121. Mark, H., The Interaction of a Reflected Shock Wave with the Boundary Layer in a Shock Tube, NACA TM 1418, March 1958.

122. Byron, S. and Rott, N., On the Interaction of the Reflected Shock Wave with the Laminar Boundary Layer on the Shock Tube Walls, Proceedings of 1961 Heat Transfer and Fluid Mechanics Institute, Univ. of So. California, June 19-21, 1961.

123. Mirels, H., Attenuation in a Shock Tube Due to Unsteady-Boundary-Layer Action, NACA TN 3278, August 1956.

124. Mirels, H. and Braun, W. H., Nonuniformities in Shock-Tube Flow Due to Unsteady-Boundary-Layer-Action, NACA 4021, May 1957.

125. Trimpi, R. L. and Cohen, N. B., A Theory for Predicting the Flow of Real Gases in Shock Tubes with Experimental Verification, NACA TN 3375, March 1955.

126. Trimpi, R. L. and Cohen, N. B., A Nonlinear Theory for Predicting the Effects of Unsteady Laminar, Turbulent, or Transitional Boundary Layers on the Attentuation of Shock Waves in a Shock Tube with Experimental Comparison, NACA TN 4347, September 1958.

127. Boyer, D. W., Effects of Kinematic Viscosity and Wave Speed on Shock Wave Attenuation, Univ. Toronto, Inst. Aerophysics, Tech. Note. No. 8, May 1956.

128. Wheeler, D. B. Jr., Density Variation in Shock Tube Flow, Lehigh Univ., Inst. of Res. Tech. Rept. 8, August 1956.

129. Rose, P. H. and Nelson, W., On the Effects of Attentuation of Gas Dynamic Measurements made in Shock Tubes, AVCO Res. Rept. 24, March 1958.

130. Stalder, J. R., Rubesin, M. W. and Eberly, D. K., Study of Real Gas and Heat Transfer Effects on the Design of Hotshot Wind Tunnels, Sandia Corp. Monograph SCR-166, March 1960.

SYMBOLS

The notation not explicitly defined in the text or figures is given below. Where several definitions are given for a single symbol, the correct meaning is clear from the usage in the text.

A	area
C	proportionality constant in linear viscosity-temperature relation, $C = \frac{\mu/\mu_\infty}{T/T_\infty}$
c	specific heat of backing material for resistance thermometers
C_D	drag coefficient, Drag $/ \frac{1}{2}\rho_\infty U_\infty^2 \left(\frac{\pi}{4} d^2\right)$
C_H	heat transfer coefficient, $q / \rho_\infty U_\infty (H_0 - H_w)$
C_L	lift coefficient, Lift $/ \frac{1}{2}\rho_\infty U_\infty^2 A$
C_m	pitching moment coefficient, Pitching Moment $/ \frac{1}{2}\rho_\infty U_\infty^2 \left(\frac{\pi}{4} d^2\right)$
C_{m_α}	static stability derivative, $\left(\partial C_m / \partial \alpha\right)_{\alpha \to 0,\ \dot{\alpha} = q' = 0}$
$C_{m_{\dot{\alpha}}}$	dynamic stability derivative, $\left[\partial C_m / \partial \left(\frac{\dot{\alpha} L}{U}\right)\right]_{\dot{\alpha} \to 0,\ \alpha = q' = 0}$
$C_{m_{q'}}$	dynamic stability derivative, $\left[\partial C_m / \partial \left(\frac{q' L}{U}\right)\right]_{q' \to 0,\ \alpha = \dot{\alpha} = 0}$
D	drag; blunt-cone nose diameter; nozzle diameter
d	diameter
d_c	parameter in analysis of boundary-layer displacement effect on a cone (Ref. 80), $\frac{0.968}{M_c^2} \frac{T_w}{T_c} + 0.145(\gamma - 1)$
E_i	energy in specified mode of freedom
F_1	parameter in boundary-layer displacement analysis for a cone (Ref. 80)
H	enthalpy

H_F	chemical energy frozen out in nonequilibrium flow
h	altitude
k	nose or leading-edge drag coefficient, Drag $/ \frac{1}{2}\rho_\infty U_\infty^2 \left(\frac{\pi}{4} D^2\right)$ or Drag $/ \frac{1}{2}\rho_\infty U_\infty^2 t$; thermal conductivity of backing material for resistance thermometers
k_F, k_R	forward and reverse reaction rate constants
K	parameter in analysis of stagnation region flow at low Reynolds numbers, $\sqrt{\rho_\infty R / \mu_\infty U_\infty C}$
K_ϵ	parameter controlling inviscid leading-edge bluntness effect, $M^3 k \epsilon t / x$
L	length; nozzle throat radius
ℓ	ratio of nozzle throat radius to tangent of the asymptotic angle, $L / \tan\theta$
M	Mach number
p	pressure
Pr	Prandtl number
q	heat transfer rate; dynamic pressure, $\frac{1}{2}\rho U^2$
q'	angular velocity
R	radius, gas constant
Re	Reynolds number
S	entropy
St	Stanton number, $q / \rho U (H_{aw} - H_w)$
T	temperature
t	time; leading-edge thickness
U	velocity

X	distance along plate surface, cone axis, or free-stream direction
Y_i	concentration of certain species in mixture
Y_s	shock-wave coordinate measured normal to plate surface
α	angle of attack
$\dot{\alpha}$	rate of change of angle of attack, $d\alpha/dt$
α_f	frozen degree of dissociation
β	parameter in combined leading-edge bluntness boundary-layer displacement analysis, $\chi_\epsilon K_\epsilon^{-2/3}$
γ	specific-heat ratio
δ^*	boundary-layer displacement thickness
ϵ	$\frac{\gamma-1}{\gamma+1}$
θ	angle
μ	viscosity
ρ	density
τ	relaxation time; time variable of integration; testing time per foot of shock tube
χ, $\overline{\chi}$	viscous interaction parameter, $M^3/\sqrt{Re}$, $M^3\sqrt{C}/\sqrt{Re}$
χ_ϵ	$\epsilon(0.664 + 1.73\frac{H_w}{H_0})\overline{\chi}$

Subscripts

AW	conditions at adiabatic wall temperature
B	body
C	cone
$C.R.$	center of rotation

Subscripts (Cont.)

EQ	equilibrium flow conditions
$L.E.$	leading-edge
0	stagnation conditions
S	shock wave
t	conditions referenced to leading-edge thickness
W	wall conditions
X	conditions referenced to length x
∞	free-stream ambient conditions

Superscript

$'$	conditions behind normal shock

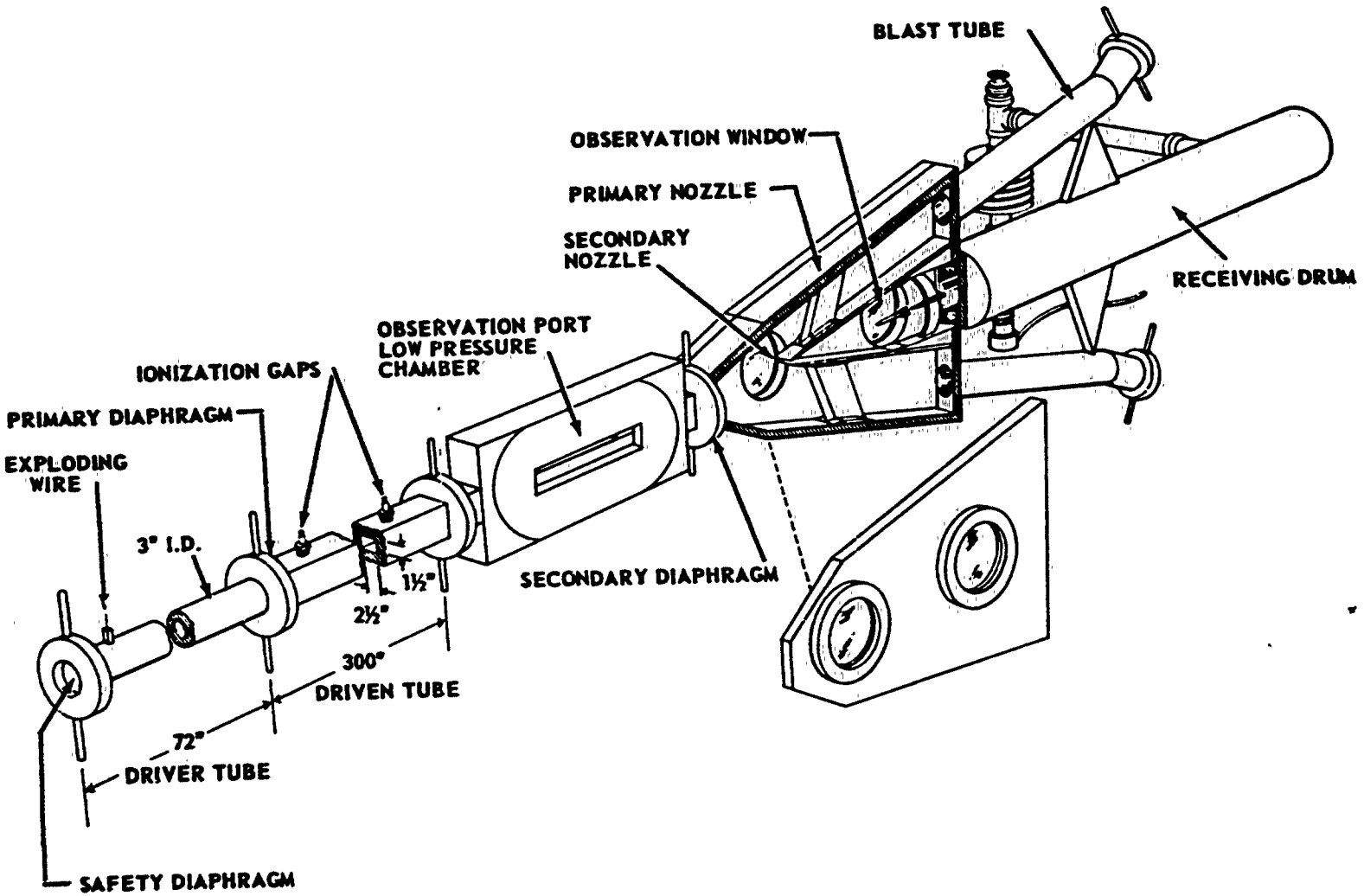

Figure 1 SKETCH OF THE EARLY C.A.L. HYPERSONIC SHOCK TUNNEL

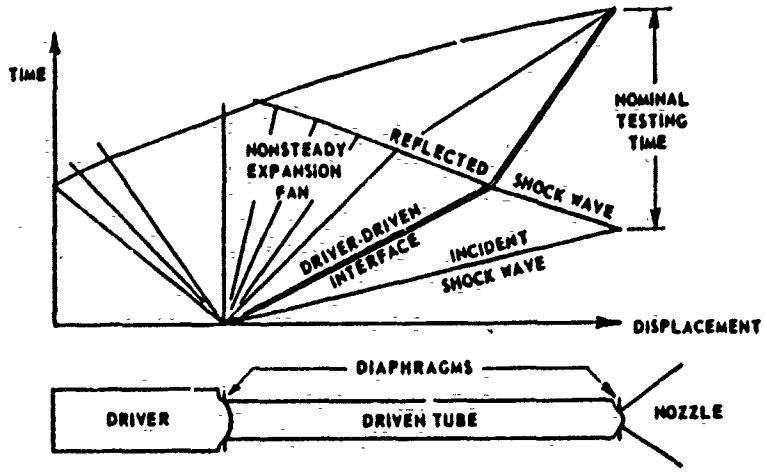

Figure 2 WAVE DIAGRAM FOR THE TAILORED INTERFACE SHOCK TUNNEL

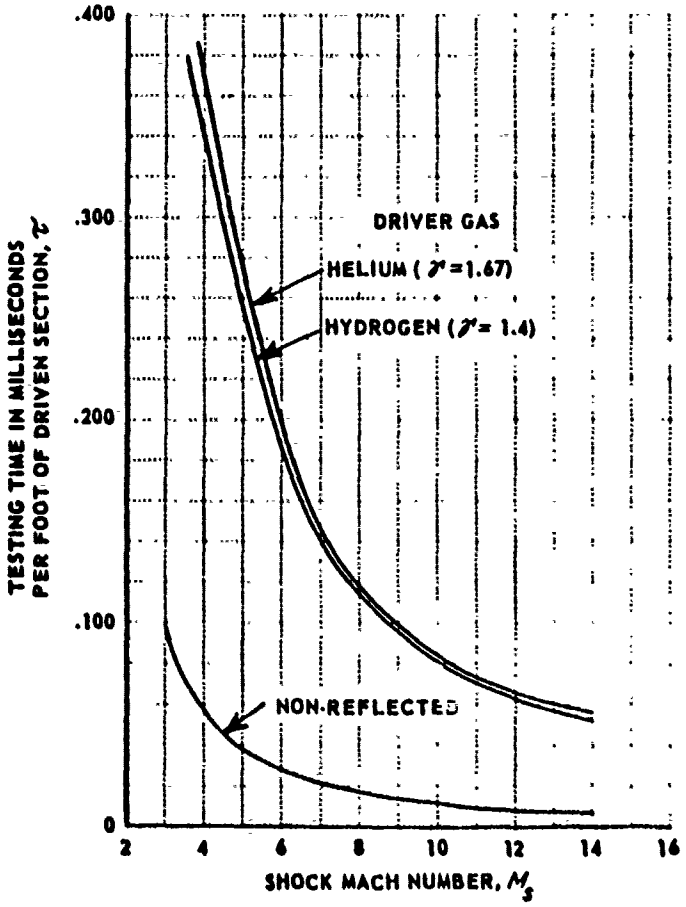

Figure 3 TESTING TIME vs. SHOCK MACH NUMBER

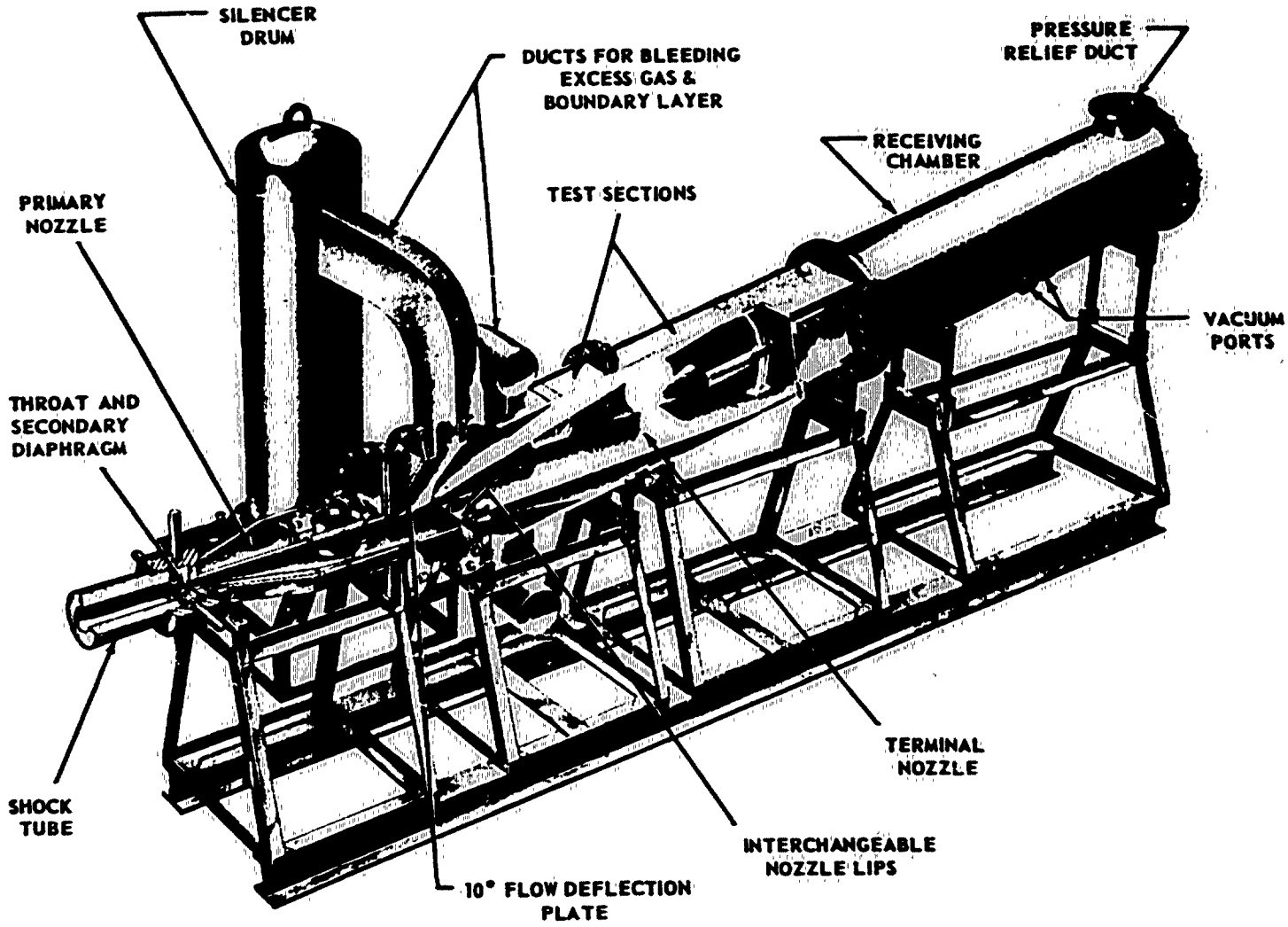

Figure 4 CORNELL AERONAUTICAL LABORATORY 11 INCH BY 15 INCH HYPERSONIC SHOCK TUNNEL

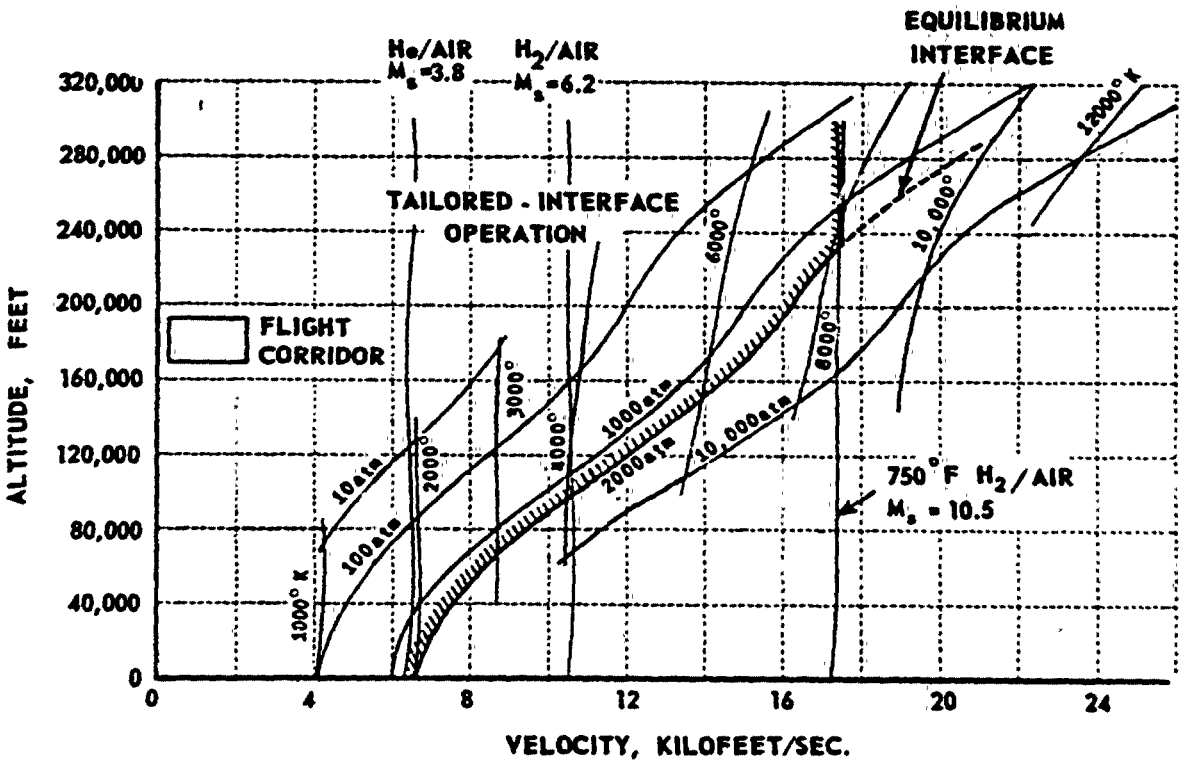

Figure 5 TUNNEL STAGNATION PRESSURES AND STAGNATION TEMPERATURES REQUIRED FOR FLIGHT DUPLICATION

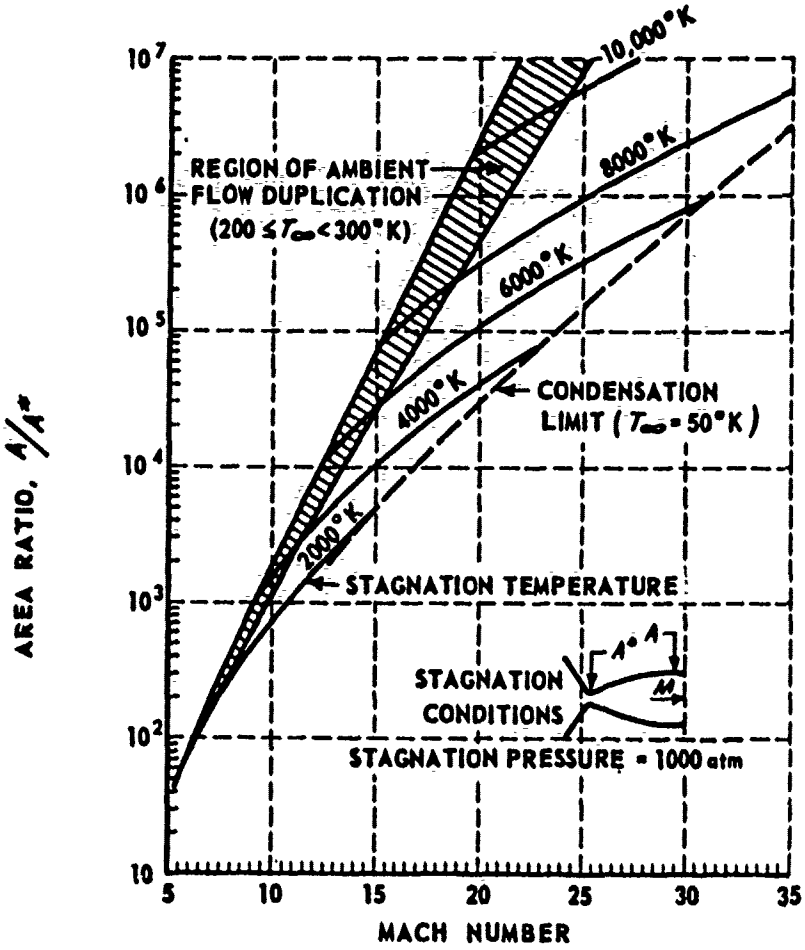

Figure 6 AREA RATIO vs. MACH NUMBER

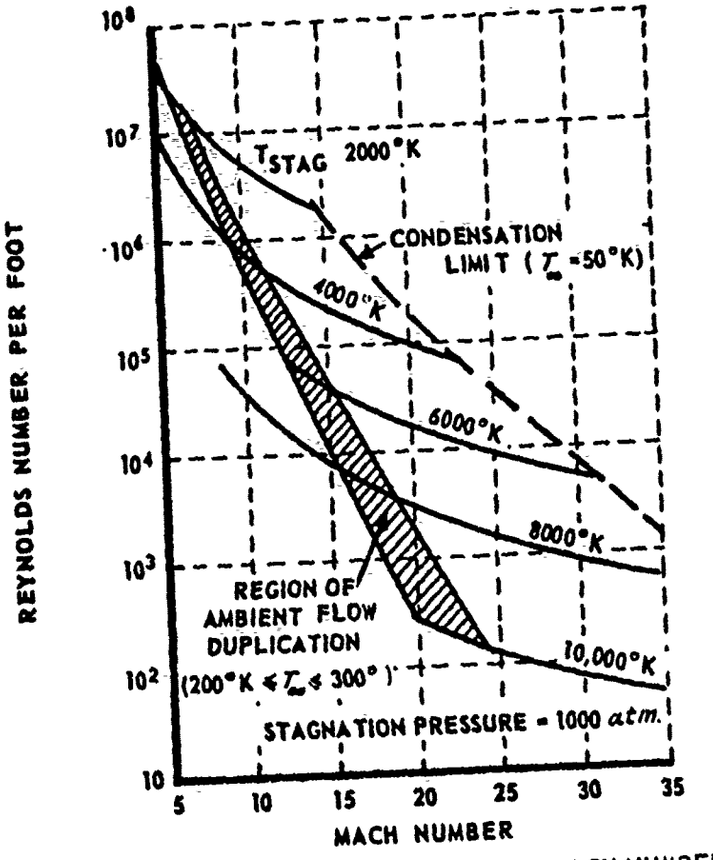

Figure 7 REYNOLDS NUMBER PER FOOT vs. MACH NUMBER

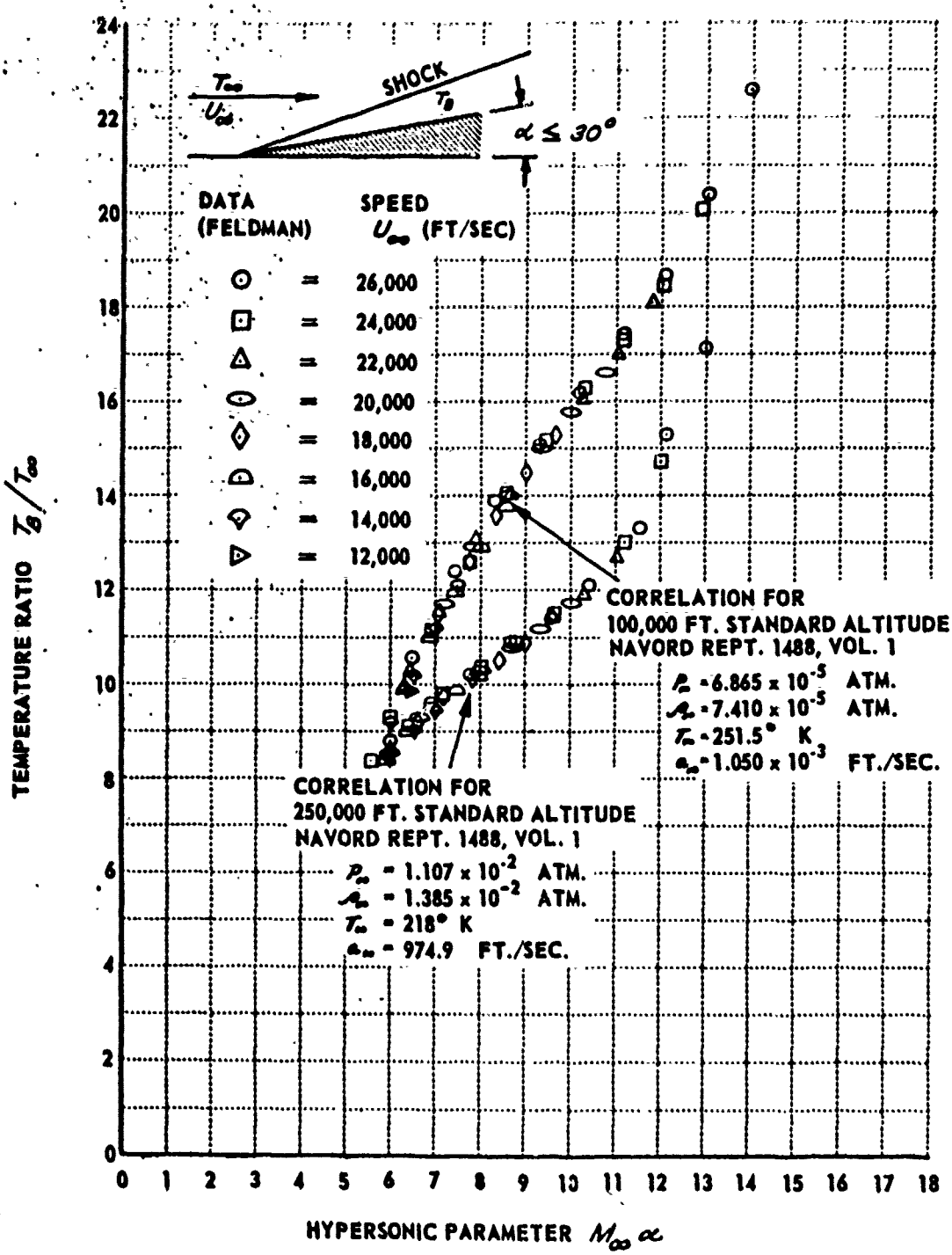

Figure 8 CORRELATIONS OF THE TEMPERATURE RATIO FOR EQUILIBRIUM WEDGE FLOWS OF ARGON-FREE AIR

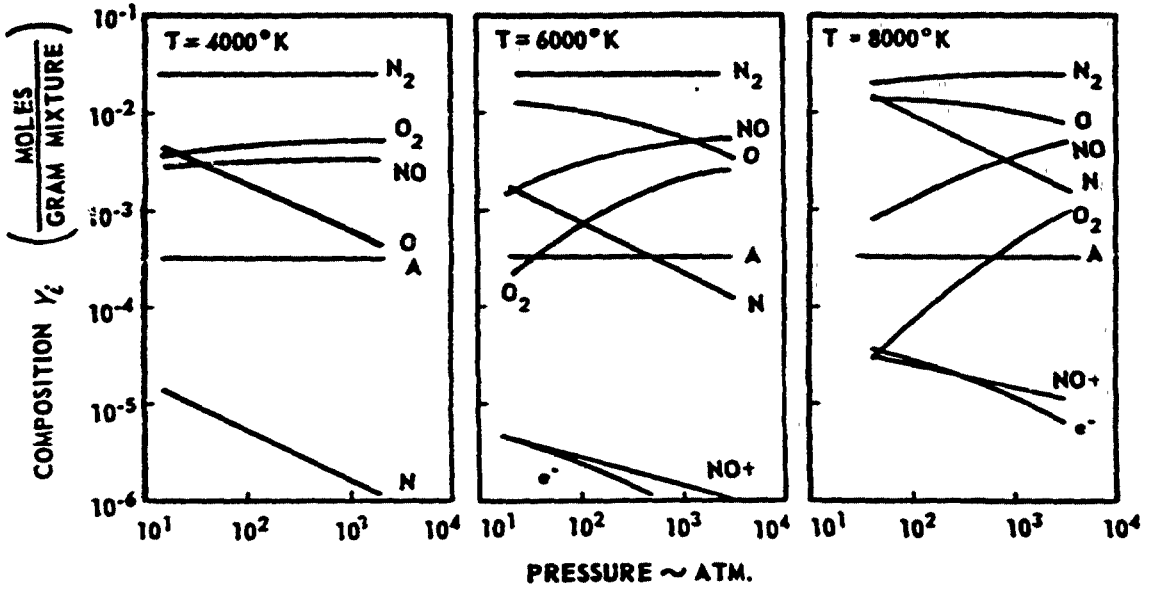

Figure 9 COMPOSITION OF EQUILIBRIUM AIR
(REFERENCE: CAL REPORT NO. BE-1007-A-3)

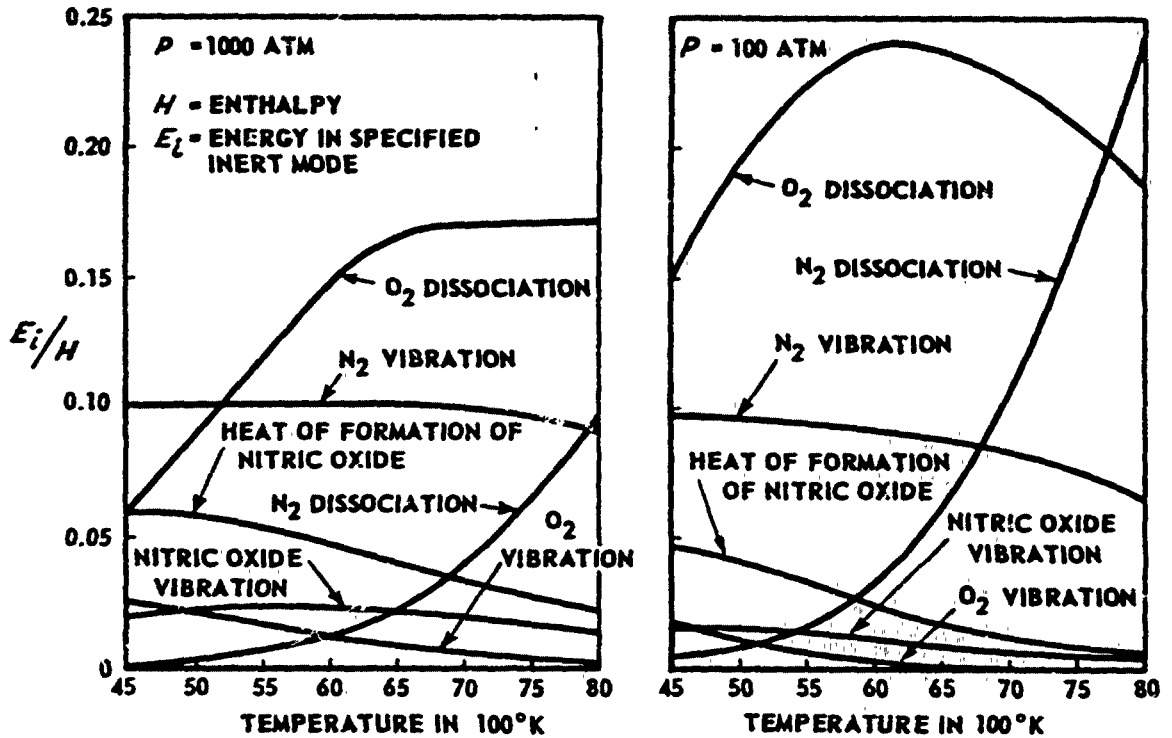

Figure 10 FRACTION OF THE ENTHALPY OF EQUILIBRIUM AIR IN SPECIFIED ENERGY MODE

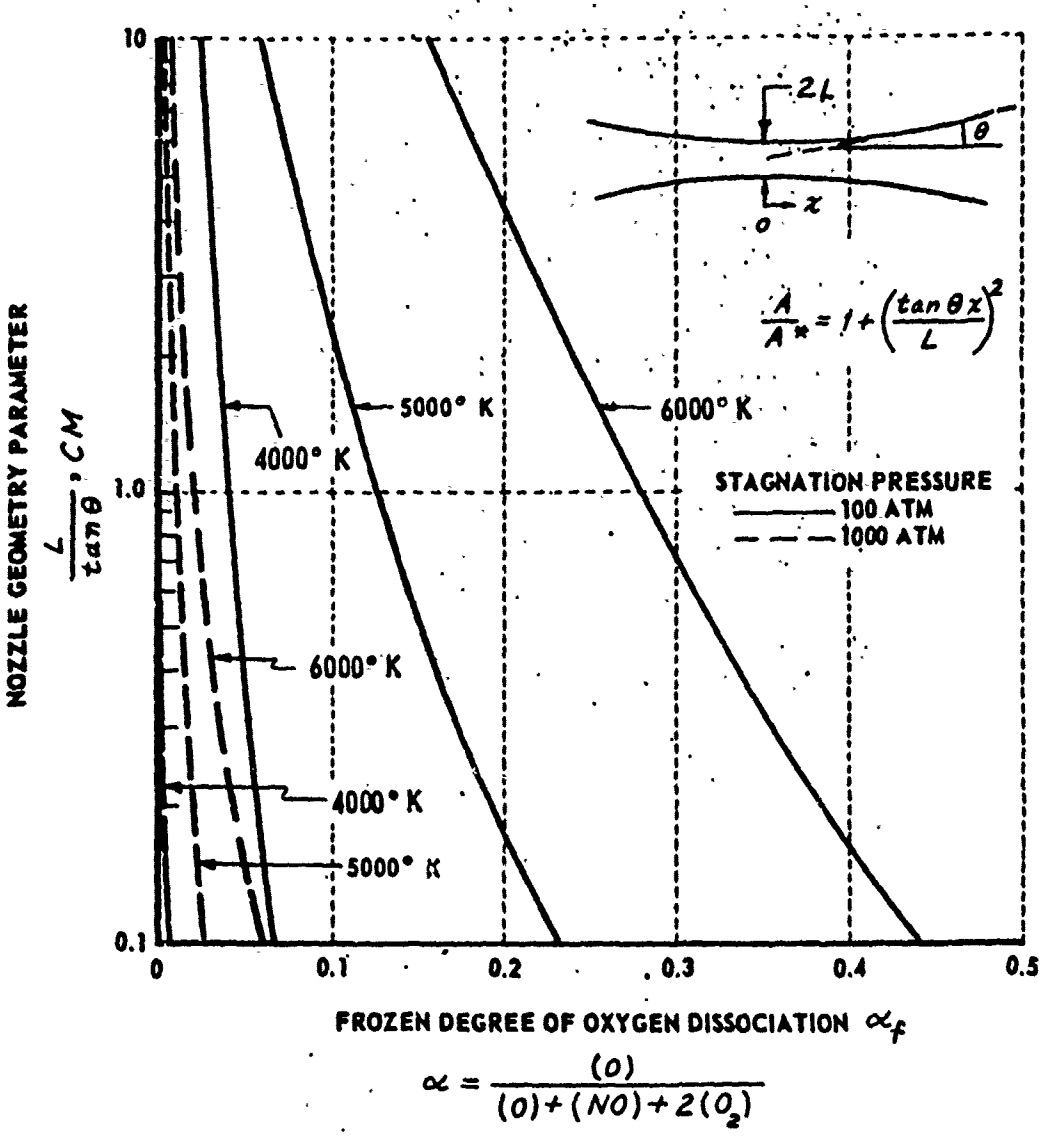

Figure 11 THE EFFECT OF STAGNATION TEMPERATURE AND PRESSURE AND NOZZLE GEOMETRY FOR A HYPERBOLIC AXISYMMETRIC NOZZLE ON THE FROZEN DEGREE OF OXYGEN DISSOCIATION FOR A SIMPLIFIED AIR MODEL

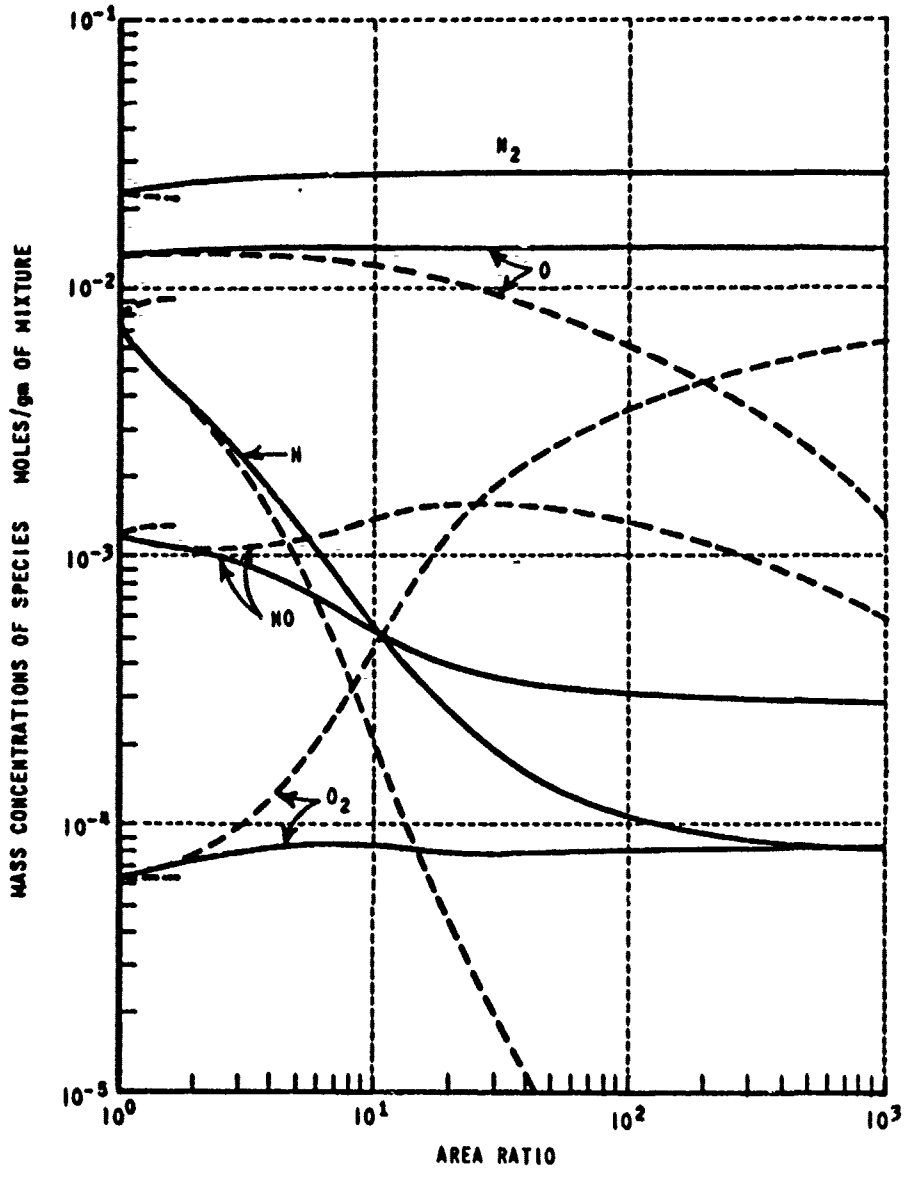

FIG. 12 SPECIES DISTRIBUTIONS FOR AIRFLOW IN A HYPERSONIC NOZZLE

T_0 = 8000°K, P_0 = 100 ATM ℓ = 1 cm

——— FINITE RATE NONEQUILIBRIUM

– – – – – INFINITE RATE EQUILIBRIUM

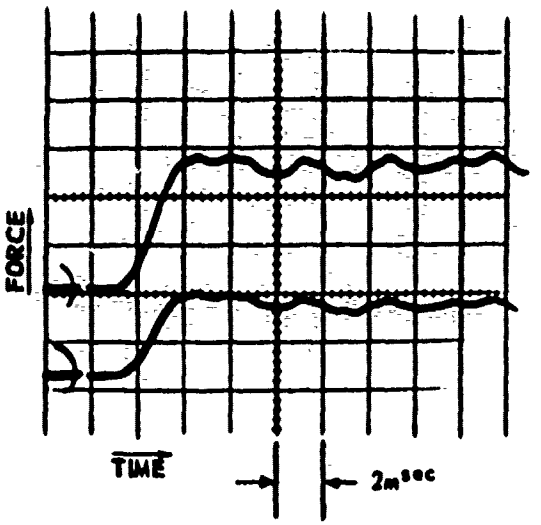

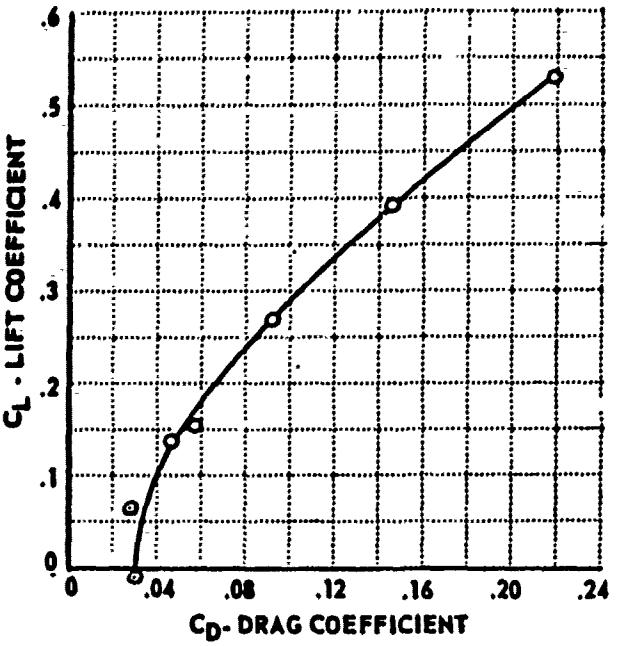

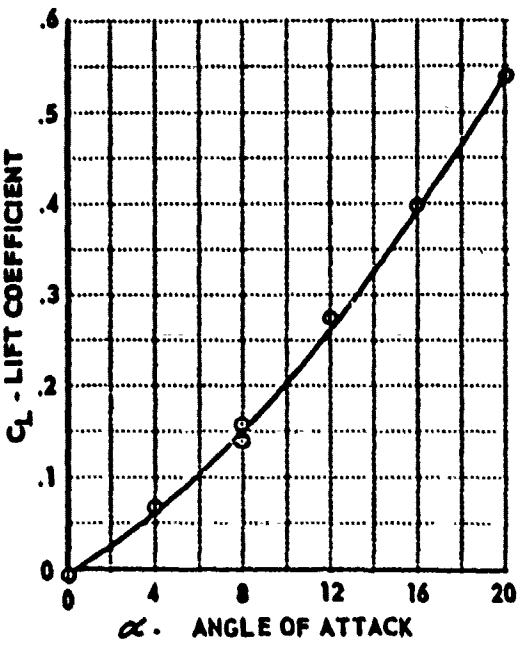

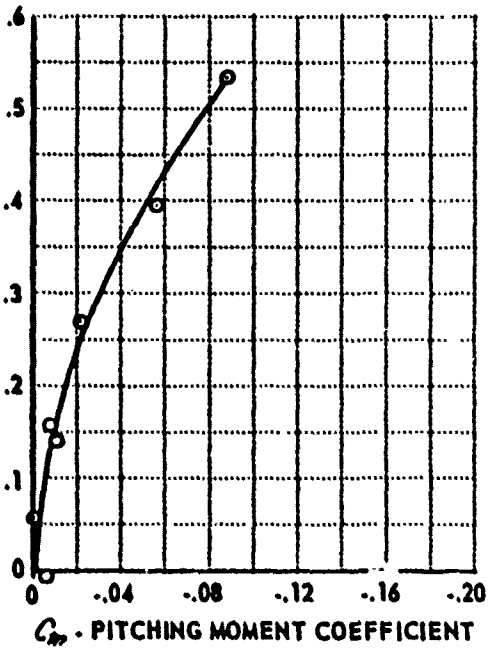

Figure 13 TYPICAL RAW DATA OSCILLOGRAPH RECORDS AND REDUCED DATA FOR HYPERSONIC AIRCRAFT CONFIGURATION AT MACH 8

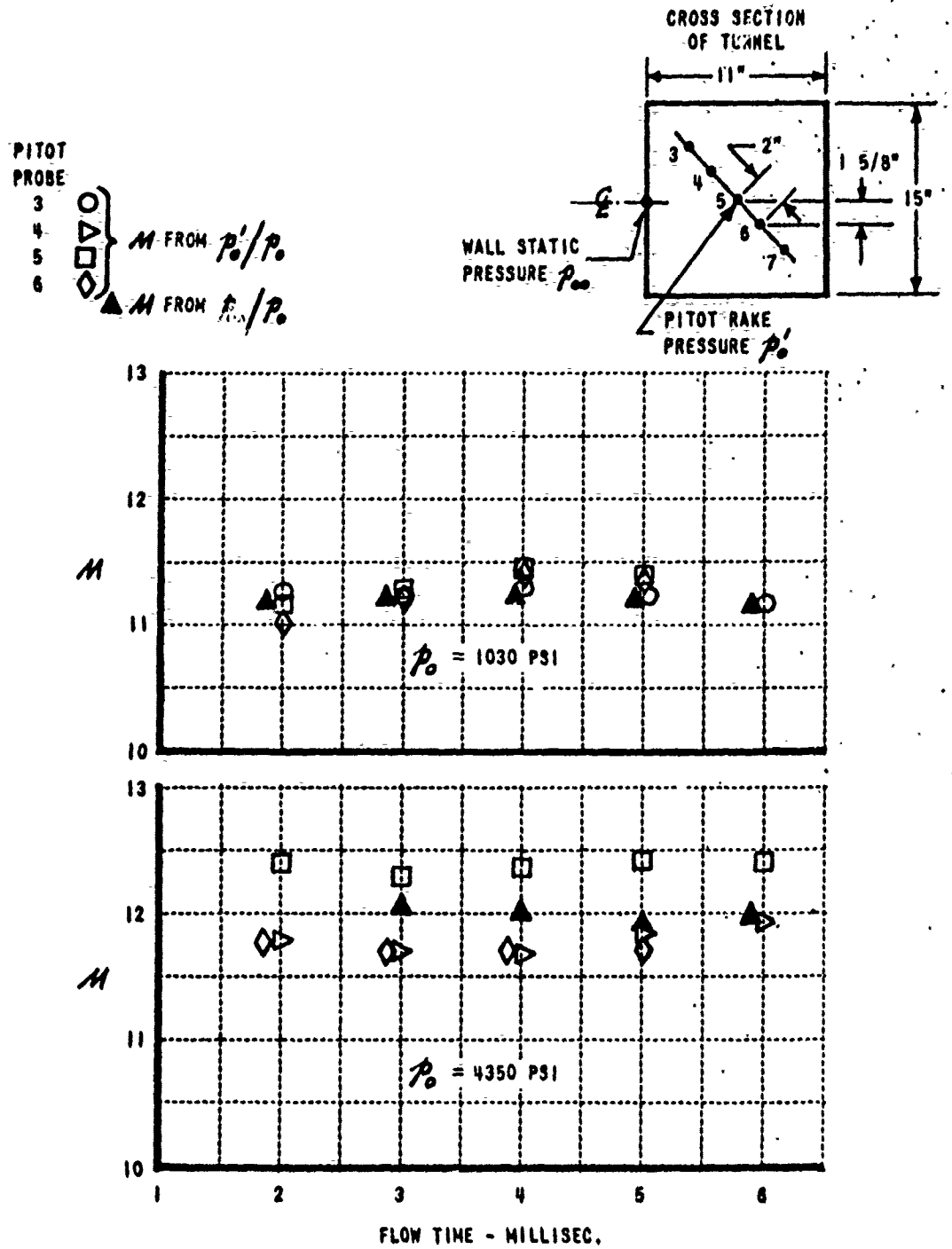

Figure 14 TYPICAL CALIBRATION RESULTS FOR MACH NUMBER (M) SURVEY

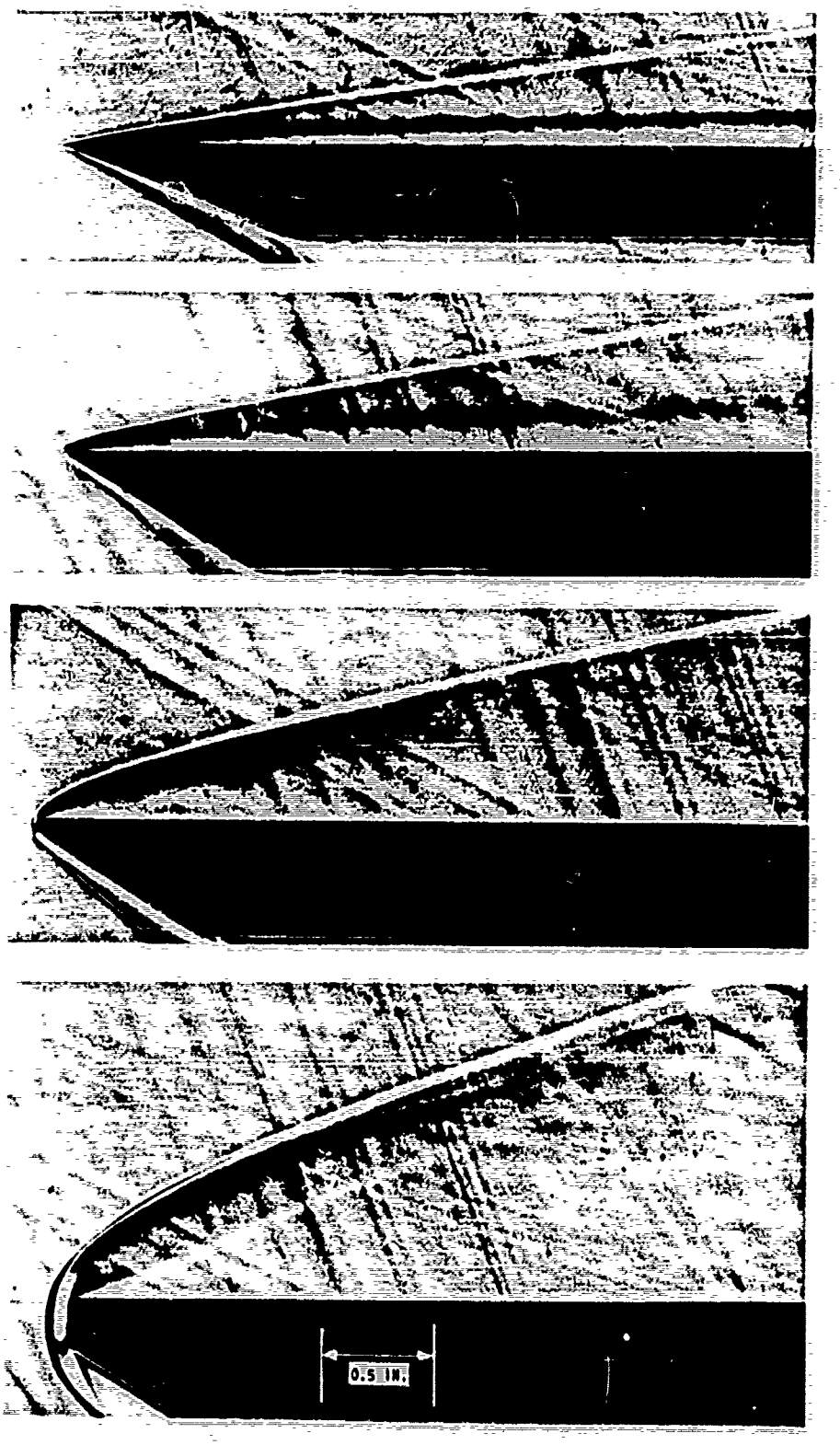

Figure 15 SCHLIEREN PHOTOGRAPHS OF SHOCK-WAVE SHAPES ($\alpha = 0°$, $T_0 \sim 2000°K$)

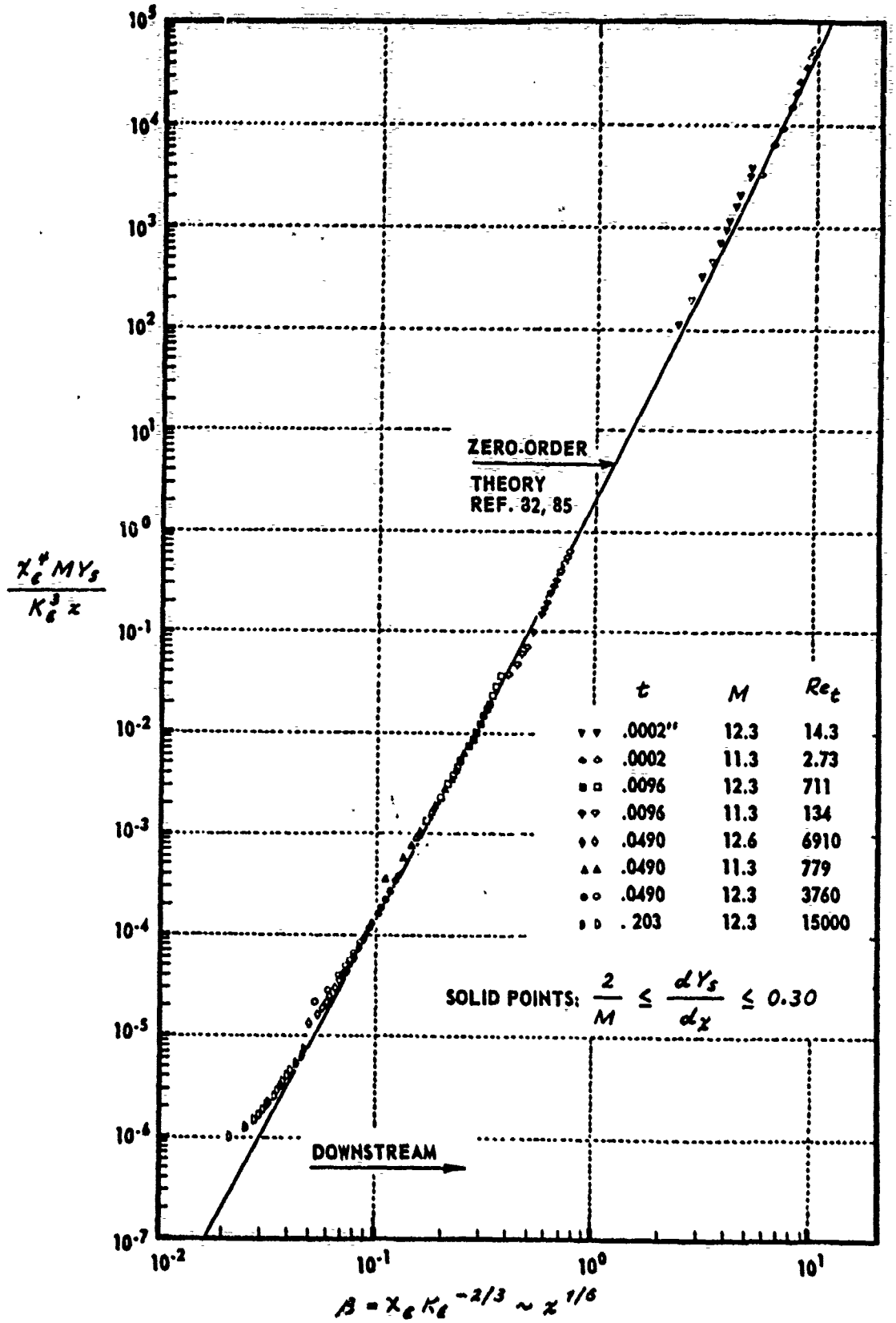

Figure 16 GENERAL CORRELATION OF SHOCK-WAVE SHAPES FOR ARBITRARY β (α = 0°, $T_o \sim$ 2000°K)

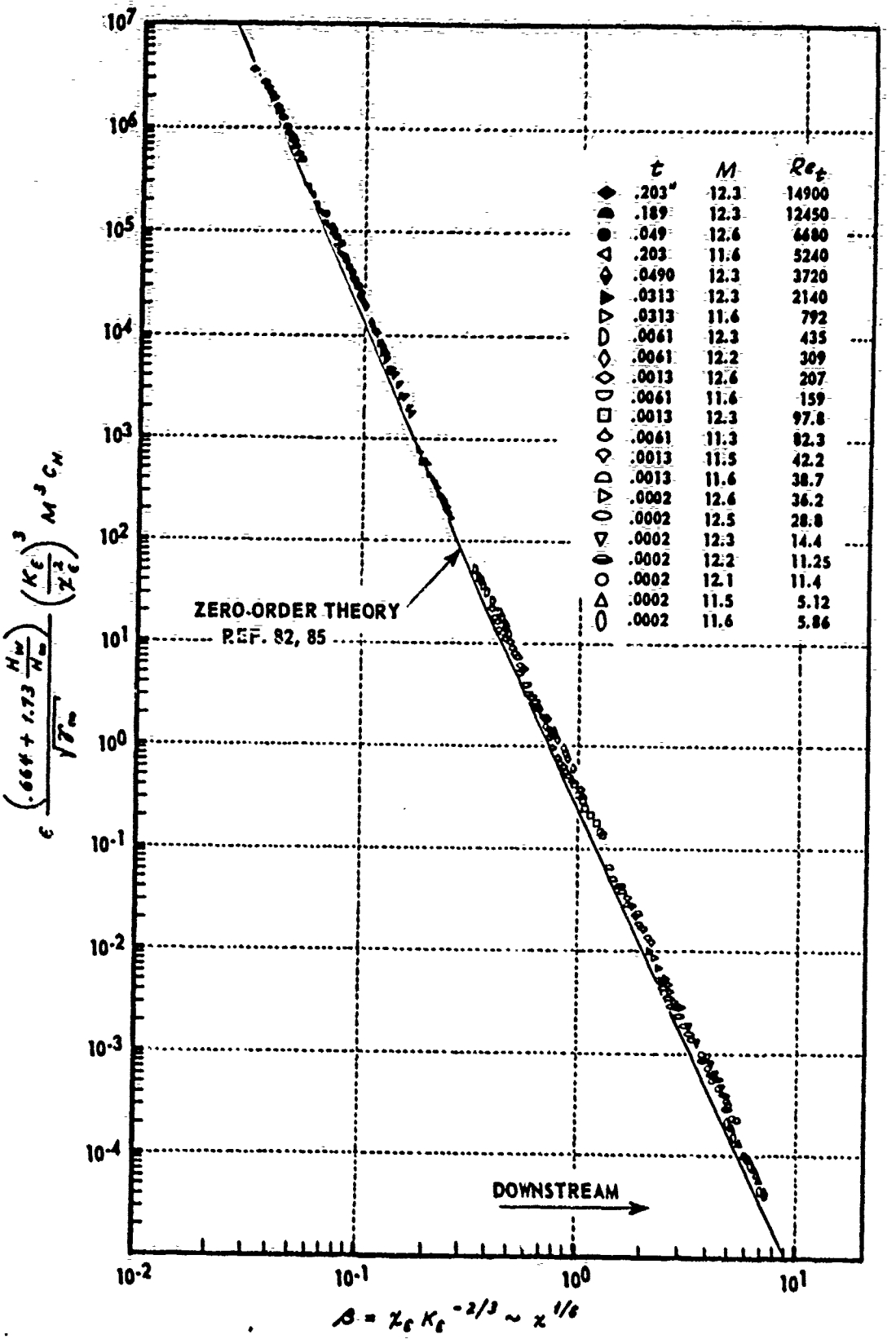

Figure 17 GENERAL CORRELATION OF EXPERIMENTAL HEAT TRANSFER FOR ARBITRARY β (α = 0°, $T_o \sim 2000°$ K)

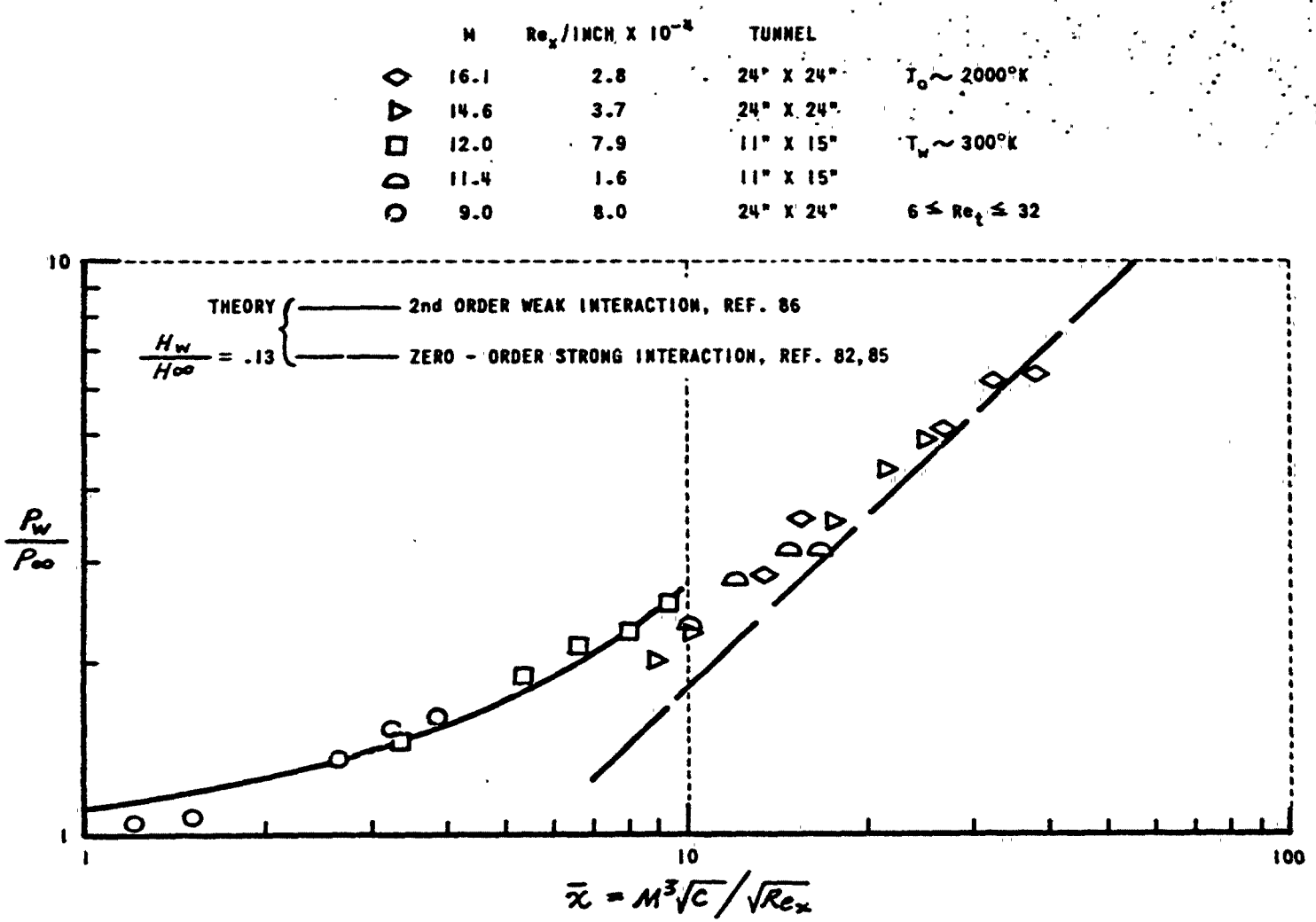

Figure 18 CORRELATION OF EXPERIMENTAL PRESSURES ON SHARP PLATE ($\alpha = 0$)

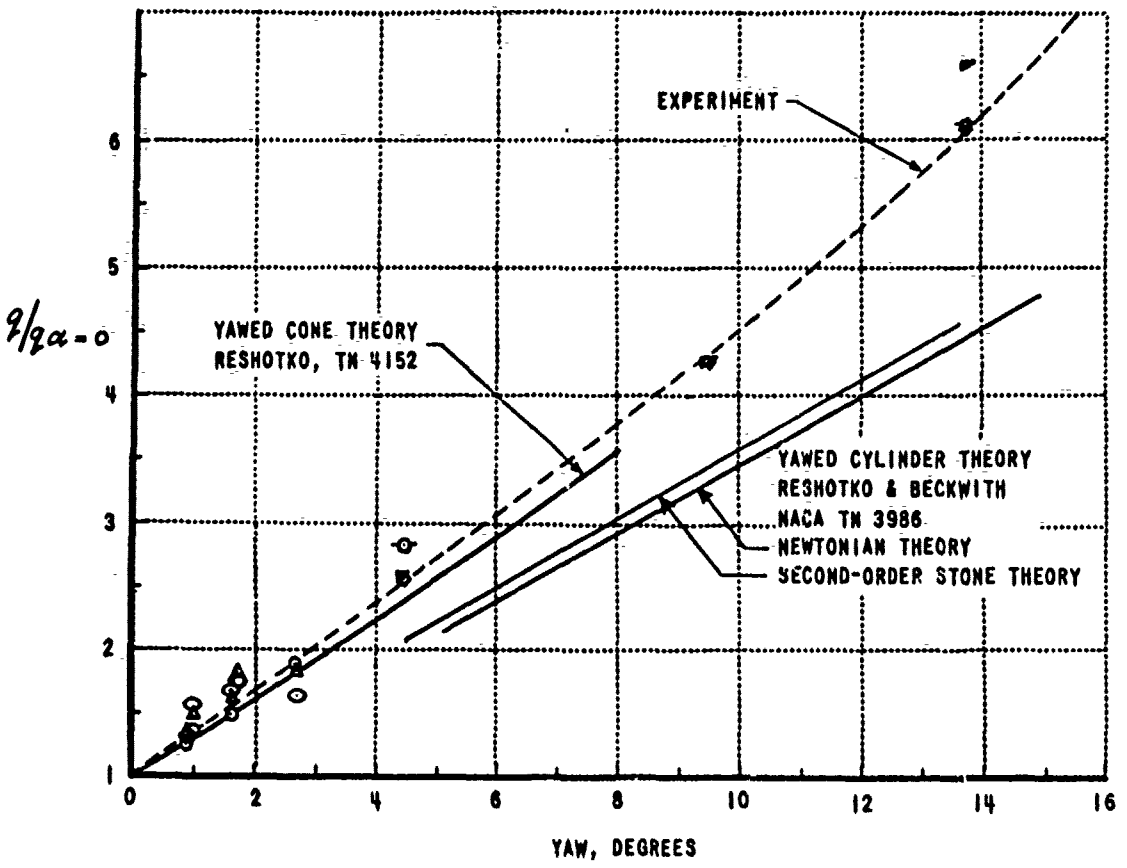

Figure 19 RATIO OF HEAT TRANSFER ALONG MOST WINDWARD STREAMLINE TO ZERO YAW HEAT TRANSFER - 5° HALF-ANGLE CONE AT M = 12, T_o = 2000°K

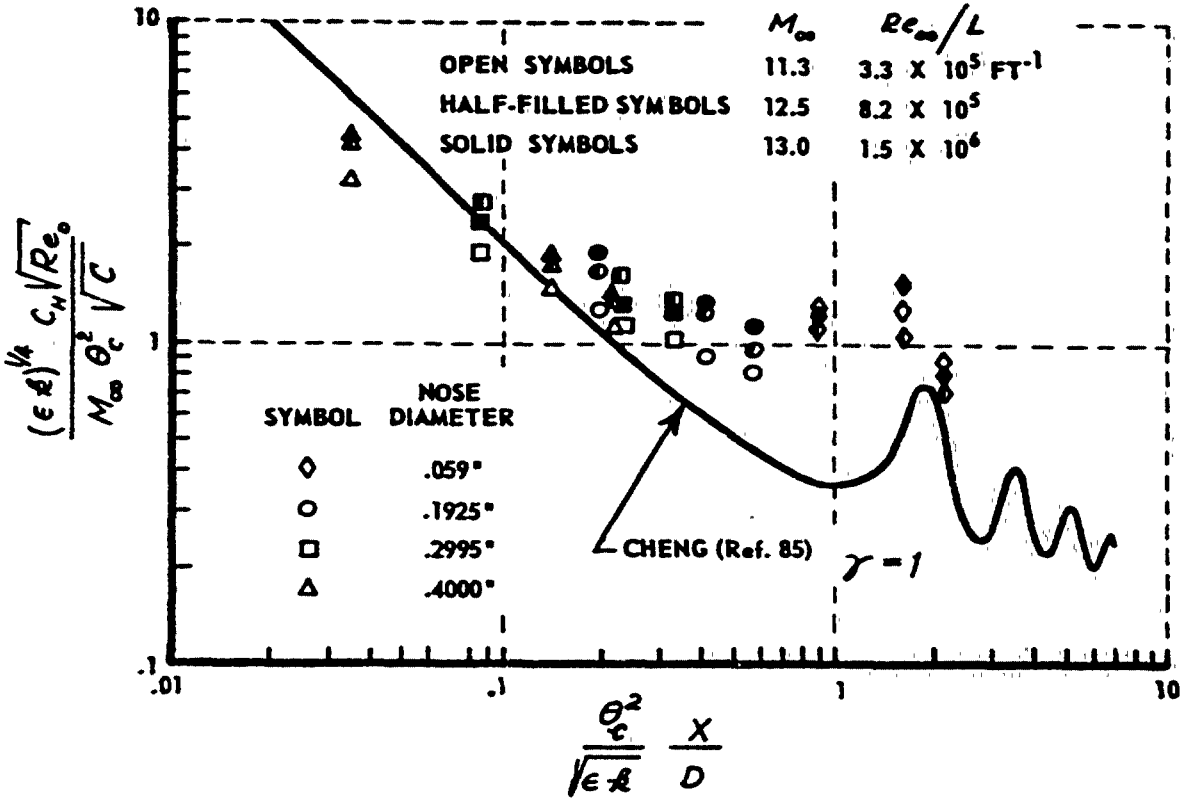

Figure 20 HEAT TRANSFER TO A BLUNT 5° HALF-ANGLE CONE AT ZERO YAW

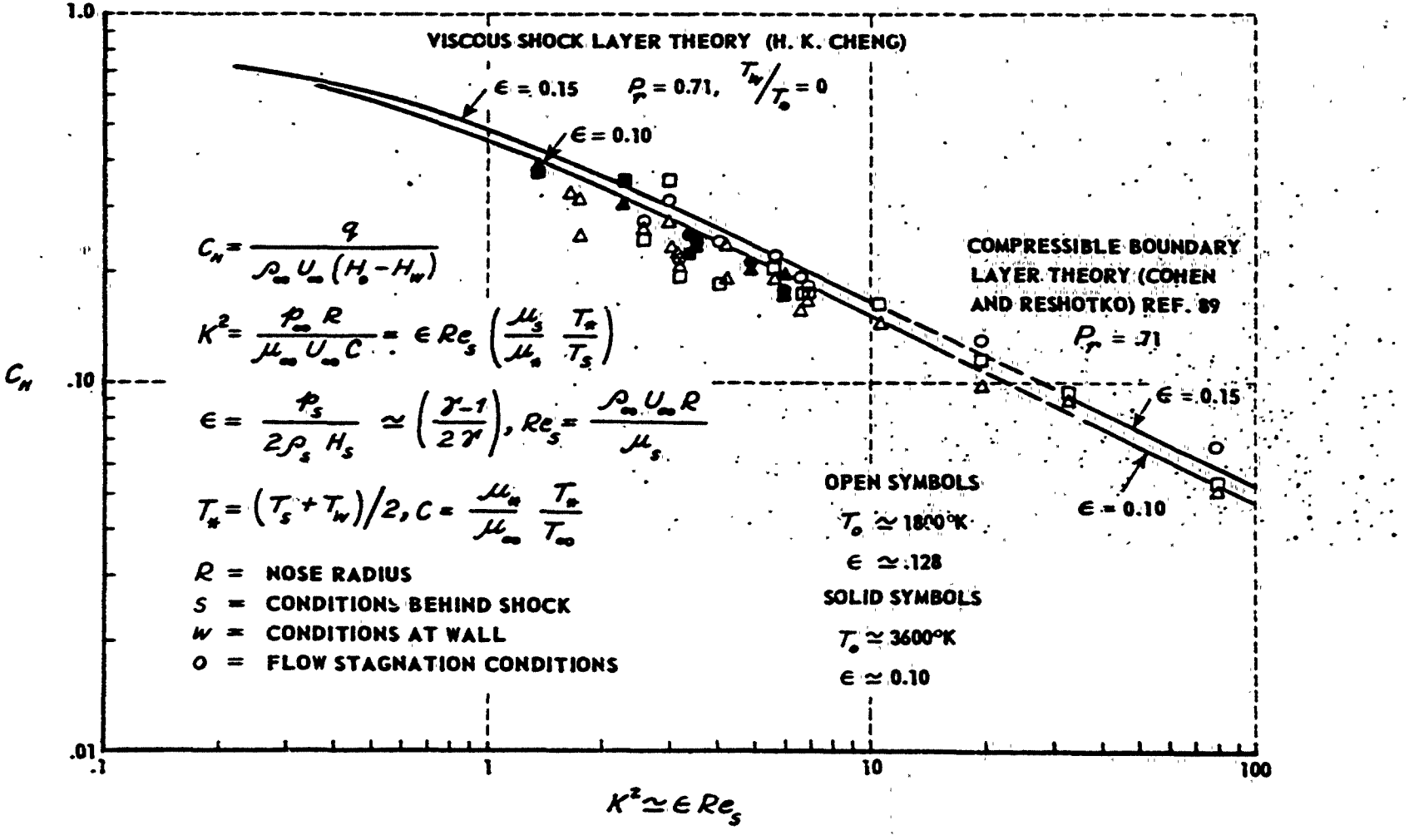

Figure 21 STAGNATION-POINT HEAT TRANSFER TO A TRANSVERSE CYLINDER IN HYPERSONIC AIR FLOW

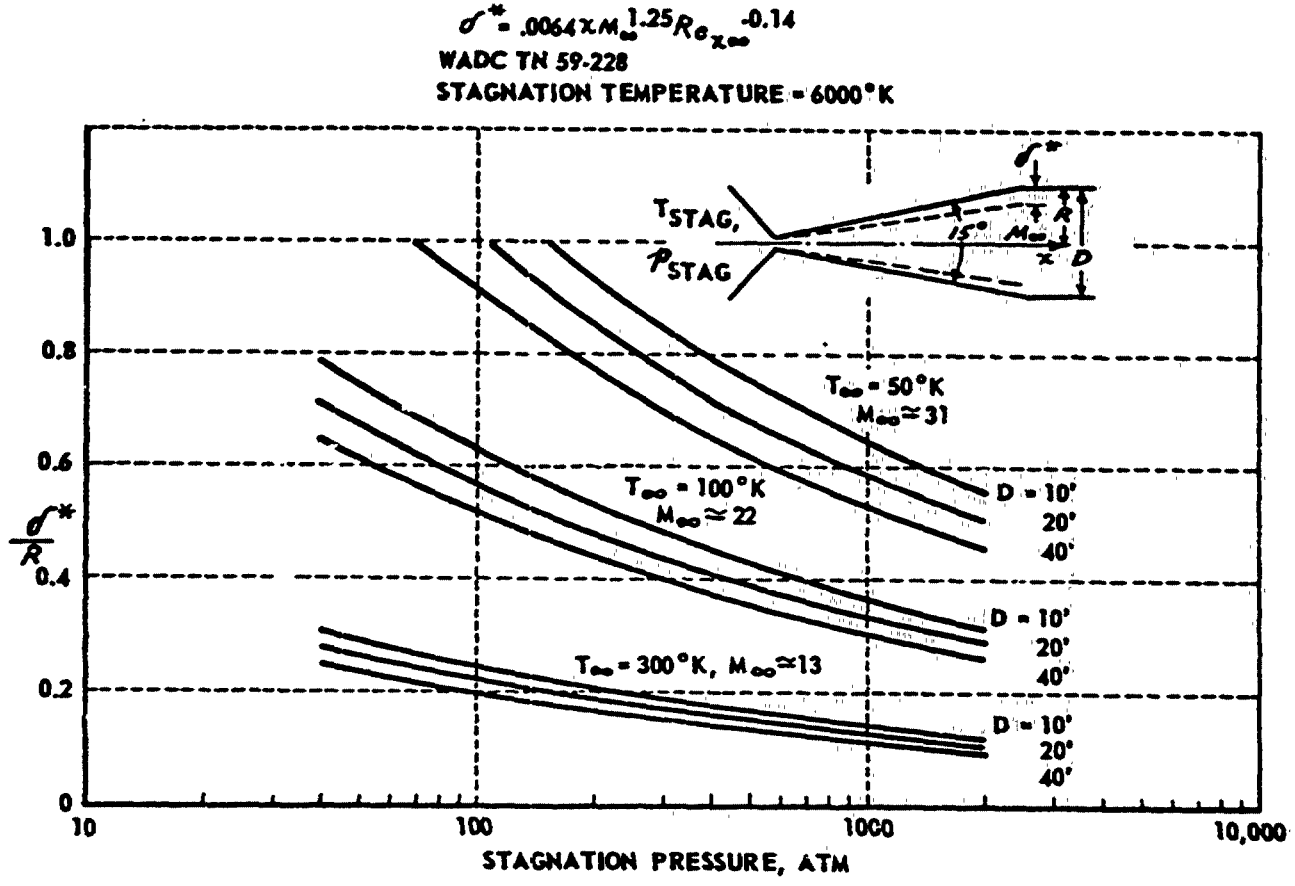

Figure 22 BOUNDARY LAYER DISPLACEMENT THICKNESS IN A CONICAL NOZZLE

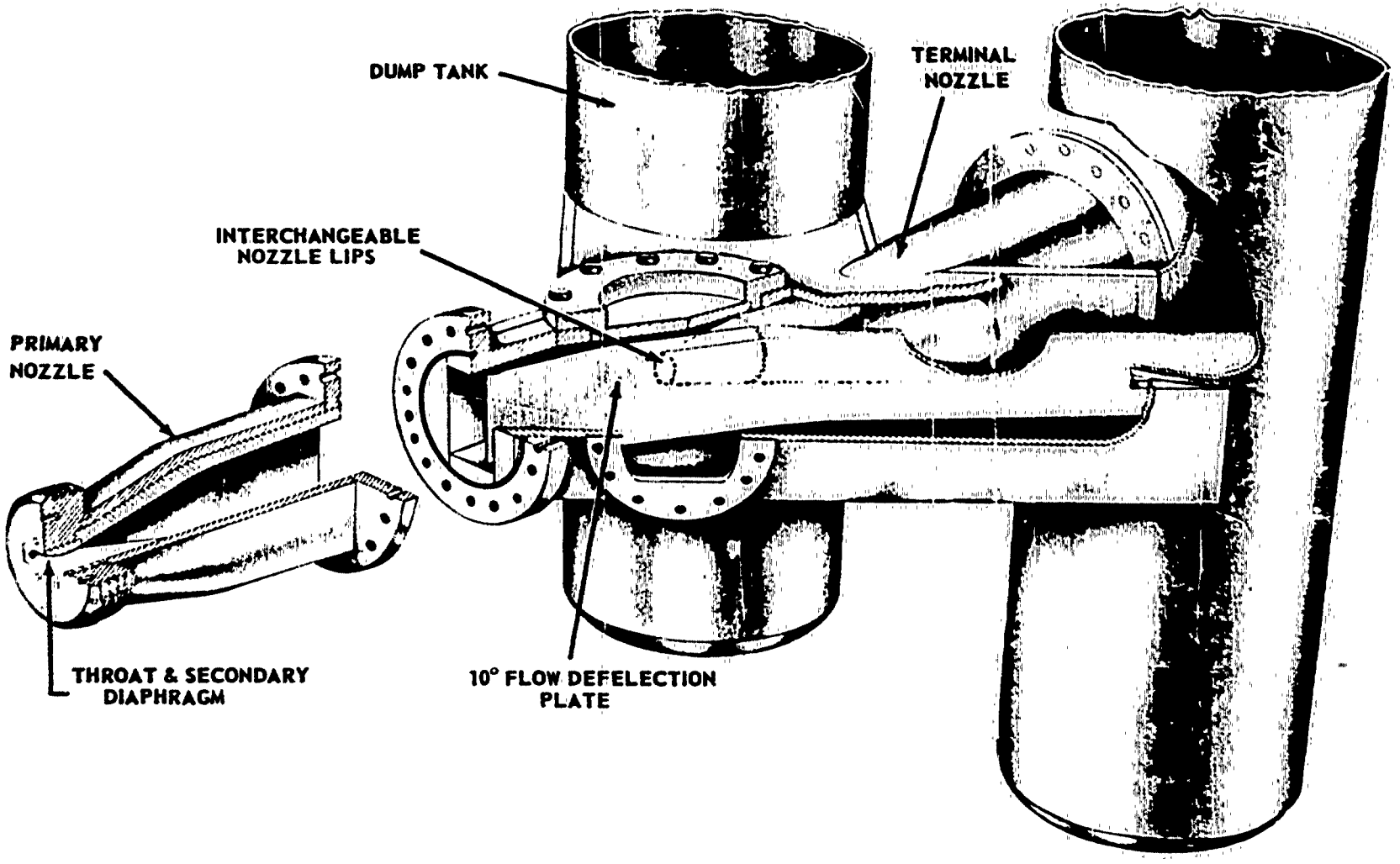

Figure 23 PRIMARY NOZZLE, FLOW-TURNING SECTION, AND CONICAL NOZZLE ENTRANCE FOR THE CORNELL AERONAUTICAL LABORATORY 6 FT HYPERSONIC SHOCK TUNNEL

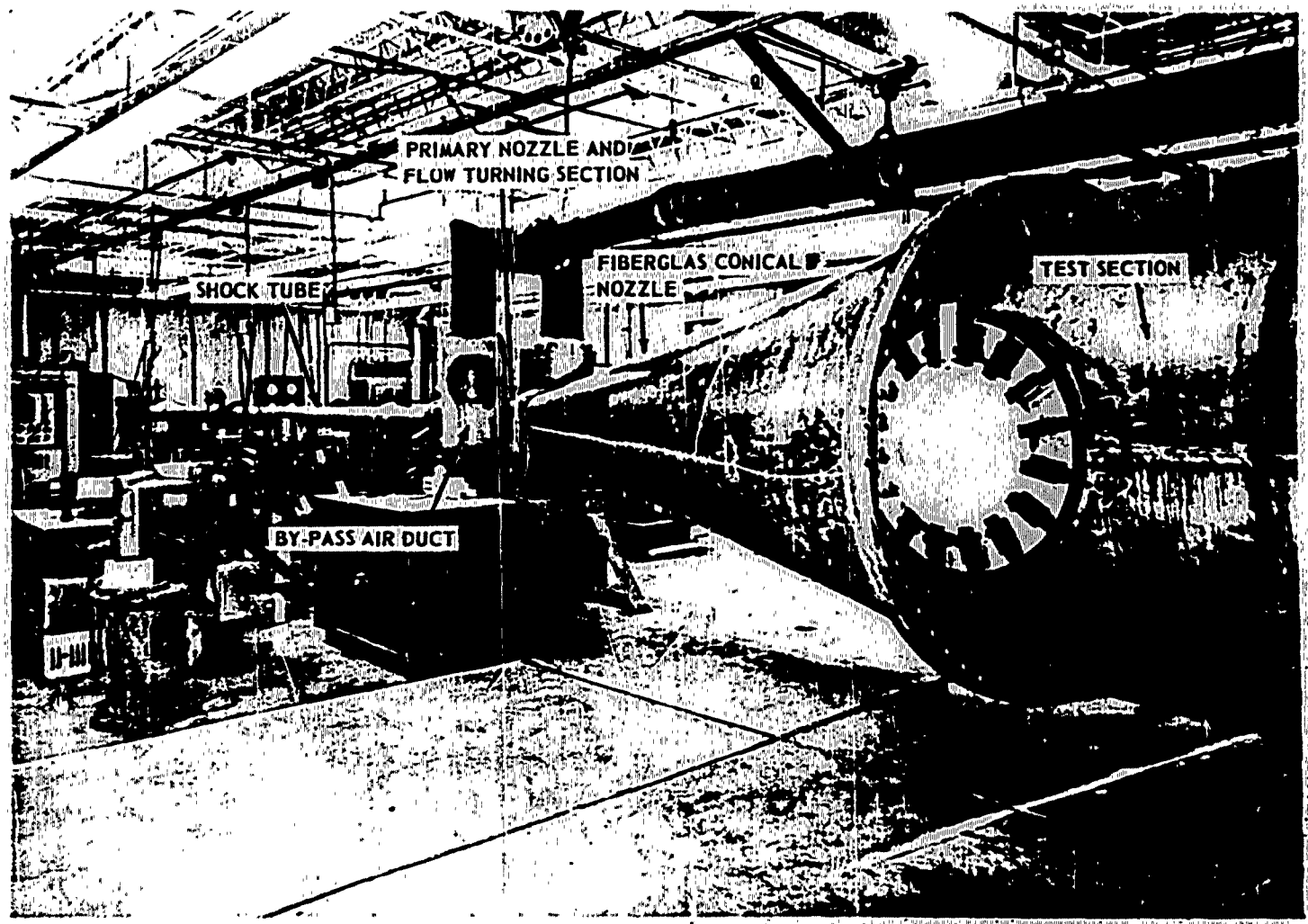

Figure 24 PHOTOGRAPH OF THE CAL 6-FT HYPERSONIC SHOCK TUNNEL